UNIVERSITY OF CALIFORNIA
RIVERSIDE

Characterization of *Xylella fastidiosa* Lipopolysaccharide-Induced Plant Defense Priming, Endoglucanase-Regulated Exopolysaccharide Production, and Type IV Pili

A Dissertation submitted in partial satisfaction
of the requirements for the degree of

Doctor of Philosophy

in

Plant Pathology

by

Claudia Alejandra Castro

December 2021

Dissertation Committee:
Dr. M. Caroline Roper, Chairperson
Dr. Patricia Manosalva
Dr. Ansel Hsiao

The Dissertation of Claudia Alejandra Castro is approved:

_____

_____

_____

Committee Chairperson

University of California, Riverside

Acknowledgements

Pursuing a PhD is a difficult task but it is worthwhile. As I look back to when I began graduate school, I see that I have grown so much as a scientist and individual. During these years, I learned that I shouldn't take failed experiments and rejected fellowship applications personally. I learned that these "failures" are not a reflection of who I am as a person. I learned resilience. I learned to celebrate the small and big successes. I learned that my anxiety disorder is not always my enemy, but that it helps me be a better scientist and it encourages me to strive for perfection, although perfection is impossible to achieve. This chapter of my life is coming to an end and I feel extremely grateful and lucky to have been given this opportunity.

Caroline, thank you for guiding me through this process and for your encouragement to learn new skills and attend conferences. You always treated me as an independent thinker even when I was a young scientist and I didn't trust myself yet. Your respect, enthusiasm, and positive attitude really made this experience better for me. I will carry these things with me as I navigate my career as a scientist and leader. I will always be proud to be a graduate from the Roper lab!

I want to thank my other mentors. Patty, thank you for always giving me meaningful feedback on my research and for helping carve the way for other Latina scientists in plant pathology. Ansel, thank you for serving on my dissertation committee and for always letting me know you were available to discuss my research. Quinn McFrederick, thank you for your time, openness, and kindness during the CUSP program. Ravi Palanivelu, I cannot thank you enough. Your time, guidance, and patience for me as

an undergraduate student really changed everything for me and my career. You're a never ending inspiration for me. I also want to thank Jennifer Noble, Xunliang Liu, and Yanbing Wang for being great mentors in the Palanivelu lab at the University of Arizona. Thank you to my research collaborators for your incredible work and diligence.

Many thanks to the current and former students of the Roper lab and the Manosalva lab. You are all incredible individuals and I consider myself lucky to have worked alongside you. Tash, my confidant, I'm so glad I got to experience this journey with you. I'm going to miss our gym sessions and coffee breaks. Brian, my battle buddy, thank you for teaching me so much about *Xylella* and for being such a good friend and listener during the long hours we spent in the greenhouse. Pol, thank you for your friendship, kindness, and selflessness. You never hesitated to answer my questions and provide help even when you were in the middle of something important. Nichole, my peer hero, thank you for always cheering me on and for inspiring me to be more tenacious. Alex and Flavia, thank you for those long bike rides and for helping me stay sane during the pandemic. I'll miss our adventures! Biagio, what can I say? Your friendship really helped my morale and improved my well-being during very tough times. Thank you. Chris, my bestie, thank you for the never ending laughs and for understanding my love for chihuahuas. Matt, thank you for being the best undergrad! It was such a pleasure working with you. Normita, thank you for your hard work and help. I am excited to see your achievements during your PhD y acuerdate que sí se puede. Thank you to Lindsey Burbank, Jeannette Rapicavoli, Nancy Her, Gretchen Heimlich, Alicia Serrano Gómez, and Barbara Jablonska.

Thank you to my Arizona friends for being patient with me when I couldn't make it to weddings and other important life events. Thank you to my friends and roommates, Kelley Clark and Hannah Shulman. I really enjoyed our time together on bachelor nights and shopping trips. Many thanks to Loretta Mead, for providing me with the tools to better understand myself and become a better version of me. Thank you to my brothers, Juan and José, for always cheering me up and for your genuine excitement about what I study. Gracias a mis papás, a quiénes les dedico este trabajo. Gracias por su amor y sonrisas. Son lo máximo. Los quiero muchísimo. Finally, I want to thank Benjamin Cornell, my partner. You've shown me incredible patience and love since I've met you. I cannot thank you enough. I'm thrilled to begin the next chapter with you.

ABSTRACT OF THE DISSERTATION

Characterization of *Xylella fastidiosa* Lipopolysaccharide-Induced Plant Defense Priming, Endoglucanase-Regulated Exopolysaccharide Production, and Type IV Pili

by

Claudia Alejandra Castro

Doctor of Philosophy, Graduate Program in Plant Pathology
University of California, Riverside, December 2021
Dr. M. Caroline Roper, Chairperson

Xylella fastidiosa is a re-emerging, Gram-negative bacterium that causes disease in many economically important crops including grape, olive, and citrus. *X. fastidiosa* subsp. *fastidiosa*, the causal agent of Pierce's disease of grapevine, remains a significant problem for grape growers in California. This plant-pathogenic bacterium resides exclusively in the foregut of its insect vectors and in the plant host xylem. Bacterial lipopolysaccharide (LPS) covers most of the cell surface of Gram-negative bacteria, like *X. fastidiosa*. This molecule is a well-described microbe-associated molecular pattern that elicits immune responses in mammals and plants. Vitis vinifera grapevines pre-treated with the *X. fastidiosa* MAMP, lipopolysaccharide (LPS), as a priming stimulus had a significant decrease in both external and internal symptoms of PD as well as the rate of overall disease progression indicating that LPS primes the grapevine immune response to better defend itself against future challenge with the *X. fastidiosa* pathogen. This enhanced defense was phenotypically manifested in a suppression of both internal and

external symptoms. Differential gene expression analysis revealed major transcriptomic reprogramming in primed vines in response to pathogen challenge at the point of inoculation and 20 nodes distal to the point of inoculation when compared to naive, untreated vines. Furthermore, a weighted gene co-expression analysis identified modules of co-expressed genes common to the point inoculation and 20 nodes above indicating that primed vines mount a temporally and spatially synchronous response to initial pathogen challenge. These responses included genes involved in signal perception, signal transduction, as well as auxin-related pathways.

X. fastidiosa produces exopolysaccharides (EPS) and forms robust biofilms in the plant host xylem and in the mouthparts of its insect vectors. Here we demonstrate that the *X. fastidiosa* EPS is a β-1,4-glucan backbone with alternating 3-linked side chains, one with terminal β-glucuronic acid and α-1,2-mannose residues, and the other with a terminal β-glucose and α-1,2-mannose residues. An endoglucanase mutant, Δ*engXCA2*, has a hypermucoid colony morphotype *in vitro* suggesting that EngXCA2 is involved in EPS processing and/or turnover. Additionally, Δ*engXCA2* was severely impaired in several key steps in biofilm development that included cell-cell aggregation, attachment to surface substrata and biofilm maturation. *In vitro*, Δ*engXCA2* biofilms were structurally compromised compared to wildtype biofilms. In planta, Δ*engXCA2* biofilms were encased in copious amounts of EPS compared to wild type biofilms which corroborates our *in vitro* findings. Recombinant EngXCA2 digested *X. fastidiosa* EPS confirming that EngXCA2 utilizes the EPS as a substrate. These results demonstrate that

EngXCA2 plays an important role in regulating *X. fastidiosa* biofilm formation through enzymatic degradation of the β-1,4-glucan backbone of EPS.

X. fastidiosa is nonflagellated and relies upon its type IV pili (T4P) for movement. T4P are filamentous appendages that quickly polymerize and depolymerize to pull and drag the cell along a surface. These structures are also involved in biofilm formation by linking cells to each other. Finally, to explore the role of T4P in X. fastidiosa pathogenesis in grapevines, we created three mutant strains in genes involved in the T4P machinery: *pilB, pilA1,* and *pilA2*. Δ*pilB* and Δ*pilA1* strains were deficient in cell-cell aggregation compared to wildtype and Δ*pilA2* strains. Moreover, Δ*pilB*- and Δ*pilA1*-inoculated grapevines had significantly less overall disease and lower *X. fastidiosa* titer while Δ*pilA2* behaved similarly to wildtype. Our results indicate that PilB, a putative ATPase that drives pili extension, and PilA1, a putative pilin subunit, are necessary for PD symptom development and grapevine colonization.

Table of Contents

List of Figures

Chapter II

Chapter III

Chapter IV

Appendix

List of Tables

Chapter II

Chapter IV

Chapter I

Introduction

Vitis vinifera subsp. *vinifera,* the source of wine and table grapes, is the most economically important horticultural crop in the world [1,2]. In the state of California alone, grapes were valued at $6.25 in 2018 [3]. Although *V. vinifera* has large genetic diversity that could be exploited for the breeding of beneficial traits, this monoecious, perennial crop has been clonally propagated for many years [1,2]. *V. vinifera* subsp. *vinifera* was domesticated from its wild progenitor approximately 22,000 to 30,000 years ago [2]. Its geographical origin is unknown but it is commonly hypothesized to be the Middle East [1,2]. *V. vinifera* was introduced to California in 1769 when Franciscan missionaries arrived in San Diego from the Baja California mission Nuestra Señora de Loreto. The Catholic missionaries traveled along the coast until reaching Sonoma in Northern California during the early 1800s. Missionaries planted grapevines and made wine as they established along the state. Wine-making was considered a necessity for the missionaries who used wine for the celebration of Mass, for meals, and later as a source of income [4].

Newton B. Pierce, working under the U.S. Department of Agriculture Division of Vegetable Pathology, first described a serious vine disease in 1892 in Anaheim, California that would later be known as Pierce's disease of grapevine. During his 10-month stay in California, he reported on the symptoms caused by this disease and the economic losses in the industry across the counties of Los Angeles, Orange, and San Bernardino [5]. The causal agent of Pierce's disease would not be determined until 1978 by Davis et al. who cultured the bacterium for the first time and completed Koch's

postulates [6]. This bacterium would be further described and be named *Xylella fastidiosa* by Wells *et al.* in 1987 [7].

X. fastidiosa is a fastidious, gram-negative bacterium in the class Gammaproteobacteria, order Xanthomonadales, and family *Xanthomonadaceae*. This bacterium is rod-shaped, nonflagellate, and is 0.25–0.35 by 0.9–3.5 μm in size [8]. *X. fastidiosa* can behave as a commensal endophyte or as a pathogen in its plant hosts[9]. This bacterium has an extremely wide host range that includes over 300 hosts from 63 different plant families and is pathogenic in approximately 100 plant species [8]. Besides PD, *X. fastidiosa* is the causal agent of other economically important diseases such as olive quick decline syndrome, almond leaf scorch, and citrus variegated chlorosis whose bacterial strain, 9a5c, was the first plant pathogenic bacterial genome to be sequenced [8,10]. *X. fastidiosa* is endemic to the Americas and recently emerged in Europe in 2013 for the first time [11]. Currently, olive quick decline syndrome is causing a severe epidemic in southern Italy's olive growing regions. Because *X. fastidiosa* is exceptionally good at colonizing the xylem of plants either as a pathogen or commensal endophyte and it can easily undergo natural recombination, it is a serious threat to crop production in Europe and the rest of the world.

PD remains a significant problem for raisin, table, and wine grape growers. PD costs the state of California $104 million and $50 million in preventative strategies every year [12,13]. Currently, there is no effective control against PD with the exception of PD-resistant vines from a UC Davis breeding program that were released in 2019. However, these hybrid vines are wine grape varieties only [14]. Other management strategies

include eradication of vines, severe pruning, and the control of the sharpshooter vectors. PD symptoms include leaf margin discoloration quickly followed by scorching, leaf abscission from the petiole (also known as "matchstick petiole"), irregular periderm development, cane stunting, and fruit desiccation. Disease ultimately results in vine death. Growers are advised to eradicate vines if symptoms reappear after one year. Cane pruning is often an unsuccessful control method because *X. fastidiosa* cells are able to migrate to the cordons and trunk of the vine where they overwinter [15]. PD can be graft-transmitted, therefore distribution of clean material from nurseries is critical since grapevines are clonally propagated through cuttings. Another strategy is the conventional use of insecticide sprays against *X. fastidiosa* vectors, specifically sharpshooters. Coordinated imidacloprid sprays, a neonicotinoid, against sharpshooters in the Temecula Valley have been able to mitigate the disease to a profitable level but California grape growers still suffer significant economic losses. In addition, areas in the southeast region of the U.S. are still not able to grow grapes profitably [8,12,16].

X. fastidiosa is introduced into the xylem of its host by hemipteran, xylem-feeding insect vectors of the leafhopper (Cicadellidae) and spittlebug (Cercopidae) families [17,18]. There are several vectors of PD in California, two of which are the blue-green sharpshooter, *Graphocephala atropunctata*, and the glassy-winged sharpshooter, *Homalodisca vitripennis*. Both vectors are polyphagous insects, meaning that they feed on many plant species. Thus, they can transmit *X. fastidiosa* to many plant species where the bacterium can behave as a commensal endophyte or pathogen. The blue-green sharpshooter is native to riparian areas in California while the glassy-winged

sharpshooter is an invasive species and a more effective vector of the disease because of its ability to feed on both green and woody tissues and fly longer distances [15,19]. This insect can also harbor more than one *X. fastidiosa* subspecies in its mouthparts, meaning it could presumably spread more than one strain of *X. fastidiosa* [20].

When sharpshooters feed on the xylem of infected vines, *X. fastidiosa* is acquired and cells multiply to establish biofilms in the insect foregut where they are retained in a non-circulative but persistent manner. Both nymphs and adults can transmit *X. fastidiosa* but cells are lost with each molt [18,21]. Once acquired, bacterial cells dislodge from the insect cuticle and are inoculated directly into the xylem of healthy vines where they cause infection [22]. *X. fastidiosa* systemically colonizes the grapevine by using several cell wall-degrading enzymes to break down xylem vessel interconnections called pit membranes [23,24]. These structures have pores that allow water passage but these are too small for bacterial cells to go through. Within the xylem, *X. fastidiosa* forms bacterial cell aggregates and biofilms that attach to the xylem wall [25].

During early PD infection, the O antigen in *X. fastidiosa's* lipopolysaccharide (LPS) prevents the grapevine immune system from recognizing the bacterium as a biotic stress. Instead, grapevines respond to the infection as an abiotic stress, specifically drought stress, and it induces ethylene-signaling pathways that are most likely involved in the systemic overproduction of tyloses in the xylem which worsen PD symptoms [26,27]. Interestingly, *X. fastidiosa* tends to colonize approximately 15% of xylem vessels while tylose occlusions are found in at least 40% of the vessels[28]. During late infection, grapevines become starch-deprived (starch is the storage form of carbon) most

likely because photosynthesis is suppressed and genes involved in ethylene signaling and drought stress continue to be significantly up-regulated [28]. Although grapevines do not initially perceive *X. fastidiosa* as a biotic stress, Rapicavoli et al. showed that LPS-treatment prior to *X. fastidiosa* inoculation reduced PD symptoms compared to the control plants that did not receive LPS, suggesting that LPS application allowed the grapevine host to recognize *X. fastidiosa* and that a priming effect occurred [26].

Plants have developed complex mechanisms to defend themselves from constant biotic and abiotic challenges presented by a fluctuating environment. One of these mechanisms, called plant defense priming, is a tool that exploits plant 'memory' to counteract pathogens and abiotic stress. Microorganisms have signature molecules called microbe-associated molecular patterns (MAMPs), such as bacterial LPS, that can act as stimuli to induce the primed state. This 'memory' allows plants to quickly recognize pathogens and activate strong immune responses that result in disease resistance or tolerance [29–31].

X. fastidiosa forms robust biofilms in the xylem and in the insect mouthparts. Biofilms are organized bacterial aggregates enclosed in a matrix that can be self-produced. Biofilm formation begins with the reversible attachment of a planktonic cell to a surface. If the surface is suitable, the bacterial cell undergoes irreversible attachment that is mediated by cell surface charges and fimbrial and afimbrial adhesins. After attachment, cells will multiply and self-aggregate to form microcolonies. At this point, cells begin secreting polymeric substances such as extracellular polysaccharides (EPS), extracellular DNA, proteins, and lipids to form the matrix. Once the biofilm is mature, it

can be reconfigured and degraded to promote fluidity, growth of the biofilm or cell dispersal. The release from the biofilm allows planktonic cells to explore and begin the colonization of a new niche [32,33].

The development of a biofilm within the insect foregut and plant host is crucial for the PD cycle. Non-aggregating and biofilm-impaired mutant strains in *X. fastidiosa* are often hypervirulent[34–37]. It is currently hypothesized that *X. fastidiosa* forms biofilms to limit its spread in the xylem to attenuate its virulence and preventing killing its host too quickly. This would presumably increase the probability of being acquired by a sharpshooter and transmitted to a new host. It is also hypothesized that *X. fastidiosa* limits its spread by forming biofilms in a commensal relationship [9].

X. fastidiosa creates robust biofilms within its insect vector. During acquisition, *X. fastidiosa* uses type I pili and afimbrial adhesins for initial attachment to the foregut cuticle [38–41]. *X. fastidiosa's* rhamnose-rich LPS contributes to the overall cell surface charge of the bacterium that promotes adhesion between cells and the chitinous cuticle of the insect [42]. EPS, an adhesive and structural component of mature biofilms, is also involved in surface attachment and is necessary for insect transmission [43,44].

There are many advantages to forming a biofilm. The biofilm matrix can provide protection against antimicrobial peptides and reactive oxygen species and aid in nutrient and cation capture [45–48]. The architecture and viscosity of the biofilm matrix can also aid in withstanding fluid shear stress [49]. The matrix also provides a habitat where cell-to-cell proximity permits communication via quorum sensing and horizontal gene transfer [32,50]. On the contrary, there are also benefits to the planktonic lifestyle such as

exploration for nutrients and subsequent colonization of a new niche. During the late stages of the biofilm life cycle, bacterial cells use enzymes to modify or degrade matrix components (i.e. EPS, eDNA, proteins) [33,51,52]. For instance, *Pseudomonas aeruginosa* degrades its EPS alginate by using alginate lyase to cleave polymannuronic acid chains and promote cell dispersal [33]. The plant pathogenic bacterium, *Xanthomonas campestris* uses an endo-1,4-beta-mannosidase to induce the dispersal of cells from the biofilm [53]. Additionally, modifications to the biofilm can increase biofilm persistence and cell migration [49,54]. The early stages of biofilm development in *X. fastidiosa* are relatively well-characterized. However, EPS and biofilm modifications during the middle and late stages of biofilm development in *X. fastidiosa* have not been investigated.

The regulation of virulence factors required for *X. fastidiosa* colonization is density-dependent via the diffusible signaling factor (DSF) molecule [35]. High levels of DSF promote the up-regulation of surface adhesins and EPS and the down-regulation of type IV twitching motility. The opposite is observed at low levels of DSF. It is hypothesized that when cells are in high numbers inside xylem vessels, the accumulation of DSF causes *X. fastidiosa* cells to become stickier allowing them to be easily acquired by the sharpshooter [55]. Additionally, X. *fastidiosa*'s genome contains several two-component regulatory systems and response regulators that could promote fine-tuning of gene expression necessary for colonization of the plant host and insect vector [25].

X. fastidiosa has two types of pili, type I and type IV (T4P), that are polarly attached to one end of the cell [38,59]. X. fastidiosa type I pili are short, approximately

0.4 to 1 μm in length. Type I pili are involved in individual cell attachment and biofilm formation. T4P are much longer than type I, approximately 1 to 6 μm in length [38]. *X. fastidiosa* is nonflagelleted and relies upon its T4P for twitching motility [38,59]. The T4P machinery extends, binds, and retracts long filamentous appendages to pull the bacterial cell along a surface. PilB, an ATPase, drives the quick polymerization of thousands of pilin subunits called PilA to form and extend the T4P filaments while PilT, a different ATPase, drives the depolymerization of the filaments pulling the cell in a retracting movement. Besides movement, T4P can pick up extracellular DNA from the environment and participate in cell-cell aggregation, a key process for biofilm formation [56–58].

In nature, bacteria can exist attached to a surface as a part of a biofilm community where cells are continually exposed to physical forces such as fluid shear force. Recent advances in bacterial sensing have incorporated mechanics on the biophysical interactions of bacteria with their environment through their T4P and how this affects bacterial gene expression [58,60–62]. Meng et al. previously showed *X. fastidiosa* responds to unidirectional liquid flow in a microfluidic flow cell, causing the bacterium to move upstream against flow via type IV pili-mediated [59]. *X. fastidiosa* resides exclusively in the xylem and in the mouthparts of its vector where both environments expose *X. fastidiosa* to shear stress created by flow that could potentially be perceived by T4P.

X. fastidiosa continues to be a critical plant pathogenic bacterium that threatens crops globally because of its extremely broad host range and its ability to colonize the

mouthparts of many xylem-feeding insects. A better understanding of the mechanisms governing the pathogen, vector, and host interactions will help pave the way for control strategies against PD and other diseases caused by *X. fastidiosa*. As a result, this dissertation aims to further understand the mechanisms by which *X. fastidiosa* LPS primes the grapevine immune system, how *X. fastidiosa* regulates EPS production, and how T4P are involved in *X. fastidiosa* pathogenicity.

Literature Cited

1. Myles S, Boyko AR, Owens CL, Brown PJ, Grassi F, Aradhya MK, et al. Genetic structure and domestication history of the grape. Proc Natl Acad Sci U S A. 2011;108: 3530–3535.

2. Zhou Y, Massonnet M, Sanjak JS, Cantu D, Gaut BS. Evolutionary genomics of grape (Vitis vinifera ssp. vinifera) domestication. Proc Natl Acad Sci U S A. 2017;114: 11715–11720.

3. California Department of Food, Agriculture. CDFA - Statistics. [cited 22 Nov 2019]. Available: https://www.cdfa.ca.gov/statistics/

4. Amerine MA. An Introduction to the Pre-Repeal History of Grapes and Wines in California. Agric Hist. 1969;43: 259–268.

5. Pierce NB. The California Vine Disease: A Preliminary Report of Investigations. U.S. Government Printing Office; 1892.

6. Davis MJ, Purcell AH, Thomson SV. Pierce's disease of grapevines: isolation of the causal bacterium. Science. 1978;199: 75–77.

7. Wells JM, Raju BC, Hung H-Y, Weisburg WG, Mandelco-Paul L, Brenner DJ. Xylella fastidiosa gen. nov., sp. nov: Gram-Negative, Xylem-Limited, Fastidious Plant Bacteria Related to Xanthomonas spp. Int J Syst Bacteriol. 1987;37: 136–143.

8. Rapicavoli J, Ingel B, Blanco-Ulate B. Xylella fastidiosa: An examination of a re-emerging plant pathogen. Mol Plant. 2017. Available: http://onlinelibrary.wiley.com/doi/10.1111/mpp.12585/full

9. Roper C, Castro C, Ingel B. Xylella fastidiosa: bacterial parasitism with hallmarks of commensalism. Curr Opin Plant Biol. 2019;50: 140–147.

10. Simpson AJG, Reinach FC, Arruda P, Abreu FA, Acencio M, Alvarenga R, et al. The genome sequence of the plant pathogen Xylella fastidiosa. Nature. 2000;406: 151–157.

11. Saponari M, Boscia D, Nigro F, Martelli GP, Others. Identification of DNA sequences related to Xylella fastidiosa in oleander, almond and olive trees exhibiting leaf scorch symptoms in Apulia (Southern Italy). J Plant Pathol. 2013;95. Available: https://www.cabdirect.org/cabdirect/abstract/20153279019

12. Tumber K, Alston J, Fuller K. Pierce's disease costs California $104 million per year. Calif Agric. 2014. Available: http://calag.ucanr.edu/Archive/?article=ca.v068n01p20

13. Alston JM, Fuller KB, Kaplan JD, Tumber KP. Assessing the returns to R&D on perennial crops: the costs and benefits of Pierce's disease research in the California winegrape industry. Aust J Agric Resour Econ. 2015;59: 95–115.

14. UC Davis releases 5 grape varieties resistant to Pierce's disease. [cited 28 Oct 2021]. Available: https://ucanr.edu/blogs/blogcore/postdetail.cfm?postnum=39023

15. Janse JD, Obradovic A. XYLELLA FASTIDIOSA: ITS BIOLOGY, DIAGNOSIS, CONTROL AND RISKS. Supplement), S. 2010;1: 35–S1.

16. Daugherty MP, O'Neill S, Byrne F, Zeilinger A. Is Vector Control Sufficient to Limit Pathogen Spread in Vineyards? Environ Entomol. 2015;44: 789–797.

17. Hill BL, Purcell AH. Acquisition and retention of Xylella fastidiosa by an efficient vector, Graphocephala atropunctata. Phytopathology. 1995. Available: https://www.apsnet.org/publications/phytopathology/backissues/Documents/1995Articles/Phyto85n02_209.PDF

18. Almeida RPP, Blua MJ, Lopes JRS, Purcell AH. Vector Transmission of Xylella fastidiosa: Applying Fundamental Knowledge to Generate Disease Management Strategies. Ann Entomol Soc Am. 2005;98: 775–786.

19. Castro C, DiSalvo B, Roper MC. Xylella fastidiosa: A reemerging plant pathogen that threatens crops globally. PLoS Pathog. 2021;17: e1009813.

20. Stenger DC, Burbank LP, Krugner R, Sisterson MS. Individual field-collected glassy-winged sharpshooter vectors harbor sequences from two Xylella fastidiosa subspecies. Eur J Plant Pathol. 2019;155: 329–338.

21. Purcell AH, Finlay AH. Evidence for noncirculative transmission of Pierce's disease bacterium by sharpshooter leafhoppers. Phytopathology. 1979. Available: https://www.apsnet.org/publications/phytopathology/backissues/Documents/1979Articles/Phyto69n04_393.PDF

22. Backus EA, Shugart HJ, Rogers EE, Morgan JK, Shatters R. Direct Evidence of Egestion and Salivation of Xylella fastidiosa Suggests Sharpshooters Can Be "Flying Syringes." Phytopathology. 2015;105: 608–620.

23. Roper MC, Greve LC, Warren JG, Labavitch JM, Kirkpatrick BC. Xylella fastidiosa requires polygalacturonase for colonization and pathogenicity in Vitis vinifera grapevines. Mol Plant Microbe Interact. 2007;20: 411–419.

24. Pérez-Donoso AG, Sun Q, Roper MC, Greve LC, Kirkpatrick B, Labavitch JM. Cell wall-degrading enzymes enlarge the pore size of intervessel pit membranes in healthy and Xylella fastidiosa-infected grapevines. Plant Physiol. 2010;152: 1748–1759.

25. Voegel TM, Doddapaneni H, Cheng DW, Lin H, Stenger DC, Kirkpatrick BC, et al. Identification of a response regulator involved in surface attachment, cell-cell aggregation, exopolysaccharide production and virulence in the plant pathogen Xylella fastidiosa. Mol Plant Pathol. 2013;14: 256–264.

26. Rapicavoli JN, Blanco-Ulate B, Muszyński A, Figueroa-Balderas R, Morales-Cruz A, Azadi P, et al. Lipopolysaccharide O-antigen delays plant innate immune recognition of Xylella fastidiosa. Nat Commun. 2018;9: 390.

27. Sun Q, Sun Y, Walker MA, Labavitch JM. Vascular occlusions in grapevines with Pierce's disease make disease symptom development worse. Plant Physiol. 2013;161: 1529–1541.

28. Ingel B, Reyes C, Massonnet M, Boudreau B, Sun Y, Sun Q, et al. Xylella fastidiosa causes transcriptional shifts that precede tylose formation and starch depletion in xylem. Mol Plant Pathol. 2020. doi:10.1111/mpp.13016

29. Westman SM, Kloth KJ, Hanson J, Ohlsson AB, Albrectsen BR. Defence priming in Arabidopsis - a Meta-Analysis. Sci Rep. 2019;9: 13309.

30. Conrath U, Beckers GJM, Langenbach CJG, Jaskiewicz MR. Priming for enhanced defense. Annu Rev Phytopathol. 2015;53: 97–119.

31. Mauch-Mani B, Baccelli I, Luna E, Flors V. Defense Priming: An Adaptive Part of Induced Resistance. Annu Rev Plant Biol. 2017;68: 485–512.

32. Flemming H-C, Wingender J, Szewzyk U, Steinberg P, Rice SA, Kjelleberg S. Biofilms: an emergent form of bacterial life. Nat Rev Microbiol. 2016;14: 563–575.

33. Boyd A, Chakrabarty AM. Role of alginate lyase in cell detachment of Pseudomonas aeruginosa. Appl Environ Microbiol. 1994;60: 2355–2359.

34. Gouran H, Gillespie H, Nascimento R, Chakraborty S, Zaini PA, Jacobson A, et al. The Secreted Protease PrtA Controls Cell Growth, Biofilm Formation and Pathogenicity in Xylella fastidiosa. Sci Rep. 2016;6: 31098.

35. Newman KL, Almeida RPP, Purcell AH, Lindow SE. Cell-cell signaling controls Xylella fastidiosa interactions with both insects and plants. Proc Natl Acad Sci U S A. 2004;101: 1737–1742.

36. Burbank LP, Stenger DC. The DinJ/RelE Toxin-Antitoxin System Suppresses Bacterial Proliferation and Virulence of Xylella fastidiosa in Grapevine. Phytopathology. 2017;107: 388–394.

37. Guilhabert MR, Hoffman LM, Mills DA, Kirkpatrick BC. Transposon mutagenesis of Xylella fastidiosa by electroporation of Tn5 synaptic complexes. Mol Plant

Microbe Interact. 2001;14: 701–706.

38. Li Y, Hao G, Galvani CD, Meng Y, De La Fuente L, Hoch HC, et al. Type I and type IV pili of Xylella fastidiosa affect twitching motility, biofilm formation and cell-cell aggregation. Microbiology. 2007;153: 719–726.

39. Feil H, Feil WS, Lindow SE. Contribution of Fimbrial and Afimbrial Adhesins of Xylella fastidiosa to Attachment to Surfaces and Virulence to Grape. Phytopathology. 2007;97: 318–324.

40. Guilhabert MR, Kirkpatrick BC. Identification of Xylella fastidiosa Antivirulence Genes: Hemagglutinin Adhesins Contribute to X. fastidiosa Biofilm Maturation and Colonization …. Mol Plant Microbe Interact. 2005. Available: http://apsjournals.apsnet.org/doi/abs/10.1094/MPMI-18-0856

41. De La Fuente L, Montanes E, Meng Y, Li Y, Burr TJ, Hoch HC, et al. Assessing adhesion forces of type I and type IV pili of Xylella fastidiosa bacteria by use of a microfluidic flow chamber. Appl Environ Microbiol. 2007;73: 2690–2696.

42. Rapicavoli JN, Kinsinger N, Perring TM, Backus EA, Shugart HJ, Walker S, et al. O antigen modulates insect vector acquisition of the bacterial plant pathogen Xylella fastidiosa. Appl Environ Microbiol. 2015;81: 8145–8154.

43. Roper MC. The characterization and role of Xylella fastidiosa plant cell wall degrading enzymes and exopolysaccharide in Pierce's disease of grapevine. ProQuest. 2006.

44. Sahoo PK, Janissen R, Monteiro MP, Cavalli A, Murillo DM, Merfa MV, et al. Nanowire Arrays as Cell Force Sensors To Investigate Adhesin-Enhanced Holdfast of Single Cell Bacteria and Biofilm Stability. Nano Lett. 2016;16: 4656–4664.

45. Cuzzi B, Cescutti P, Furlanis L, Lagatolla C, Sturiale L, Garozzo D, et al. Investigation of bacterial resistance to the immune system response: cepacian depolymerisation by reactive oxygen species. Innate Immun. 2012;18: 661–671.

46. Oubekka SD, Briandet R. Correlative time-resolved fluorescence microscopy to assess antibiotic diffusion-reaction in biofilms. Antimicrob Agents Chemother. 2012. Available: http://aac.asm.org/content/56/6/3349.short

47. Horsman SR, Moore RA, Lewenza S. Calcium chelation by alginate activates the type III secretion system in mucoid Pseudomonas aeruginosa biofilms. PLoS One. 2012;7: e46826.

48. Yu S, Wei Q, Zhao T, Guo Y, Ma LZ. A Survival Strategy for Pseudomonas aeruginosa That Uses Exopolysaccharides To Sequester and Store Iron To Stimulate Psl-Dependent Biofilm Formation. Appl Environ Microbiol. 2016;82: 6403–6413.

49. Rupp CJ, Fux CA, Stoodley P. Viscoelasticity of Staphylococcus aureus biofilms in response to fluid shear allows resistance to detachment and facilitates rolling migration. Appl Environ Microbiol. 2005;71: 2175–2178.

50. Marks LR, Reddinger RM, Hakansson AP. High levels of genetic recombination during nasopharyngeal carriage and biofilm formation in Streptococcus pneumoniae. MBio. 2012;3. doi:10.1128/mBio.00200-12

51. Manuel S, Ragunath C, Sait H. Role of active-site residues of dispersin B, a biofilm-releasing β-hexosaminidase from a periodontal pathogen, in substrate hydrolysis. FEBS J. 2007. Available: http://onlinelibrary.wiley.com/doi/10.1111/j.1742-4658.2007.06121.x/full

52. Allison DG, Ruiz B a., Jose CS, Jaspe A, Gilbert P. Extracellular products as mediators of the formation and detachment of Pseudomonas £uorescens bio¢lms. FEMS Microbiol Lett. 1998;167: 179–184.

53. Dow JM, Crossman L, Findlay K, He Y-Q, Feng J-X, Tang J-L. Biofilm dispersal in Xanthomonas campestris is controlled by cell–cell signaling and is required for full virulence to plants. Proceedings of the National Academy of Sciences. 2003;100: 10995–11000.

54. Whitfield GB, Marmont LS, Howell PL. Enzymatic modifications of exopolysaccharides enhance bacterial persistence. Front Microbiol. 2015;6: 471.

55. Chatterjee S, Almeida RPP, Lindow S. Living in two Worlds: The Plant and Insect Lifestyles of Xylella fastidiosa. Annu Rev Phytopathol. 2008;46: 243–271.

56. Burdman S, Bahar O, Parker JK, De La Fuente L. Involvement of Type IV Pili in Pathogenicity of Plant Pathogenic Bacteria. Genes . 2011;2: 706–735.

57. Chang Y-W, Rettberg LA, Treuner-Lange A, Iwasa J, Søgaard-Andersen L, Jensen GJ. Architecture of the type IVa pilus machine. Science. 2016;351: aad2001.

58. Craig L, Forest KT, Maier B. Type IV pili: dynamics, biophysics and functional consequences. Nat Rev Microbiol. 2019;17: 429–440.

59. Meng Y, Li Y, Galvani CD, Hao G, Turner JN, Burr TJ, et al. Upstream migration of Xylella fastidiosa via pilus-driven twitching motility. J Bacteriol. 2005;187: 5560–5567.

60. Persat A, Inclan YF, Engel JN, Stone HA, Gitai Z. Type IV pili mechanochemically regulate virulence factors in Pseudomonas aeruginosa. Proc Natl Acad Sci U S A. 2015;112: 7563–7568.

61. Lee CK, de Anda J, Baker AE, Bennett RR, Luo Y, Lee EY, et al. Multigenerational

memory and adaptive adhesion in early bacterial biofilm communities. Proc Natl Acad Sci U S A. 2018;115: 4471–4476.

62. Rodesney CA, Roman B, Dhamani N, Cooley BJ, Katira P, Touhami A, et al. Mechanosensing of shear by Pseudomonas aeruginosa leads to increased levels of the cyclic-di-GMP signal initiating biofilm development. Proceedings of the National Academy of Sciences. 2017;114: 5906–5911.

Chapter II

Xylella fastidiosa Elicits an Early, Synchronous Response in Local and Systemic Tissue of Lipopolysaccharide-Primed Grapevines

Abstract

Plant defense priming is an adaptive mechanism that improves plant defense by enhancing activation of induced defense responses following pathogen challenge. Microorganisms have signature molecules called pathogen or microbe-associated molecular patterns (PAMPs/MAMPs) that act as stimuli to induce the primed state. The bacterium, *Xylella fastidiosa*, is the causal agent of Pierce's disease of grapevine and is limited to the xylem, a tissue compartment that is primarily non-living at maturity, but mounts a robust defense response to xylem invading pathogens. Vitis vinifera grapevines pre-treated with the *X. fastidiosa* MAMP, lipopolysaccharide (LPS), as a priming stimulus had a significant decrease in both external and internal symptoms of PD as well as the rate of overall disease progression indicating that LPS primes the grapevine immune response to better defend itself against future challenge with the *X. fastidiosa* pathogen. This enhanced defense phenotypically manifested into a suppression of both internal and external symptoms. Differential gene expression analysis revealed major transcriptomic reprogramming in primed vines in response to pathogen challenge at the point of inoculation and 20 nodes (1.5m) distal to the point of inoculation when compared to naive, untreated vines. Furthermore, a weighted gene co-expression analysis identified modules of co-expressed genes common to the point inoculation and 20 nodes above indicating that primed vines mount a temporally and spatially synchronous response to initial pathogen challenge. These responses included genes involved in signal perception, signal transduction, as well as auxin-related pathways.

Introduction

Plants integrate immune 'memory' into their biotic and abiotic defense repertoire. This mechanism, called plant defense priming, conditions plants for enhanced defense against biotic or abiotic stressors. Defense priming consists of three phases: the naive state, the priming phase, and the post-challenge primed state. In the naive phase, the plant has yet to be exposed to the priming stimulus that activates the primed state. The priming phase occurs when plants are exposed to a priming stimulus and the plant reprograms its transcriptome to enable rapid recognition of future pathogen encounters. Examples of biotic priming stimuli include pathogen or microbe-associated molecular patterns (PAMPs/MAMPs), beneficial microbes or chemical signals. Abiotic stimuli include short exposures to cold or drought. During the post-challenge primed state, the plant initiates rapid and strong immune responses to an invading pathogen that confers tolerance or resistance to the pathogen [1–4]. The molecular mechanisms underlying priming include rapid induction of components of the plant defense response such as metabolites, hormones, chromatin modification, increased levels of dormant MAPKs and PRRs and antimicrobial compounds among others [2,4–8]. In this study we focused on the transcriptional response during the post-challenge primed state in grapevines pre-treated with the PAMP/MAMP priming stimulus, lipopolysaccharide (LPS), purified from the bacterium, *Xylella fastidiosa*, and then challenged with the cognate whole live cell inoculum of *X. fastidiosa*.

X. fastidiosa is a Gram-negative, xylem-limited bacterium with a broad host range that includes economically important crops like grape, olive and citrus [9–11]. *X.*

fastidiosa subsp. fastidiosa, the causal agent of Pierce's Disease (PD) of grapevine, is responsible for millions in economic losses in the state of California alone [12]. All Vitis vinifera cultivars of wine, raisin and table grapes are susceptible to PD. External symptoms of PD include marginal leaf scorching, berry desiccation, abnormal leaf abscission, irregular periderm development and overall vine stunting [13]. Internal symptoms in the xylem include the development of an extensive amount of tyloses and the production of pectin gels and crystals. Overproduction of tyloses is a hallmark symptom of PD and these balloon-shaped structures are produced by xylem parenchyma cells to block air embolisms and movement of pathogens within the xylem. However, in response to *X. fastidiosa* infection, grapevines produce prolific numbers of tyloses in the xylem, which exacerbates PD symptoms and causes a detrimental reduction in hydraulic conductivity of the vine [14,15].

Notably, prior to any symptom development, *X. fastidiosa* has a relatively long latent period (approximately six-eight weeks) in grapevine greenhouse bioassays. However, major transcriptional reprogramming during the very early phases of disease before internal and/or external symptoms develop [15,16]. Grapevines mount a quantifiable and significant differential transcriptional response to *X. fastidiosa* in both local and systemic locations as early as four hours post-inoculation. Because of the early timing and the initial slow replication and movement of *X. fastidiosa* within the xylem, the observed systemic responses likely occur in absence of direct contact with the pathogen suggesting a signal transduction mechanism that emanates spatially over long distances as far as 1.5 meters away from the initial point of pathogen inoculation [15,16].

Lipopolysaccharide (LPS) comprises a large proportion of the outer membrane of Gram-negative bacteria and is a highly immunogenic macromolecule [13,17,18]. LPS acts as a MAMP/PAMP in both plant and animal systems. *X. fastidiosa* LPS and its derivatives are potent elicitors of the grapevine immune system and trigger defense pathways associated with a reactive oxygen species burst and salicylic acid (SA) production among other defense-related responses. Furthermore, pre-treating with LPS and then challenging with live *X. fastidiosa* cells resulted in lower PD symptoms at 12 weeks post-inoculation. These exciting and compelling findings indicated that a defense priming mechanism likely plays a role in conferring tolerance to PD [16]. Here we expanded the time frame of our original experimental design described in Rapicavoli et. al (2018) to determine the mechanisms underlying defense priming in grapevines.

By integrating genome-wide transcriptional profiling coupled with phenotyping of internal and external disease symptoms and bacterial titer, we monitored early temporal and spatial responses to *X. fastidiosa* in primed vines. Our findings indicate that primed grapevines undergo a major transcriptional reprogramming very early following pathogen challenge and that the number of differentially expressed genes increases over time and space in primed vines but not in naive vines. Network co-expression analysis identified sets of co-expressed genes common to the local point of pathogen inoculation and systemic location 20 nodes above and showed that many of these genes were synchronously modulated. This synchronicity affected the transcriptional modulation of genes involved in signal perception, signal transduction, cell wall modification and auxin-related pathways. Moreover, these transcriptional changes ocurred very early after

pathogen challenge and preceded any symptoms that developed over the course of the 22-week experiment.

Materials and Methods

Bacterial strain and growth conditions. *X. fastidiosa* subsp. *fastidiosa* was grown on PD3 solid medium for 5 days at 28°C for grapevine inoculations and LPS extraction.

LPS extraction. LPS was extracted from *X. fastidiosa* cells according to Rapicavoli et al. and treated with proteinase K. LPS was quantified using the Purpald Assay and its concentration was adjusted to 50 μg/mL for priming experiments[16,57].

Grapevine inoculations for disease bioassays and transcriptomic analyses. A total of 108 *Vitis vinifera* 'Cabernet sauvignon' grapevines (kindly provided by Foundation Plant Services, UC Davis)were used for plant defense priming and RNAseq experiments (27 plants per treatment). Grapevines were inoculated with 40 μL of LPS (50 μg/mL) and challenged with 40 μL *X. fastidiosa* in 1X PBS (10^8 CFU/mL) four hours later using the needle-inoculation method described by Hill and Purcell. For the control plants, grapevines were inoculated with either LPS and 1X PBS, H_2O and *X. fastidiosa*, or H_2O and 1X PBS. Grapevines were randomized throughout the greenhouse. PD symptom development was evaluated over 22 weeks post-inoculation using a standard PD rating scale of 0 to 5 [58].

Disease development and survival analyses. The longitudinal disease ratings are discrete, non-Gaussian, observations. Therefore, a Generalized Estimating Equations (GEE) model was used for their analysis [59,60]. The fixed effects structure of the GEE model included treatment effects, time trend effects, and interaction effects between the treatment effects and the time trend effects. The time trend effects were captured with a linear spline that included a knot at 10 weeks. Empirical standard error estimates and asymptotic Score tests were used to draw inferences from the fitted model, including construction of 95% confidence intervals for the means at each time point, and estimates and hypothesis tests of treatment contrasts that compared the rates of progression across treatments, and the effect of water versus LPS as the first injection. AUDPC and survival analysis were performed using the R scripts provided by Schandry (2017) under the supplemental data [61].

Quantification of *X. fastidiosa* titer. Three petioles were collected from both the point of inoculation and 20 nodes above in grapevines according to Ginnan et al. 2020 with some modifications. Specifically, petioles were lyophilized for about 24 hours and transferred to a 5 mL tube with a steel grinding ball (size ⅜ in., BC Precision). Samples were pulverized using a Geno/Grinder machine (2010 model, SPEX SamplePrep) at 1680 rpm for 40s. Then, 2 mL of guanidine buffer (4M guanidine thyocyanate, 0.2 M NaOAc, 25 mM EDTA, 2.5% w/v PVP-40, pH 5) were added to each sample and mixed thoroughly. Samples were incubated at 4°C for 15 min. and centrifuged at 4°C for 45 min., 20,000xg. 300 µL of the supernatant was collected for DNA extraction using

MagMAX™-96 DNA Multi-Sample Kit and MagMAX Express-96 Deep Well Magnetic Particle Processor with the "441302ForPlants" protocol (Invitrogen™, Cat. No. 4413021). Total DNA was quantified using a Qubit™ 4 Fluorometer (Invitrogen™, Cat. No. Q33226) and Qubit™ dsDNA HS Assay Kit (Invitrogen™, Cat. No. Q32854). The extracted DNA was used for absolute quantification qPCR to determine *X. fastidiosa* titer using the protocol described in Deyett et al. 2019.

Tylose quantification. Three stem internodes closest to the point of inoculation were collected per grapevine and stored in 80% ethanol, 4°C. A microtome (Hacker Instruments and Industries Inc., Winnsboro, SC, USA) was used to prepare 100 µm thick cross sections. These were rinsed with water, stained with 0.05% Toluidine Blue O, and rinsed twice with water. Cross sections were mounted on glass slides in 50% glycerol. The total number of empty and tylose-occluded xylem vessels were counted using a Leica DM4000 upright microscope (Leica Microsystems GmbH, Wetzlar, Germany).

Transcriptional analysis. For the RNA-Seq analysis, three petioles were harvested at 4 h, 24 h, and 48 h post-*X. fastidiosa* challenge from the point of inoculation and 20 nodes above the point of inoculation. The petioles were immediately frozen in liquid nitrogen and stored at -80°C. Nine plants were used per time point for each treatment. For each treatment and time point, the petioles of three plant replicates were pooled to build one biological replicate for a total of three biological replicate cDNA libraries. RNA extraction and cDNA preparation were done according to Rapicavoli et al. (2018).

cDNA libraries were sequenced using an Illumina HiSeq4000 sequencer (DNA Technologies Core, University of California, Davis, California, USA) as single-end 100-bp reads (Illumina, CA, USA). Sequences were deposited to the National Center for Biotechnology Information's Gene Expression Omnibus (GEO) and are accessible through GEO. Illumina reads were trimmed using Trimmomatic v.0.36 (Bolger et al., 2014) with the options LEADING:3 TRAILING:3 SLIDINGWINDOW:10:20 CROP:100 MINLEN:36. Trimmed single-end reads were mapped onto the predicted protein-coding sequences of *V. vinifera* 'PN40024' (version V1 from http://genomes.cribi.unipd.it/grape/) using Bowtie2 v.2.3.4.1 (Langmead and Salzberg, 2012) with parameters: -q -end-to-end -sensitive -no-unal. Counts of reads mapping uniquely onto the grape reference transcriptome (i.e., with Q > 30) were extracted using sam2counts.py v.0.91 (https://github.com/vsbuffalo/sam2counts). The Bioconductor package DESeq2 v.1.16.1 (Love et al., 2014) was used for read count normalization and for statistical testing of differential gene expression. The VitisNet functional annotations were used to assign grape genes to functional categories (Grimplet et al., 2009). Enrichment analyses of grape biological functions were computed in R using the classic Fisher method (P-value ≤ 0.05).

Weighted Gene Co-expression Analysis. Our differentially expressed genes data for WGCNA was formatted as described by Amrine et al. and Massonnet et al. [22,62]. A soft-thresholding power of 18 with a scale-free model fitting index of $R^2 > 0.42$ for primed local, $R^2 > 0.70$ for primed systemic, $R^2 > 0.90$ for naive local, and $R^2 > 0.60$ for

naive systemic networks (Figures S2.3). A relatively large minimum module size of 30, a medium sensitivity deep split of 2 to cluster splitting, and a 0.25 cut height for merging modules. These parameters were used to build all four networks (Figures 2.7 and S2.5). To determine significant module-time point associations, we calculated the correlation and their P-values for each module eigengene and time point combination (Figure S2.6). To identify significant module overlap between primed local and systemic responses for primed and naive treatments, we created a contingency table and calculated P-values using Fisher's exact test ($P \leq 0.01$) for each module intersection. The VitisNet functional annotations were used to assign grape genes to functional categories [63]. Enrichment analyses of grape biological functions were computed in R using the classic Fisher method ($P \leq 0.01$).

Results

LPS treatment prior to *X. fastidiosa* inoculation significantly reduces Pierce's disease symptoms in grapevines. Grapevines that were pre-treated with LPS (primed) prior to *X. fastidiosa* challenge exhibited significantly fewer PD symptoms over the course of the 22-week disease bioassay. We analyzed the disease severity data in three different ways to determine (i) rate of symptom progression, (ii) total disease severity of disease over time and (iii) endpoint survival rate in primed vs. naïve vines. To compare the rate of symptom progression between treatments over time, we used a generalized estimated equations (GEE) model. The model indicated that primed vines developed symptoms at a significantly slower rate than naive vines (Figure 2.2B). To quantify total

disease severity over time, we calculated area under the disease progress curve (AUDPC), which indicated that the primed vines had significantly less overall disease over the course of the entire experiment (Figure S2.1). Lastly, we conducted a vine survival analysis using the Survival R package [19]. This analysis determines the time it takes for an event of interest to occur within a population over time. The event of interest was set to a plant scoring a 2 in the PD rating scale because vines that enter this phase never revert to a score of 1 or 0 and are destined to progress to a 5 (a dead or dying vine) (Figure S2.2A). Following 7 weeks post-inoculation (wpi), the survival probability estimates were significantly higher in primed vines than naive vines indicating that primed vines have a higher chance of surviving PD than naïve vines. Specifically, the survival probability for naive plants was 0% at 10 wpi, meaning that a vine under these conditions will succumb to PD after this point. Primed plants had a survival probability of 12% at 10 wpi and for the remainder of the disease trial (Figure S2.2B).

LPS pre-treatment results in lower *X. fastidiosa* bacterial titer. We quantified *X. fastidiosa* populations in primed and naive grapevines collected from the point of inoculation (local) and 20 nodes above the point of inoculation (systemic). *X. fastidiosa* titer was significantly lower in both local and systemic petioles of primed plants than in naive plants indicating that pre-treatment with LPS inhibits *X. fastidiosa* growth *in planta*.

Primed vines have fewer xylem vessels that are occluded with tyloses. Tyloses are a hallmark internal symptom in the xylem of PD-infected grapevines [14]. Qualitatively, primed vines produced no or a very small number of tyloses, whereas naive plants had many xylem vessels that were heavily occluded with tyloses at the end of the disease bioassay (Figure 2.3A). Quantitatively, primed vines had a significantly lower percentage of vessels occluded with tyloses as compared to naïve vines (Figure 2.3B). Negative control vines that were treated with water or LPS only prior to PBS buffer inoculation did not develop any vessel occlusions.

Primed grapevines have a differential transcriptional response to pathogen challenge than naive grapevines. Because LPS pre-treatment resulted in the observed systemic phenotypes of disease suppression, reduced bacterial titer and fewer internal responses to *X. fastidiosa* (tyloses), we sought to better understand local and systemic host responses and their temporal patterns during early pathogen challenge in both LPS-primed and naive grapevines. To accomplish this, we profiled the transcriptomes of local petioles (those closest to the point of inoculation (POI)) and systemic petioles (20 nodes above the POI) in primed and naive vines at 4, 24, and 48 hours after challenging with *X. fastidiosa*. Using RNA-Seq analysis, we obtained an average of 11.7 million high-quality reads that aligned to the grapevine transcriptome. Overall, in local petioles, there were more differentially expressed genes (DEGs, $P < 0.05$) in primed vines (5,408 DEGs) as compared to those in naive vines (3,543 DEGs) across all time points. The number of DEGs in naive, local petioles decreased after 4 hpi, whereas the number of DEGs in local

petioles of primed vines was relatively stable over time with a slight decrease at 48 hpi (Figure 2.4A). At 20 nodes above the point of inoculation (systemic) across all timepoints, there were 9,823 DEGs in local petioles of primed vines and 7,081 DEGs in local petioles of naive vines. The number of DEGs increased over time in systemic petioles of primed vines while the number of DEGs in systemic petioles of naïve vines decreased over time, similar to the decrease in DEGs in local petioles of naive vines. Across all time points, systemic petioles primed and naive vines each had 3,853 and 1,814 unique DEGs, respectively (Figure 2.4B).

To determine the enriched functional categories among the significant DEGs in local and systemic petioles of primed and naive vines, we utilized an enrichment analysis (Fisher's exact test, $P < 0.05$). The category "WRKY family transcription factor" was significantly enriched among up-regulated genes in local petioles of primed plants and not in naive at 4 hpi. Among the eleven WRKY transcription factors in this category, seven of them are implicated in response to pathogens. These include WRKY18, WRKY22, and WRKY53 (*VIT_04s0008g05760*, *VIT_15s0046g02190*, and *VIT_15s0046g01140*) (Figure 2.5A) [20,21]. However, among the up-regulated genes in systemic petioles at 4 hpi, the "WRKY family transcription factor" category was enriched in both primed (7 genes) and naive (8 genes) vines and included the genes, *WRKY11*, *WRKY18*, and *WRKY53* (*VIT_04s0069g00920*, *VIT_04s0008g05760*, and *VIT_15s0046g01140*). *WRKY18* and *WRKY53* are implicated in biotic stress [20,21]. Pathogen challenge induces an early (4 hpi), localized WRKY-modulated response in primed vines that is absent in naive vines. However, in systemic locations, pathogen

challenge induces a similar WRKY-modulated response in systemic locations in both primed and naive vines. This suggests that infection with *X. fastidiosa* potentiates induction of a complex network of WRKYs in both local and systemic locations that is both dependent and independent of LPS pre-treatment.

At 48 hpi, the functional category, "Cell wall organization and biogenesis" was significantly enriched in both local and systemic petioles (65 and 57 genes, respectively) of primed vines but not in naive vines. The up-regulated DEGs in this category that were enriched in both primed local and systemic petioles include several pectin esterases, expansins, polygalacturonases, as well as cellulose synthases. Cell wall modification and rearrangement is a typical response to infection in woody plants and is linked to tylose production [13,15,22].

Among the down-regulated genes, the categories "Photosynthesis" and "Drought stress" were enriched in primed systemic petioles at 4 hpi and 48 hpi. The genes belonging to the "Photosynthesis" category included genes are involved in the Calvin cycle and in Photosystems I and II. The down-regulation of photosynthesis-related genes suggests that primed vines reduce photosynthesis in response to pathogen challenge. Down-regulation of photosynthesis-related genes was also previously observed in *X. fastidiosa*-infected grapevines as well as grapevines infected with the vascular fungal pathogen, *Neofusicoccum parvum* [15,22,23].

Responses that occurred solely in naive systemic tissue included "Abiotic stress" and "Ethylene signaling." Ethylene signaling is linked to tylose formation.

Primed vines have a temporally and spatially synchronous response to *X. fastidiosa* challenge. Primed vines had a higher number of DEGs that were shared between local and systemic petioles than in naive vines. Specifically, we identified a total of 2,777 genes that were differentially expressed in both local and systemic petioles across all three time points (approximately 45% of total DEGs) in primed vines compared to 1,453 genes (approximately 26% of total DEGs) for naive vines (Figures 2.6A and C). We then sorted these DEGs to determine the number of DEGs that were shared between both local and systemic tissue at two or more timepoints for both treatments (Figures 2.6B & C). In primed vines, this included 157 genes at 4 hpi, 246 genes at 24 hpi, and 332 genes at 48 hpi (Figures 2.6B & C, highlighted with an asterisk). On the contrary, naive vines had a lower number of DEGs in common. This suggested a temporally and spatially synchronous response to pathogen challenge in primed vines, which prompted us to perform a weighted gene co-expression network analysis (WGCNA, R package) to define groups of synchronously co-expressed genes (modules) that had similar temporal patterns of up- and down-regulation in local and systemic locations.

In primed plants, the WGCNA analysis identified 6 modules in the co-expression network of local DEGs and 9 modules in the co-expression network of systemic DEGs (Figures 2.7A and B). For naive plants, we found 5 modules in the co-expression network of local DEGs and 6 in the co-expression network of systemic DEGs (Figure S2.5A and B). Each individual module was assigned a unique color identifier that was used for downstream analyses in the WGCNA pipeline. Next, we calculated module eigengenes (gene expression profile representative) for each network to determine the time point

where each group of co-expressed genes occurred (Figure S2.6). To determine if the network modules between local and systemic were preserved and reproducible, we calculated the $Z_{summary}$, that summarizes several density preservation and connectivity statistics. Our $Z_{summary}$ results indicated the majority of the primed modules were strongly preserved with a few that were moderately preserved (Figures S2.7A and B) [24]. We obtained similar results for the naive modules with the exception of two naive local modules that were not preserved, "green" and "turquoise" (Figures S2.7C and D).

To identify significant co-expressed genes shared between primed local and systemic responses at each time point, we created a contingency table and calculated P-values using Fisher's exact test ($P < 0.01$) for each module (Figure S2.8). The analysis indicated 13 significant overlaps between local and systemic modules in primed plants. Moreover, six of these overlaps occurred at the same time point indicating a synchronicity in their up- or down-regulation patterns that spanned from the POI to approximately 1.5 m (20 nodes) distal from the POI. Two of the six synchronous overlaps corresponded to the 4 hpi time point, two to the 24 hpi time point, and two to the 48 hpi time point (Figure 2.7C). A total of 684 genes were found in synchronous overlapping modules (Table 1). A similar analysis in naive plants indicated 11 significant overlaps between local and systemic modules. Three of these synchronous overlaps occurred at the same time point: one at the 4 hpi time point, one at the 24 hpi time point, and one at the 48 hpi time point (a total of 356 genes) (Figure 2.7D and Table S2.1). These results indicate that primed vines have more synchronicity between local and systemic responses to *X. fastidiosa* challenge as compared to naive vines.

To get a better understanding of what comprised the synchronicity of the host response to pathogen challenge, we performed a FCT analysis (Fisher's exact test, $P < 0.01$) for all significant overlaps occurring at the same time points. At 4 hpi, co-expressed genes shared in primed local and systemic modules were enriched in the category "Protein Kinase", which included various types of kinases such as two leucine-rich repeat (LRR) receptor-like kinases (*VIT_06s0004g03930* and *VIT_14s0108g00280*) and two wall-associated kinases (WAKs; *VIT_14s0006g02600* and *VIT_17s0000g03340*). These WAKs participate in plant defense as Damage Associated Molecular Patterns (DAMPs) receptors[25–29]. Additionally, the categories "Auxin signaling" and "Auxin transport" were enriched (Table 1). Auxin is classically studied as a growth promoting phytohormone, however there are several studies reporting its function in immunity against necrotrophic pathogens [30,31].

At 24 hpi, the functional category "CCAAT family transcription factor-HAP5-type" was enriched in both locations and included two Mtn21-like genes encoding for bidirectional transporters of auxin (*VIT_01s0026g00360* and *VIT_01s0026g00520*) and a transcription factor (*VIT_14s0128g00250*) involved in drought tolerance and resistance against *Xanthomonas oryzae* in rice [32].

The largest module overlap group was "Blue-Blue" with 222 up-regulated genes and occurred at the 48 hpi timepoint. The enriched categories within this module overlap were diverse, and included cell wall modification, photosynthesis, transcription, and signaling peptides/molecules (Table 1). The functional categories "Signaling peptide" and "Signaling molecules" included two overlapping genes that were up-regulated in both

local and systemic tissues at 48 hpi, a phytosulfokine receptor (PSKR; *VIT_09s0002g00080*) and a rapid alkalinization factor 33 (RALF33; *VIT_14s0060g02150*; Table 1). Phytosulfokines (PSKs) are small sulfated peptides involved in plant development and immunity, some of which are considered DAMPs, that bind to receptors as a response to environmental cues. Rapid alkalinization factor 33 (RALF33) is involved in the alkalinization of the plant apoplast and interacts with PSK1/PSKs to trigger a cytosolic Ca^{2+} influx that results in auxin-dependent immune response [31–34].

Two functional categories associated with the cell wall, "Cell wall structural protein" and "Cell wall organization and biogenesis", were also among the overlapping genes and included genes involved in cell wall modification/strengthening, some of which induced in other systems following pathogen perception[15,16,22]. These included several fascilin arabinogalactan protein genes, two hydroxyproline-rich glycoprotein genes, and two extensin genes, one of them containing a leucine rich repeat domain (*VIT_00s0533g00050* and *VIT_11s0016g02900*) (Table 1). These three types of proteins belong to the hydroxyproline-rich glycoprotein superfamily and participate in various plant functions including plant-microbe interactions [35–37]. For example, plant extensins can modify the structural and mechanical properties of cell walls to restrict pathogen movement. Leucine-rich repeat extensins or LRXs, are embedded in the plant cell wall and monitor cell wall integrity. LRXs have high-affinity binding sites for rapid alkalinization factor peptides (RALFs) that regulate plant development, cell wall integrity, and stress responses [36,38]. The enriched functional categories that were

synchronously co-expressed between local and systemic locations in naive plants can be found in the Supplementary Table 1.

Discussion

Vines that were initially exposed to the priming stimulus, LPS, and then challenged with the cognate pathogen four hours later had a higher number of DEGs and a higher degree of synchronicity between the transcriptional responses occurring in local and systemic locations, whereas there was a more disconnected transcriptional response to pathogen challenge in naive vines between local and systemic locations. This indicated an early, persistent and spatial differential response to pathogen challenge in primed vines that phenotypically culminated in less overall disease and a higher vine survival probability than in naive vines over the course of the 22-week disease bioassay. Internally, primed vines also exhibited fewer internal xylem blockages, namely, tyloses. These balloon-shaped structures are produced by neighboring living xylem parenchyma and protrude into the xylem to restrict the movement of air embolisms and pathogens inside the xylem vessels (Figure 2.3A) [14,15]. However, in susceptible grapevines, tyloses fail to stop the systemic spread of *X. fastidiosa* within the xylem and actually exacerbate PD symptoms by blocking water transport and decreasing hydraulic conductivity [14]. Tylose production is linked to ethylene signaling in grapevines and other plants [15,39,40]. Interestingly, in primed vines there was a delay in enrichment of genes related to the “Ethylene signaling” pathway in local petioles and a non-enrichment in systemic petioles when compared to naive vines. In contrast, the ethylene signaling

pathway was significantly enriched as early as 4 hpi in both local and systemic tissues in naive vines. Ethylene are both linked to tylose production [41]. Our data indicate that transcriptional responses related to ethylene signaling pathways precede tylose production in PD-infected vines suggesting that disrupting the timing of the induction of the ethylene pathways early in the infection process may mitigate downstream tylose over-production and lead to less severe PD symptoms.

From a spatial perspective early in the infection process, DEGs increased over time in systemic locations in primed vines but not in naive, suggesting a propagative signaling mechanism that emanates from the point of inoculation in primed vines as early as 4 hpi that increases over time. In contrast, DEGs decreased in local and systemic tissues in naive vines over the same temporal interval. In addition, we observed more DEGs that were co-expressed between local and systemic petioles of primed plants as compared to naive vines. Taken together, we hypothesized that LPS-priming induces a synchronous, coordinated response that is more efficient in responding to a *X. fastidiosa* infection and results in less overall disease. WGCNA analysis enabled us to test this hypothesis and identified genes that were co-expressed in both local and systemic tissues at each time point. Primed vines had more synchronicity among co-expression modules when compared to the naive vines supporting our hypothesis that primed vines modulate a systemic coordinated response to *X. fastidiosa* infection that spatially spans a long distance between the POI in systemic petioles that are 20 nodes (approximately 1.5 meters) above the point where the pathogen was initially inoculated.

Specifically, the WGCNA analysis indicated that several auxin signaling and transport genes were among the genes that were modulated as part of a systemic, synchronous response to pathogen challenge in primed vines. Auxin is a phytohormone involved in a wide variety of plant physiological processes like maintaining apical dominance, phototropism, and root growth, but has also been implicated in defense priming and induced systemic resistance in tomato [42–44]. Auxin related genes were also up-regulated following early *X. fastidiosa* infection in Citrus Variegated Chlorosis (CVC)-resistant Citrus reticulata [45]. In grapevine, we observed the induction of two MtN21 genes that encode for bidirectional auxin transporters in local and systemic petioles of primed vines (24 hpi) that was absent in naive vines suggesting that auxin signaling pathways is linked to the priming response to *X. fastidiosa* [46,47]. Moreover, genes encoding PSKR1, a phytosulfokine receptor 1, and RALF33, rapid alkalinization factor peptide 33, were synchronously expressed at 48 hpi in primed local and systemic tissues. Both PSKR1 and RALF33 are linked to auxin production. Specifically, RALF33 is a small peptide that is involved in immune responses and the alkalinization of the plant apoplast by interacting with PSK1 and its PSK ligand to trigger a cytosolic Ca^{2+} influx that results in auxin-dependent immune responses. The PSK signaling pathway is activated by PAMPs and is thought to suppress SA signaling pathways. Overexpression of PSKR1 confers resistance to *Xanthomonas oryzae*, a closely related pathogen to *X. fastidiosa* [32].

Moreover, RALF peptides interact with leucine-rich repeat extensin proteins (LRXs) are part of a plant cell wall-integrity sensing mechanism that mediates plant cell

growth and expansion, but can also sense cell wall damage caused by biotic and abiotic stresses. LRXs are anchored in the plant cell wall and relay information from the plant cell wall into the cytosol of plants cells, thereby serving as an important link between the cell wall and the plasma membrane. LRXs also serve as receptors that bind hormones, such as RALF peptides [36,38]. *X. fastidiosa* harbors several cell wall degrading enzymes that hydrolyze the primary cell wall of xylem pit membranes to facilitate their systemic movement throughout the xylem tissue [13,48–50]. We speculate that *X. fastidiosa* mediated cell wall degradation is recognized by LRXs in the living xylem parenchyma adjacent to the xylem vessels [15]. Moreover, LRXs interact with pectin, a major component of the primary plant cell wall and target of *X. fastidiosa* polygalacturonase, thus, LRXs may be ideally positioned to detect perturbation to the cell wall by *X. fastidiosa* [49].

At 4 hpi, primed local and systemic responses also include the expression of two LRR receptor-like kinases and two WAKs. Accumulation of these receptors is a key mechanism of plant defense priming [2,28,29] and enrichment of these genes suggests the host is perceiving MAMPs and/or DAMPs at the point of inoculation and communicating that to systemic locations in the xylem tissue in advance of the bacterial colonization front. In addition to polygalacturonase, *X. fastidiosa* produces endoglucanases that target the plant cell wall and are known virulence factors in the *X. fastidiosa*-grapevine pathosystem [48,49,51–53]. These CWDEs digest the primary cell walls of the xylem pit membranes to facilitate movement of the pathogen through the xylem network. This

enzymatic degradation likely liberates cell-wall derived oligosaccharides that may serve as DAMPs that signal damage incurred by a pathogen attack.

Overall, the synchronicity of gene expression between local and systemic tissues in primed vines indicates communication occurs between these two locations. Long-distance communication is typically mediated through systemic acquired resistance (SAR), a plant immunity mechanism triggered by the perception of a microorganism that results in a systemic and potent immune response that provides broad-spectrum defense against a secondary infection [54–56]. SAR is typically associated with production of the phytohormone salicylic acid (SA) and earlier transcriptome work suggested that a strong SA mediated response was induced and maintained both spatially and over time in plants inoculated with a mutant lacking the O-antigen portion of its LPS. Interestingly, we did not observe up-regulation of SA pathways in LPS primed vines following pathogen challenge. Instead, we observed enrichment of genes involved in auxin signaling and transport and the related PSK signaling pathway that is thought to suppress SA signaling pathways. Biphasic patterns of SA production can occur in plants as part of the defense priming mechanism. The first phase is elicited by PAMPs, like LPS, and the second phase is induced by pathogen challenge. It is hypothesized that the first phase potentiates the second phase and enables the systemic resistance observed in defense priming. We speculate that our timepoints may fall within the two phases because we did not observe enrichment of SA-related pathways in any of our post pathogen challenge timepoints. SAR can also be activated independent of SA and the SA-independent SAR is thought to be of lower magnitude than SA-dependent SAR, but robust enough to elicit an effective

host immune response [55,56]. Thus, it is possible that partial SA-independent SAR response is what facilitates the defense-priming we observed in our study and the long-distance communication between local and distal tissues rather than biphasic SA production.

This study begins to dissect the complexities of plant defense priming in V. vinifera in response to the xylem-limited bacterium, X. fastidiosa. Our data indicate that significant responses occur in systemic tissue distal to the point where the pathogen was introduced in primed vines and these responses occur in advance of detectable levels of pathogen in the systemic location. The xylem is fundamentally considered non-living at maturity and the mechanism by which grapevines mount systemic responses to xylem pathogens remains an open biological question.

Literature Cited

1. Martinez-Medina A, Flors V, Heil M, Mauch-Mani B, Pieterse CMJ, Pozo MJ, et al. Recognizing Plant Defense Priming. Trends Plant Sci. 2016;21: 818–822.

2. Conrath U, Beckers GJM, Langenbach CJG, Jaskiewicz MR. Priming for enhanced defense. Annu Rev Phytopathol. 2015;53: 97–119.

3. Balmer A, Pastor V, Gamir J, Flors V, Mauch-Mani B. The “prime-ome”: towards a holistic approach to priming. Trends Plant Sci. 2015;20: 443–452.

4. Conrath U. Molecular aspects of defence priming. Trends Plant Sci. 2011;16: 524–531.

5. Ton J, Jakab G, Toquin V, Flors V, Iavicoli A, Maeder MN, et al. Dissecting the beta-aminobutyric acid-induced priming phenomenon in Arabidopsis. Plant Cell. 2005;17: 987–999.

6. Baccelli I, Mauch-Mani B. Beta-aminobutyric acid priming of plant defense: the role of ABA and other hormones. Plant Mol Biol. 2016;91: 703–711.

7. Návarová H, Bernsdorff F, Döring A-C, Zeier J. Pipecolic acid, an endogenous mediator of defense amplification and priming, is a critical regulator of inducible plant immunity. Plant Cell. 2012;24: 5123–5141.

8. Jung HW, Tschaplinski TJ, Wang L, Glazebrook J, Greenberg JT. Priming in systemic plant immunity. Science. 2009;324: 89–91.

9. Davis MJ, Purcell AH, Thomson SV. Pierce’s disease of grapevines: isolation of the causal bacterium. Science. 1978;199: 75–77.

10. Saponari M, Boscia D, Nigro F, Martelli GP, Others. Identification of DNA sequences related to Xylella fastidiosa in oleander, almond and olive trees exhibiting leaf scorch symptoms in Apulia (Southern Italy). J Plant Pathol. 2013;95. Available: https://www.cabdirect.org/cabdirect/abstract/20153279019

11. Chang CJ, Garnier M, Zreik L, Rossetti V, Bové JM. Culture and serological detection of the xylem-limited bacterium causing citrus variegated chlorosis and its identification as a strain ofXylella fastidiosa. Curr Microbiol. 1993;27: 137–142.

12. Tumber K, Alston J, Fuller K. Pierce’s disease costs California $104 million per year. Calif Agric. 2014. Available: http://calag.ucanr.edu/Archive/?article=ca.v068n01p20

13. Rapicavoli J, Ingel B, Blanco-Ulate B, Cantu D, Roper C. Xylella fastidiosa: an examination of a re-emerging plant pathogen. Mol Plant Pathol. 2017.

doi:10.1111/mpp.12585

14. Sun Q, Sun Y, Walker MA, Labavitch JM. Vascular occlusions in grapevines with Pierce's disease make disease symptom development worse. Plant Physiol. 2013;161: 1529–1541.

15. Ingel B, Reyes C, Massonnet M, Boudreau B, Sun Y, Sun Q, et al. Xylella fastidiosa causes transcriptional shifts that precede tylose formation and starch depletion in xylem. Mol Plant Pathol. 2020. doi:10.1111/mpp.13016

16. Rapicavoli JN, Blanco-Ulate B, Muszyński A, Figueroa-Balderas R, Morales-Cruz A, Azadi P, et al. Lipopolysaccharide O-antigen delays plant innate immune recognition of Xylella fastidiosa. Nat Commun. 2018;9: 390.

17. Caroff M, Karibian D. Structure of bacterial lipopolysaccharides. Carbohydr Res. 2003;338: 2431–2447.

18. Erbs G, Newman M-A. The role of lipopolysaccharides in induction of plant defence responses. Mol Plant Pathol. 2003;4: 421–425.

19. Therneau TM. A Package for Survival Analysis in R. 2021. Available: https://CRAN.R-project.org/package=survival

20. Phukan UJ, Jeena GS, Shukla RK. WRKY Transcription Factors: Molecular Regulation and Stress Responses in Plants. Front Plant Sci. 2016;7: 760.

21. Luna E, Bruce TJA, Roberts MR, Flors V, Ton J. Next-generation systemic acquired resistance. Plant Physiol. 2012;158: 844–853.

22. Massonnet M, Figueroa-Balderas R, Galarneau ERA, Miki S, Lawrence DP, Sun Q, et al. Neofusicoccum parvum Colonization of the Grapevine Woody Stem Triggers Asynchronous Host Responses at the Site of Infection and in the Leaves. Front Plant Sci. 2017;8: 1117.

23. Bilgin DD, Zavala JA, Zhu J, Clough SJ, Ort DR, DeLucia EH. Biotic stress globally downregulates photosynthesis genes. Plant Cell Environ. 2010;33: 1597–1613.

24. Langfelder P, Luo R, Oldham MC, Horvath S. Is my network module preserved and reproducible? PLoS Comput Biol. 2011;7: e1001057.

25. Yuan M, Jiang Z, Bi G, Nomura K, Liu M, Wang Y, et al. Pattern-recognition receptors are required for NLR-mediated plant immunity. Nature. 2021;592: 105–109.

26. Tang D, Wang G, Zhou J-M. Receptor Kinases in Plant-Pathogen Interactions: More Than Pattern Recognition. Plant Cell. 2017;29: 618–637.

27. Zhou J-M, Zhang Y. Plant Immunity: Danger Perception and Signaling. Cell. 2020;181: 978–989.

28. Brutus A, Sicilia F, Macone A, Cervone F, De Lorenzo G. A domain swap approach reveals a role of the plant wall-associated kinase 1 (WAK1) as a receptor of oligogalacturonides. Proc Natl Acad Sci U S A. 2010;107: 9452–9457.

29. Rosli HG, Zheng Y, Pombo MA, Zhong S, Bombarely A, Fei Z, et al. Transcriptomics-based screen for genes induced by flagellin and repressed by pathogen effectors identifies a cell wall-associated kinase involved in plant immunity. Genome Biol. 2013;14: R139.

30. Qi L, Yan J, Li Y, Jiang H, Sun J, Chen Q, et al. Arabidopsis thaliana plants differentially modulate auxin biosynthesis and transport during defense responses to the necrotrophic pathogen Alternaria brassicicola. New Phytol. 2012;195: 872–882.

31. Zhang H, Hu Z, Lei C, Zheng C, Wang J, Shao S, et al. A Plant Phytosulfokine Peptide Initiates Auxin-Dependent Immunity through Cytosolic Ca2+ Signaling in Tomato. Plant Cell. 2018;30: 652–667.

32. Yang W, Zhang B, Qi G, Shang L, Liu H, Ding X, et al. Identification of the phytosulfokine receptor 1 (OsPSKR1) confers resistance to bacterial leaf streak in rice. Planta. 2019;250: 1603–1612.

33. Shen Y, Diener AC. Arabidopsis thaliana resistance to fusarium oxysporum 2 implicates tyrosine-sulfated peptide signaling in susceptibility and resistance to root infection. PLoS Genet. 2013;9: e1003525.

34. Mosher S, Seybold H, Rodriguez P, Stahl M, Davies KA, Dayaratne S, et al. The tyrosine-sulfated peptide receptors PSKR1 and PSY1R modify the immunity of Arabidopsis to biotrophic and necrotrophic pathogens in an antagonistic manner. Plant J. 2013;73: 469–482.

35. Deepak S, Shailasree S, Kini RK, Muck A, Mithöfer A, Shetty SH. Hydroxyproline-rich glycoproteins and plant defence. J Phytopathol. 2010. doi:10.1111/j.1439-0434.2010.01669.x

36. Herger A, Dünser K, Kleine-Vehn J, Ringli C. Leucine-Rich Repeat Extensin Proteins and Their Role in Cell Wall Sensing. Curr Biol. 2019;29: R851–R858.

37. Xie D, Ma L, Samaj J, Xu C. Immunohistochemical analysis of cell wall hydroxyproline-rich glycoproteins in the roots of resistant and susceptible wax gourd cultivars in response to Fusarium oxysporum f. sp. Benincasae infection and fusaric acid treatment. Plant Cell Rep. 2011;30: 1555–1569.

38. Zhao C, Zayed O, Yu Z, Jiang W, Zhu P, Hsu C-C, et al. Leucine-rich repeat

extensin proteins regulate plant salt tolerance in Arabidopsis. Proc Natl Acad Sci U S A. 2018;115: 13123–13128.

39. Pérez-Donoso AG, Greve LC, Walton JH, Shackel KA, Labavitch JM. Xylella fastidiosa infection and ethylene exposure result in xylem and water movement disruption in grapevine shoots. Plant Physiol. 2007;143: 1024–1036.

40. Sun Q, Rost TL, Reid MS, Matthews MA. Ethylene and not embolism is required for wound-induced tylose development in stems of grapevines. Plant Physiol. 2007;145: 1629–1636.

41. Leśniewska J, Öhman D, Krzesłowska M, Kushwah S, Barciszewska-Pacak M, Kleczkowski LA, et al. Defense Responses in Aspen with Altered Pectin Methylesterase Activity Reveal the Hormonal Inducers of Tyloses. Plant Physiol. 2017;173: 1409–1419.

42. Fu J, Wang S. Insights into auxin signaling in plant-pathogen interactions. Front Plant Sci. 2011;2: 74.

43. Kazan K, Manners JM. Linking development to defense: auxin in plant-pathogen interactions. Trends Plant Sci. 2009;14: 373–382.

44. Jaiswal AK, Alkan N, Elad Y, Sela N, Philosoph AM, Graber ER, et al. Molecular insights into biochar-mediated plant growth promotion and systemic resistance in tomato against Fusarium crown and root rot disease. Sci Rep. 2020;10: 13934.

45. Rodrigues CM, de Souza AA, Takita MA, Kishi LT, Machado MA. RNA-Seq analysis of Citrus reticulata in the early stages of Xylella fastidiosa infection reveals auxin-related genes as a defense response. BMC Genomics. 2013;14: 676.

46. Lee J, Kim H, Park S-G, Hwang H, Yoo S-I, Bae W, et al. Brassinosteroid-BZR1/2-WAT1 module determines the high level of auxin signalling in vascular cambium during wood formation. New Phytol. 2021;230: 1503–1516.

47. Ranocha P, Denancé N, Vanholme R, Freydier A, Martinez Y, Hoffmann L, et al. Walls are thin 1 (WAT1), an Arabidopsis homolog of Medicago truncatula NODULIN21, is a tonoplast-localized protein required for secondary wall formation in fibers. Plant J. 2010;63: 469–483.

48. Ingel B, Jeske DR, Sun Q, Grosskopf J, Roper MC. Xylella fastidiosa Endoglucanases Mediate the Rate of Pierce's Disease Development in Vitis vinifera in a Cultivar-Dependent Manner. Mol Plant Microbe Interact. 2019; MPMI04190096R.

49. Roper MC, Greve LC, Warren JG, Labavitch JM, Kirkpatrick BC. Xylella fastidiosa requires polygalacturonase for colonization and pathogenicity in Vitis vinifera

grapevines. Mol Plant Microbe Interact. 2007;20: 411–419.

50. Pérez-Donoso AG, Sun Q, Roper MC, Greve LC, Kirkpatrick B, Labavitch JM. Cell wall-degrading enzymes enlarge the pore size of intervessel pit membranes in healthy and Xylella fastidiosa-infected grapevines. Plant Physiol. 2010;152: 1748–1759.

51. Newman KL, Almeida RPP, Purcell AH, Lindow SE. Cell-cell signaling controls Xylella fastidiosa interactions with both insects and plants. Proc Natl Acad Sci U S A. 2004;101: 1737–1742.

52. Chatterjee S, Wistrom C, Lindow SE. A cell--cell signaling sensor is required for virulence and insect transmission of Xylella fastidiosa. Proceedings of the National Academy of Sciences. 2008;105: 2670–2675.

53. Chatterjee S, Almeida RPP, Lindow S. Living in two Worlds: The Plant and Insect Lifestyles of Xylella fastidiosa. Annu Rev Phytopathol. 2008;46: 243–271.

54. Shah J, Zeier J. Long-distance communication and signal amplification in systemic acquired resistance. Front Plant Sci. 2013;4: 30.

55. Gruner K, Griebel T, Návarová H, Attaran E, Zeier J. Reprogramming of plants during systemic acquired resistance. Front Plant Sci. 2013;4: 252.

56. Bernsdorff F, Döring A-C, Gruner K, Schuck S, Bräutigam A, Zeier J. Pipecolic Acid Orchestrates Plant Systemic Acquired Resistance and Defense Priming via Salicylic Acid-Dependent and -Independent Pathways. Plant Cell. 2016;28: 102–129.

57. Lee CH, Tsai CM. Quantification of bacterial lipopolysaccharides by the purpald assay: measuring formaldehyde generated from 2-keto-3-deoxyoctonate and heptose at the inner core by periodate oxidation. Anal Biochem. 1999;267: 161–168.

58. Guilhabert MR, Kirkpatrick BC. Identification of Xylella fastidiosa Antivirulence Genes: Hemagglutinin Adhesins Contribute to X. fastidiosa Biofilm Maturation and Colonization …. Mol Plant Microbe Interact. 2005. Available: http://apsjournals.apsnet.org/doi/abs/10.1094/MPMI-18-0856

59. Liang K-Y, Zeger SL. Longitudinal data analysis using generalized linear models. Biometrika. 1986;73: 13–22.

60. McCullagh P, Nelder JA. Chapter 5. generalized linear models 2nd ed London: Chapman and Hall. 1989.

61. Schandry N. A Practical Guide to Visualization and Statistical Analysis of R. solanacearum Infection Data Using R. Front Plant Sci. 2017;8: 623.

62. Amrine KCH, Blanco-Ulate B, Cantu D. Discovery of core biotic stress responsive genes in Arabidopsis by weighted gene co-expression network analysis. PLoS One. 2015;10: e0118731.

63. Grimplet J, Cramer GR, Dickerson JA, Mathiason K, Van Hemert J, Fennell AY. VitisNet: "Omics" integration through grapevine molecular networks. PLoS One. 2009;4: e8365.

64. Young PR, Lashbrooke JG, Alexandersson E, Jacobson D, Moser C, Velasco R, et al. The genes and enzymes of the carotenoid metabolic pathway in Vitis vinifera L. BMC Genomics. 2012;13: 243.

65. Joo H, Lim CW, Han S-W, Lee SC. The Pepper RING Finger E3 Ligase, CaDIR1, Regulates the Drought Stress Response via ABA-Mediated Signaling. Front Plant Sci. 2017;8: 690.

66. Wang X, Zhang J, Song J, Huang M, Cai J, Zhou Q, et al. Abscisic acid and hydrogen peroxide are involved in drought priming-induced drought tolerance in wheat (Triticum aestivum L.). Plant Biol . 2020;22: 1113–1122.

67. Vishwakarma K, Upadhyay N, Kumar N, Yadav G, Singh J, Mishra RK, et al. Abscisic Acid Signaling and Abiotic Stress Tolerance in Plants: A Review on Current Knowledge and Future Prospects. Front Plant Sci. 2017;8: 161.

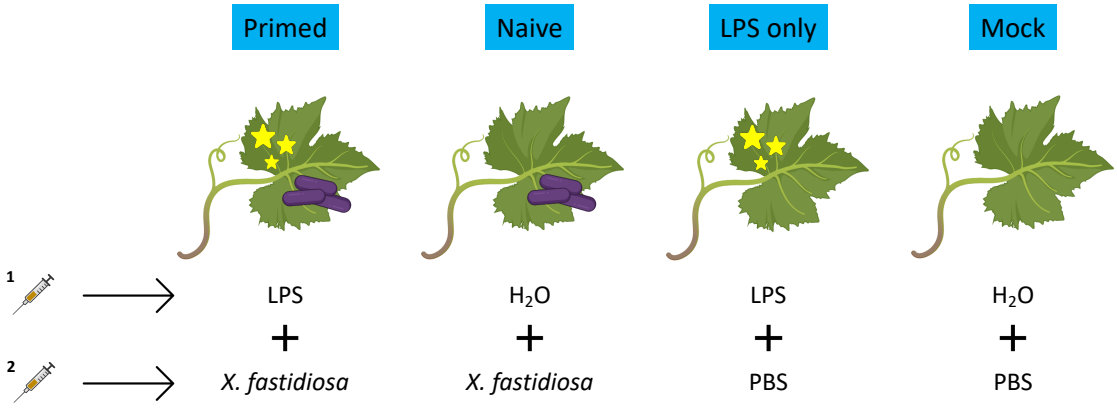

Figure 2.1. Illustration representing experimental design. Cabernet Sauvignon grapevines were treated with 2 µg *X. fastidiosa* LPS and with *X. fastidiosa* cells four hours later. These plants were designated as 'primed.' 'Naive' plants received H_2O and then *X. fastidiosa* cells. ' LPS only' plants received LPS and then PBS buffer. 'Mock' received H_2O and PBS buffer. (n = 13 vines per treatment).

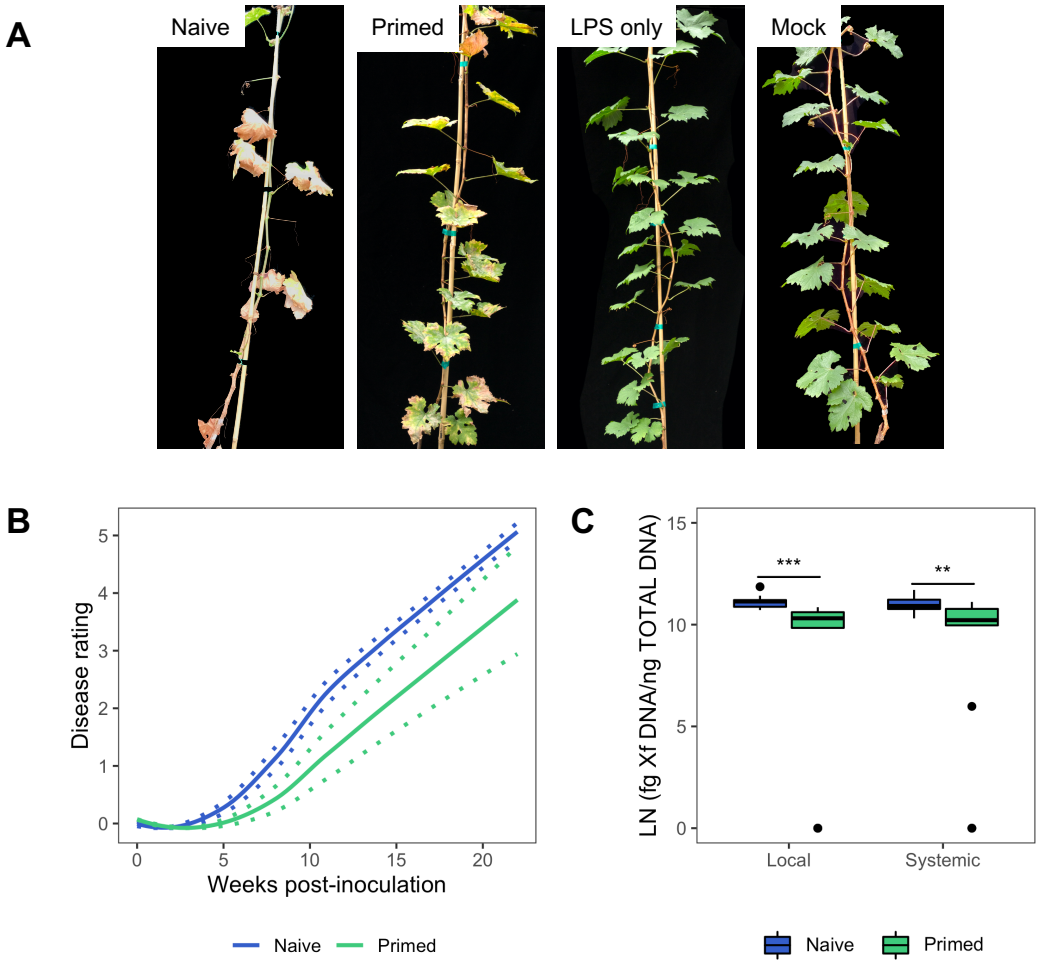

Figure 2.2. LPS treatment reduces PD symptoms and *X. fastidiosa* titer in *V. vinifera* Cabernet Sauvignon plants. (A) Pierce's disease (PD) symptoms in vines at 13 weeks post-inoculation (wpi) for each treatment. (B) A generalized estimating equations model was used to determine estimated means for PD symptom scores each week (n = 13, $P < 0.0001$). Disease scores were assigned based on the disease rating index developed by Guilhabert and Kirkpatrick (2005). Solid lines represent the estimated means for weekly PD symptom scores and dotted lines represent 95% confidence intervals. (C) *X. fastidiosa* DNA quantification in local and systemic petioles at 13 wpi via qPCR (n = 13, Kruskal-Wallis test followed by Dunn's test with Bonferroni's method for multiple-comparison correction, asterisks indicate level of significance: * $P < 0.05$, ** $P < 0.01$, *** $P < 0.001$).

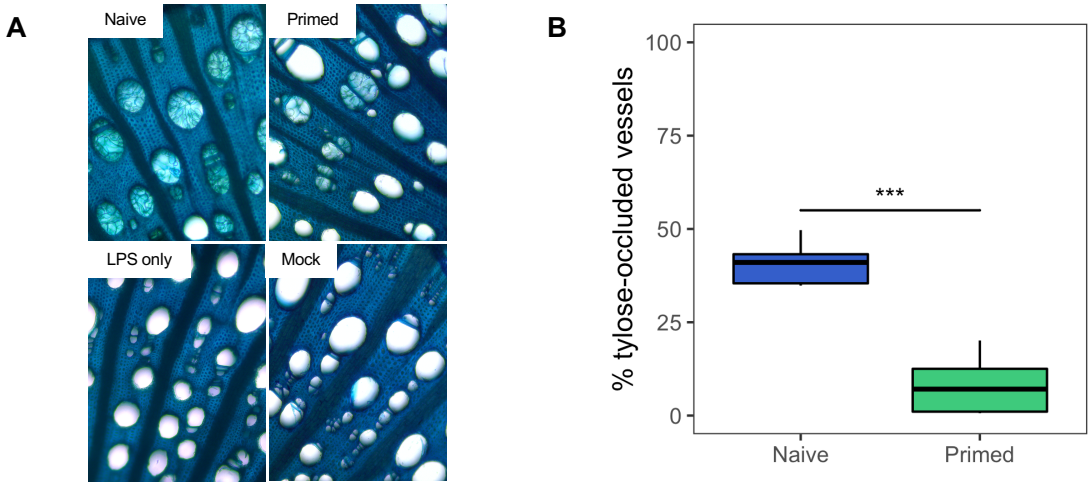

Figure 2.3. Primed grapevines have significantly lower number of tylose-occluded xylem vessels. (A) Cross sections of grapevine stems (18 wpi) stained with toluidine blue. Naive grapevines developed a high number of tyloses that led to the occlusion of many vessels while primed plants showed few to no tylose-occluded xylem vessels. Plants treated with H_2O (mock) or LPS only prior to PBS buffer did not develop any xylem vessel occlusions. (B) Quantification of tylose-occluded xylem vessels in naive and primed vine cross sections displayed as a percentage (number of occluded vessels/total number of vessels. (n = 9, Dunn's test with Bonferroni's method for multiple-comparison correction, asterisks indicate level of significance: * $P < 0.05$, ** $P < 0.01$, *** $P < 0.001$)

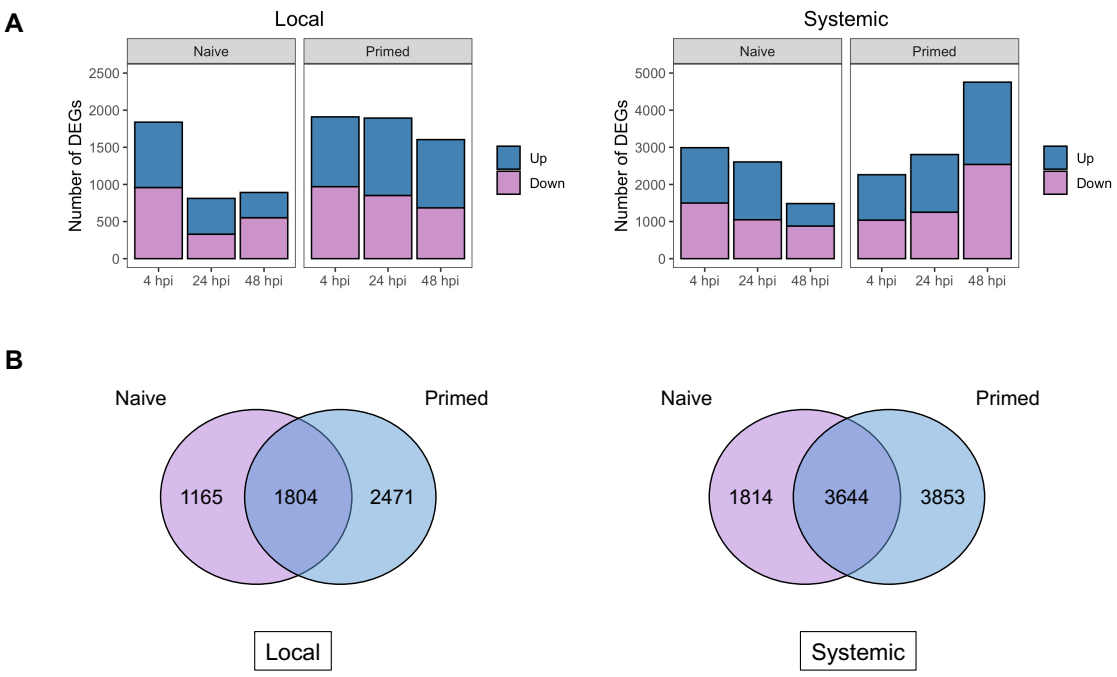

Figure 2.4. Primed vines generated a higher number of differentially expressed genes (DEGs) than naive vines. Number of DEGs in primed local tissue remain stable over time whereas in systemic tissue there is an increased number of DEGs over time. The number of DEGs for naive local and systemic tissue decrease over time. (B) Primed plants have a higher number of unique DEGs in local and systemic tissues compared to naive plants across all time points.

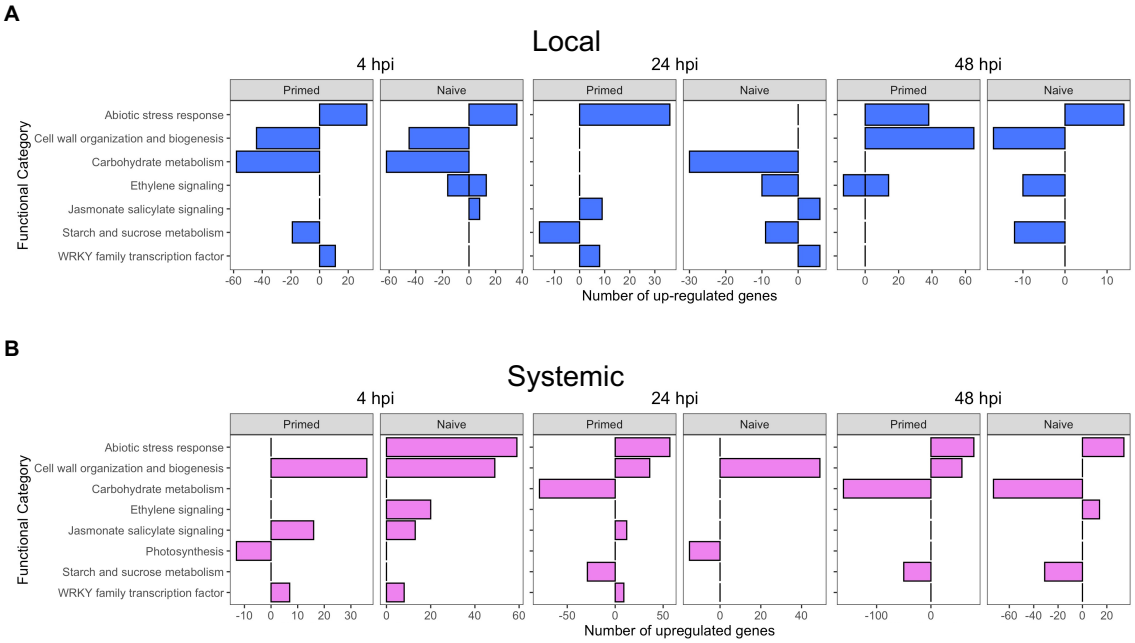

Figure 2.5. Enriched grape functional categories selected among up-regulated and down-regulated genes in primed and naive grapevines vines in response to early *X. fastidiosa* infection. (A) Functional categories for primed and naive local tissue at 4, 24, and 48 hours post-inoculation (hpi). (B) Functional categories for primed and naive systemic tissue at 4, 24, and 48 hpi. Negative gene counts represent down-regulated genes, positive gene counts represent up-regulated genes. Absent bars represent functional categories that are not significantly overrepresented among DEGs ($P < 0.05$, Fisher method).

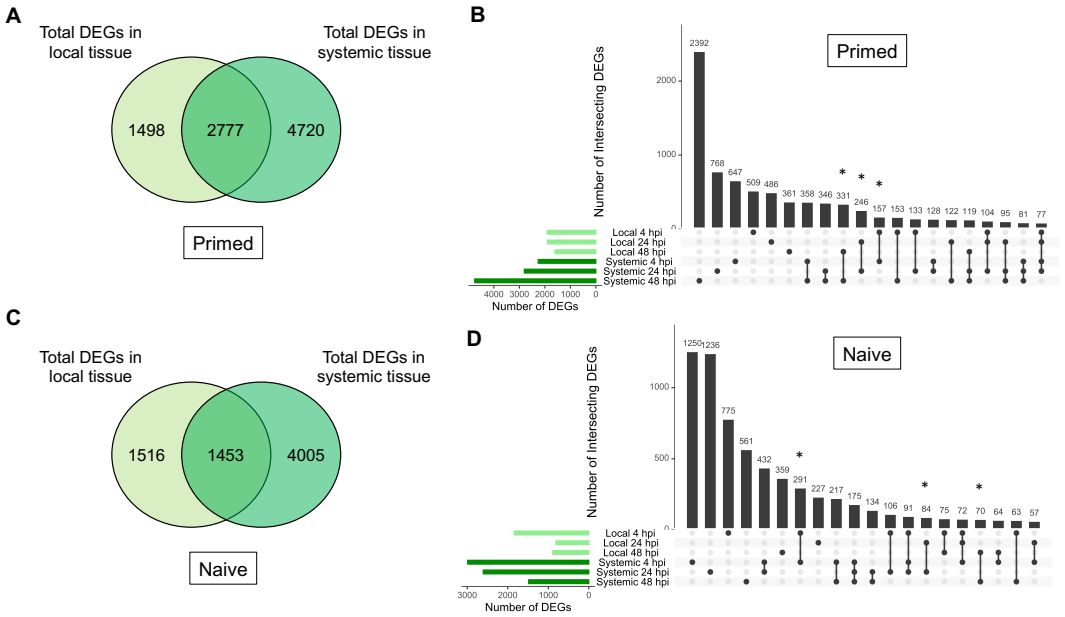

Figure 2.6. Comparison of intersecting DEGs belonging to both local and systemic tissues indicate a more synchronous response between local and systemic locations in primed vines that in naive vines. (A,C) Primed vines share approximately 45% of DEGs between local and systemic tissues whereas naive vines share only approximately 26% of the total DEGs between local and systemic tissues. (D, B) Bar plot displaying the top 20 largest intersecting DEGs sets for local and systemic time points: 4, 24, and 48 hours post-inoculation. Dashed read box indicates the DEGs shared between local and systemic responses at each time point for primed vines.

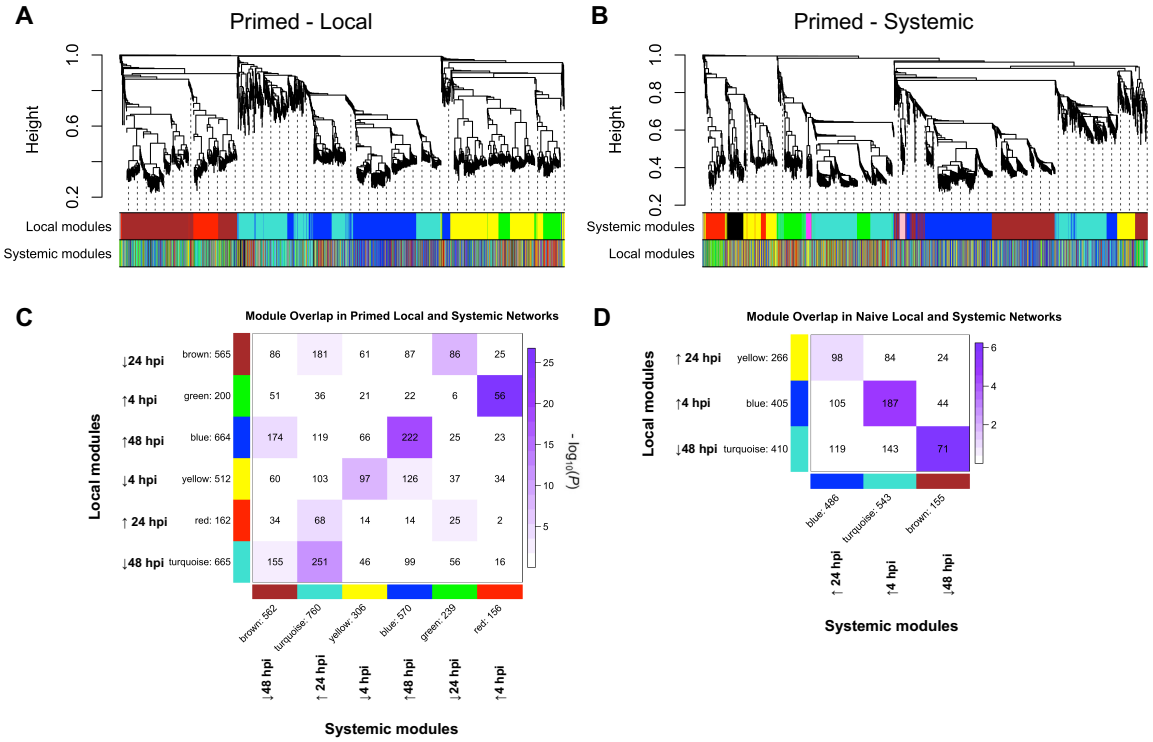

Figure 2.7. Comparison of primed local and systemic co-expression networks and their cross-tabulation. Clustering dendrogram of DEGs assigned to a module color in (A) primed local network and (B) systemic network (each line corresponds to one DEG). Rows under the dendrograms indicate module membership for (A) local modules and the comparison module membership in the systemic network and vice-versa (B). Cross-tabulation for local (rows) and systemic (columns) modules in (C) primed and (D) naive vines occurring at the same time points, either 4, 24, and 48 hours post-inoculation (hpi). Their corresponding intersecting cells indicate the number of DEGs shared by both primed/naive local and systemic modules. These cells are color-coded for their -$\log_{10}$(P-value) generated by the Fisher's exact test. Light purple to dark purple indicates a significant overlap. A darker purple color signifies a more significant overlap.

Module Overlap	Modulation			
Local-Systemic (gene number)	Local	Systemic	Enriched functional category	*P*-value
Green-Red (56)	↑ 4 hpi	↑ 4 hpi	Aluminium transport	1.87E-03
			Protein kinase	2.24E-03
			Auxin transport	4.28E-03
			Auxin Signaling	8.00E-03
Yellow-Yellow (97)	↓ 4 hpi	↓ 4 hpi	AUXIAA family transcription factor	2.51E-03
			Shikimate metabolism	3.71E-03
			Glycolipid biosynthesis	6.46E-03
			Oxylipin biosynthesis	7.46E-03
Red-Turquoise (68)	↑ 24 hpi	↑ 24 hpi	Endoplasmic Reticular Retrotranslocon	3.38E-03
			Plant Drug/Metabolite Exporter	5.57E-03
			Esterase activity	6.73E-03
			CCAAT family transcription factor-HAP5-type	9.05E-03
Brown-Green (86)	↓ 24 hpi	↓ 24 hpi	Cellular metabolism	3.38E-04
			Hormone Signaling	7.16E-04
			BHSH family transcription factor	2.87E-03
			2OG-Fe(II) oxygenase superfamily	3.59E-03
			zf-HD family transcription factor	3.82E-03
			Carbon fixation	4.25E-03
			Transcription factor	6.25E-03
			Regulation overview	6.71E-03
			Regulation of transcription	7.68E-03
			Second messenger biosynthesis	8.58E-03
			Recognized transporters of unknown biochemical mechanism	8.58E-03
			Oxidation reduction	9.28E-03
			Regulation of gene expression	9.49E-03
Blue-Blue (222)	↑ 48 hpi	↑ 48 hpi	Cell wall structural protein	1.47E-08
			Cell wall organization and biogenesis	1.54E-06
			Cellular component organization and biogenesis	1.45E-05
			Thylakoid targeting pathway	3.79E-05
			Glycine, serine, and threonine metabolism	1.09E-04
			Transcription factor	1.61E-04
			Regulation of transcription	2.51E-04
			Regulation overview	2.71E-04
			Regulation of gene expression	3.96E-04
			Photosynthesis-Antenna proteins	4.16E-04
			Cellular process	5.34E-04
			Transmembrane 1-electron transfer carriers	1.03E-03
			Transmembrane Electron Carriers	1.10E-03
			Cysteine and methionine metabolism	1.49E-03
			PseudoARR-B family transcription factor	1.49E-03
			Zinc finger C3HC4 family transcription factor	2.43E-03
			Plant Photosystem I Supercomplex	3.98E-03
			Gene family with diverse functions-GASA family	4.69E-03
			Lysine biosynthesis	4.69E-03
			Signaling peptide	6.12E-03
			Signaling molecules	8.60E-03
			HSP-mediated protein folding	9.20E-03
Turquoise-Brown (155)	↓ 48 hpi	↓ 48 hpi	Oligopeptide transport	7.29E-04
			Zinc finger B-box family transcription factor	2.67E-03
			Phenylpropanoid metabolism	4.85E-03
			Porters.Zinc (Zn2+)-Iron (Fe2+) Permease	5.74E-03
			HSF family transcription factor	6.81E-03
			Phenylpropanoid biosynthesis	7.02E-03
			Oligopeptide Transporter	8.57E-03
			Temperature stress response	9.52E-03

Table 2.1. Enriched grape functional categories among the intersecting co-expressed genes in primed local and systemic modules during early *X. fastidiosa* infection. For each local-systemic module overlap, the number of shared genes and their corresponding modulation is indicated. Only functional categories with a *P*-value < 0.01 are listed.

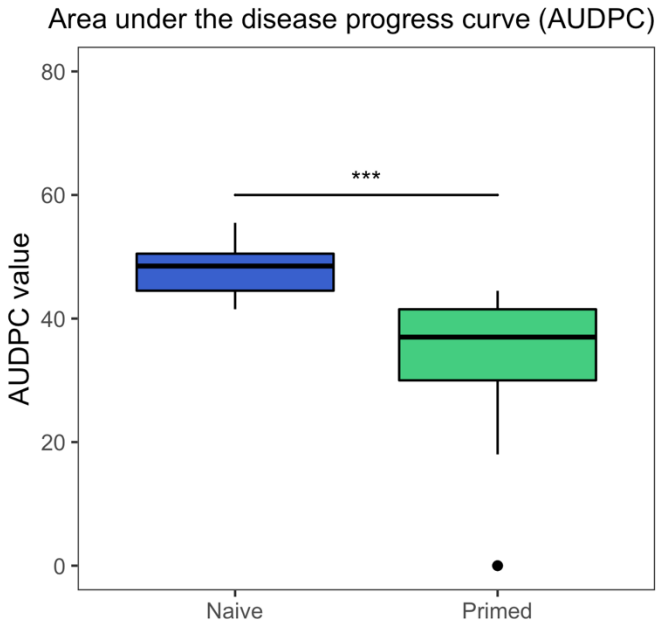

Figure S2.1. Area under the disease progress curve (AUDPC) values for naive and primed plants based on disease rating scores over the course of 22 weeks post-inoculation. LPS only and mock plants did not show any symptoms during this trial. (n = 13, Dunn's test with Bonferroni's method for multiple-comparison correction, asterisks indicate level of significance: * $P < 0.05$, ** $P < 0.01$, *** $P < 0.001$)

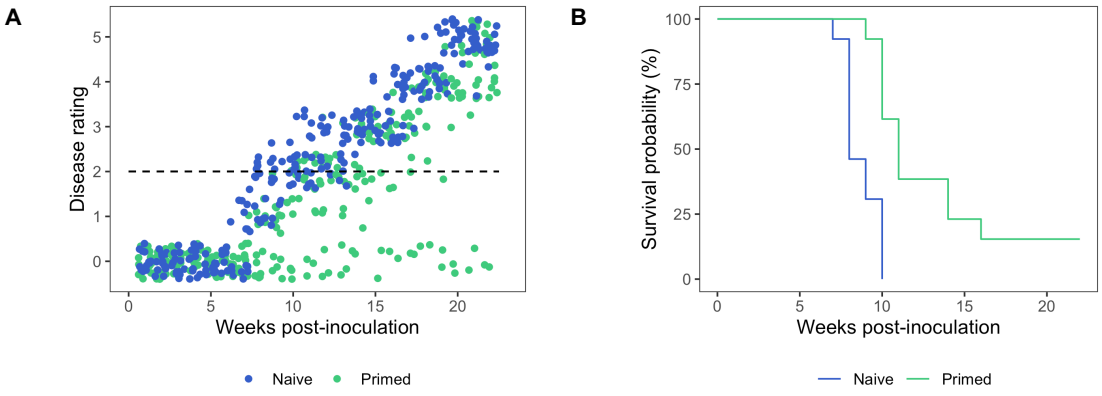

Figure S2.2. Primed plants have a higher survival probability than naive plants. (A) Data points representing weekly disease rating scores over the course of 22 weeks. Dashed line represents a cutoff of 2 as a disease rating score. (B) Survival estimates for naive and primed grapevines at each weekly time point. (n = 13, Kaplan-Meier estimates of survival, $P < 0.0001$)

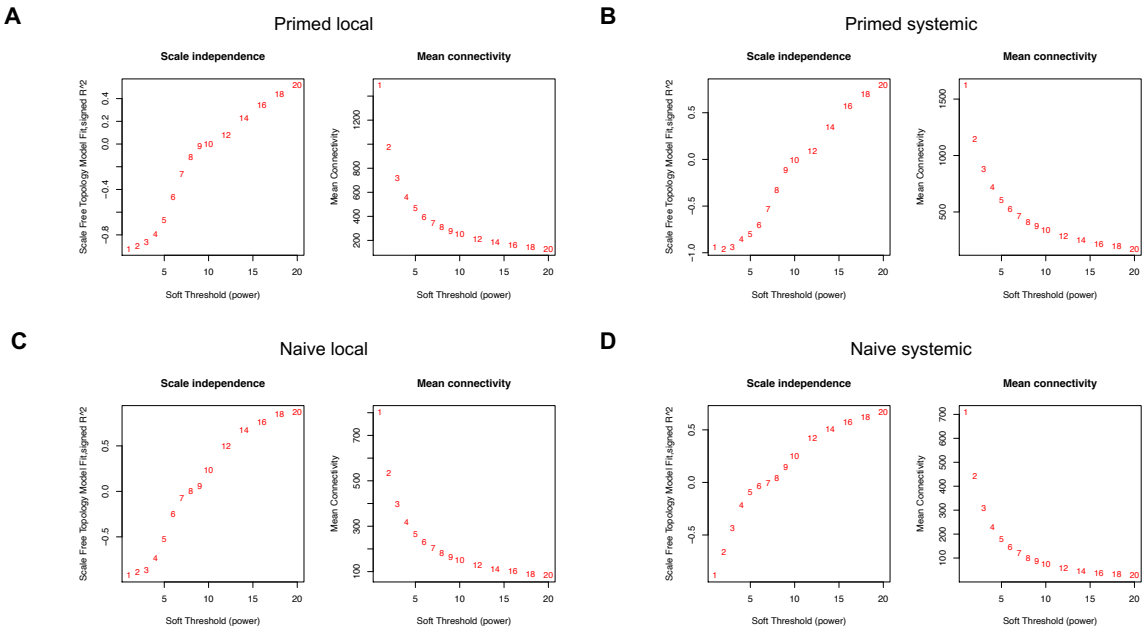

Figure S2.3. Analysis of network topology for various soft-thresholding powers for (A) primed local, (B) primed systemic, (C) naive local, and (D) naive systemic samples. Scale independence (left panel) shows the scale-free fit index (y-axis) as a function of the soft-thresholding power (x-axis). Mean connectivity (right panel, y-axis) is displayed as a function of the thresholding power (x-axis). A soft-thresholding power of 18 was selected according to Langfelder and Horvath (2017) because of lack of scale-free topology fit. Log_2-FC values (primed/mock and naive/mock) of DEGs shared by primed local and systemic samples, and naive local and systemic samples were used for this analysis and for the rest of the WGCNA workflow.

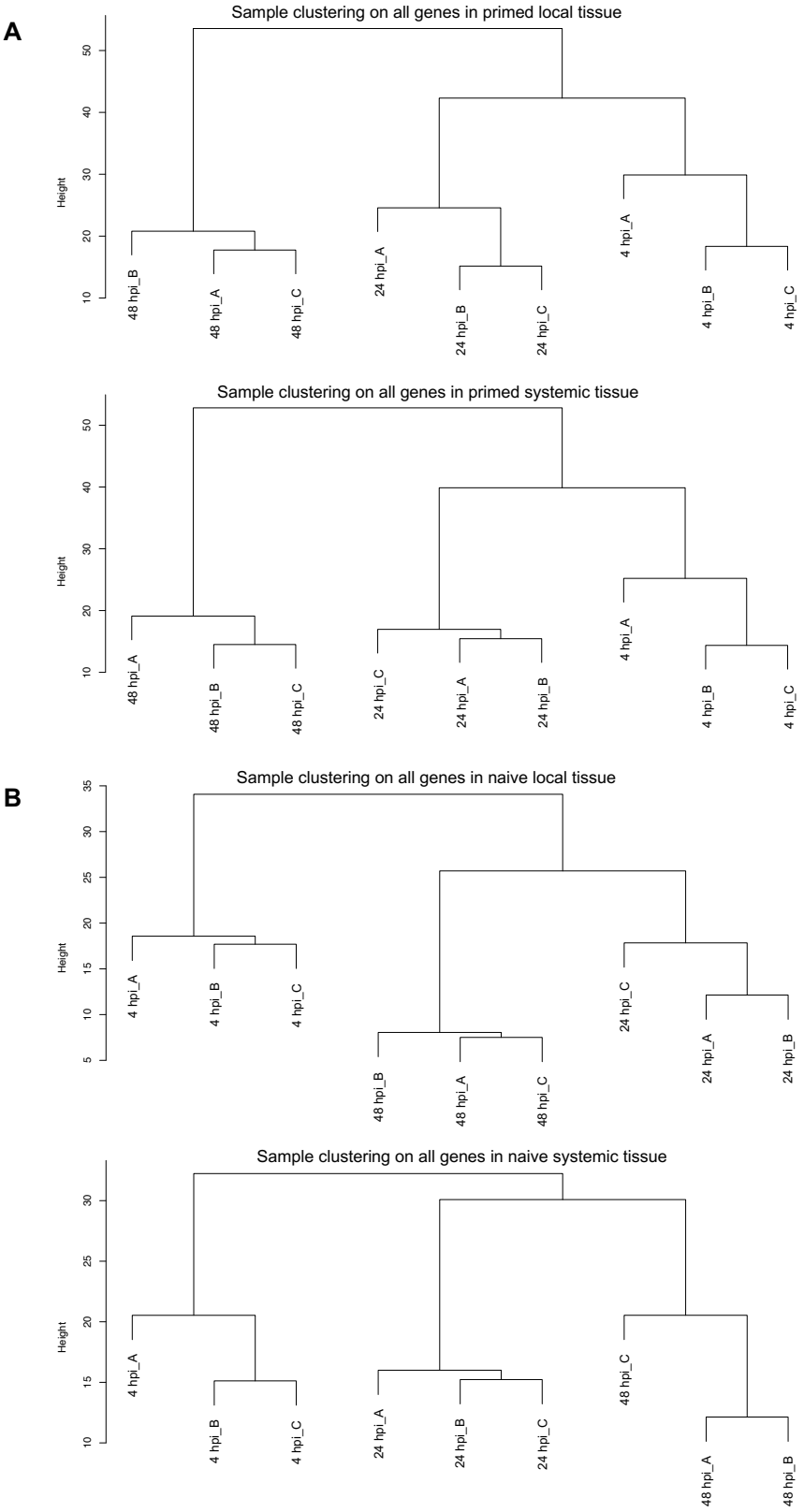
A
Sample clustering on all genes in primed local tissue
Height
48 hpi_B
48 hpi_A
48 hpi_C
24 hpi_A
24 hpi_B
24 hpi_C
4 hpi_A
4 hpi_B
4 hpi_C
Sample clustering on all genes in primed systemic tissue
Height
48 hpi_A
48 hpi_B
48 hpi_C
24 hpi_C
24 hpi_A
24 hpi_B
4 hpi_A
4 hpi_B
4 hpi_C
B
Sample clustering on all genes in naive local tissue
Height
4 hpi_A
4 hpi_B
4 hpi_C
48 hpi_B
48 hpi_A
48 hpi_C
24 hpi_C
24 hpi_A
24 hpi_B
Sample clustering on all genes in naive systemic tissue
Height
4 hpi_A
4 hpi_B
4 hpi_C
24 hpi_A
24 hpi_B
24 hpi_C
48 hpi_C
48 hpi_A
48 hpi_B

Figure S2.4. Clustering dendrograms of (A) primed local and systemic, and (B) naive local and systemic samples based on their Euclidean distance. Sample outliers were not detected.

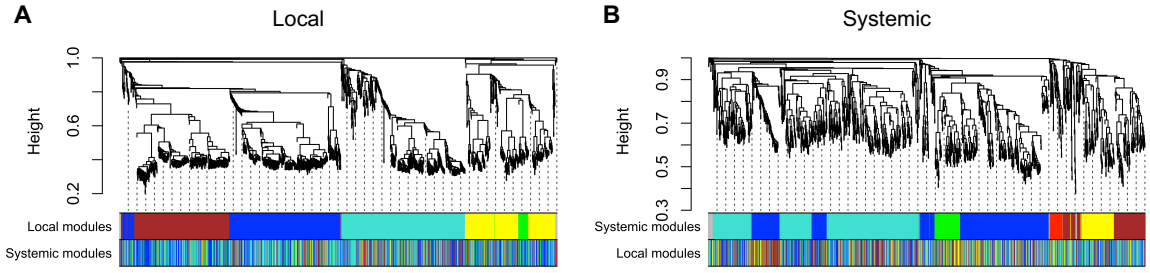

Figure S2.5. Comparison of naive local and systemic co-expression networks and their cross-tabulation. Clustering dendrogram of DEGs assigned to a module color in (A) naive local network and (B) systemic network (each line corresponds to one DEG). Rows under the dendrograms indicate module membership for (A) local modules and the comparison module membership in the systemic network and vice-versa (B).

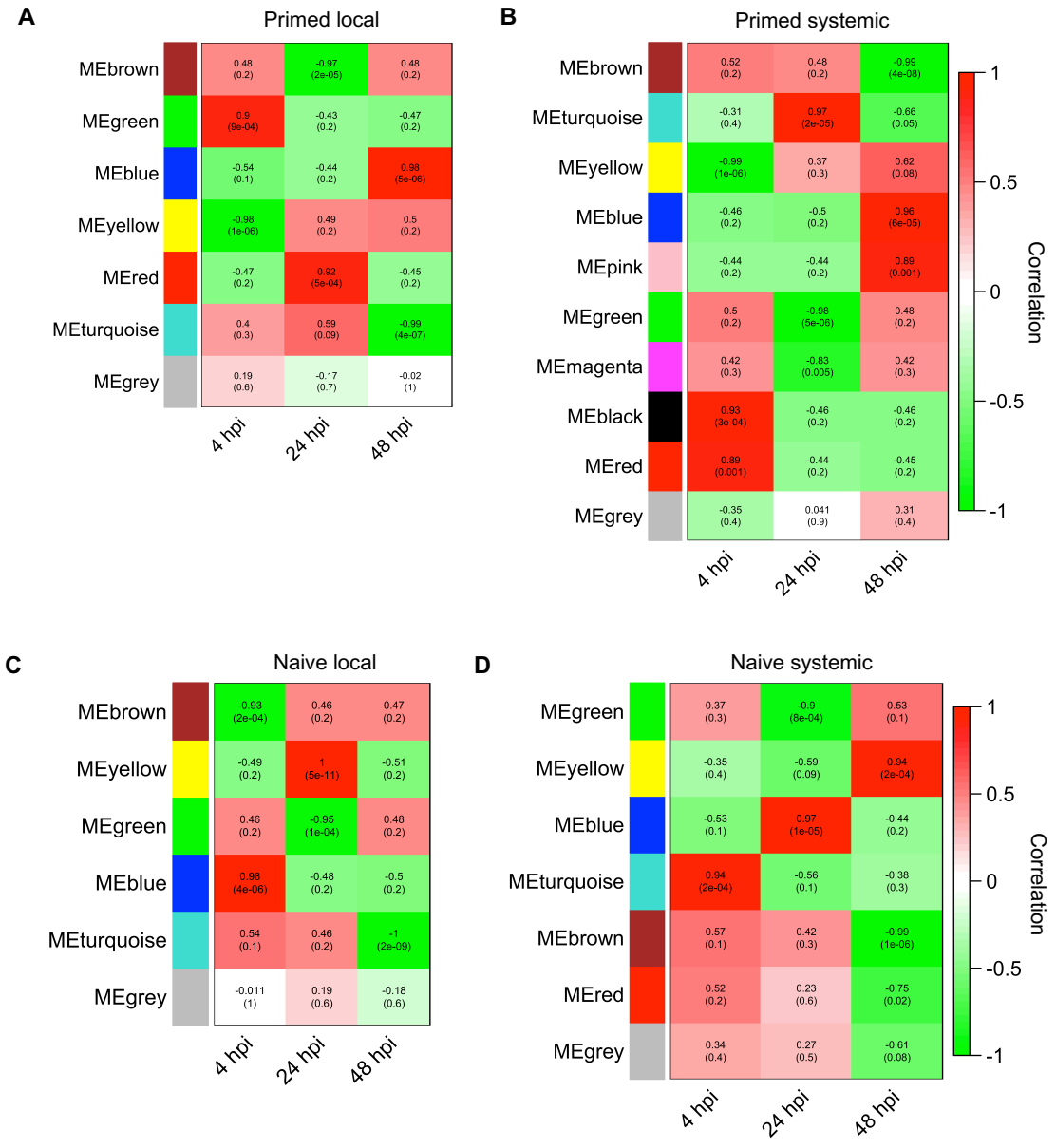

Figure S2.6. Module-trait (time point) associations for (A) primed local, (B) primed systemic, (C) naive local, and (D) naive systemic samples. Each row corresponds to a module eigengene and each column corresponds to a time point: 4, 24, or 48 hours post-inoculation (hpi). Each intersecting cell indicates the correlation and P-value (color-coded) for the corresponding module eigengene and time point.

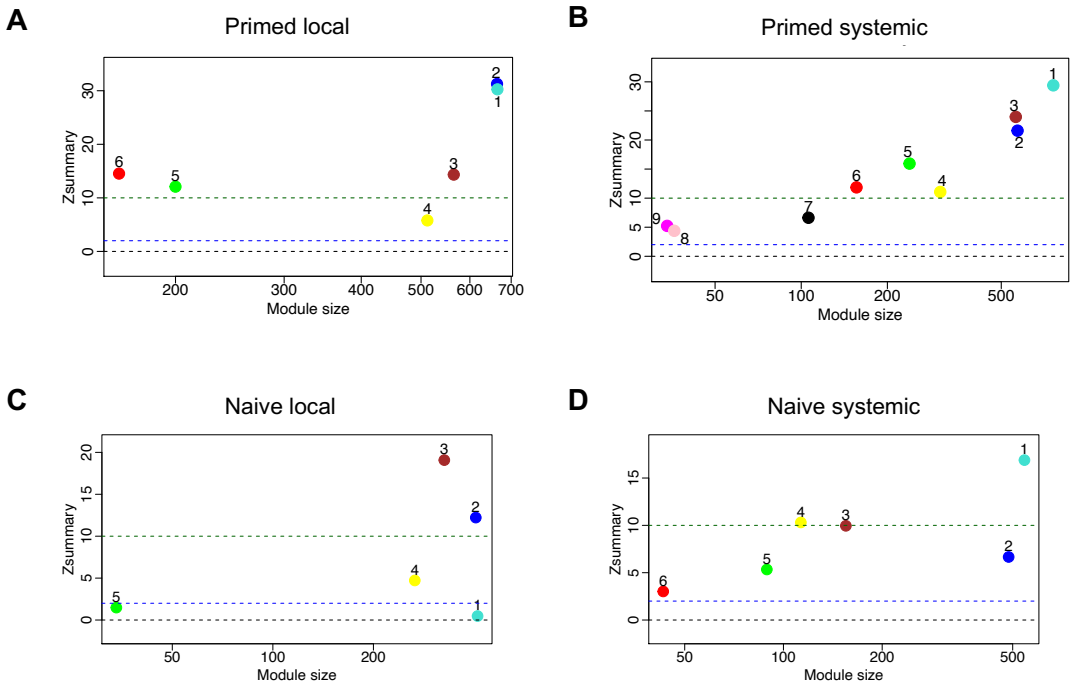

Figure S2.7. Preservation statistics using the summary statistic $Z_{summary}$ (y-axis) as a function of the module size for all samples: primed local, primed systemic, naive local, and naive systemic. Each point with a numeric label represents a module. (A) $Z_{summary}$ results for primed local modules (1=turquoise, 2=blue, 3=brown, 4=yellow, 5=green, 6=red). (B) $Z_{summary}$ results for primed systemic modules (1=turquoise, 2=blue, 3=brown, 4=yellow, 5=green, 6=red, 7=black, 8=pink, 9=magenta). (C) $Z_{summary}$ results for naive local modules (1=turquoise, 2=blue, 3=brown, 4=yellow, 5=green). (D) $Z_{summary}$ results for naive systemic modules (1=turquoise, 2=blue, 3=brown, 4=yellow, 5=green, 6=red). Based on Langfelder et al. (2011), if $Z_{summary} > 10$ there is strong evidence that the module is preserved, if $2 < Z_{summary} < 10$ there is weak to moderate evidence of preservation, and if $Z_{summary} < 2$, there is no evidence that the module is preserved. Dashed lines indicate thresholds for $Z_{summary} = 0$, $Z_{summary} = 2$, and $Z_{summary} = 10$.

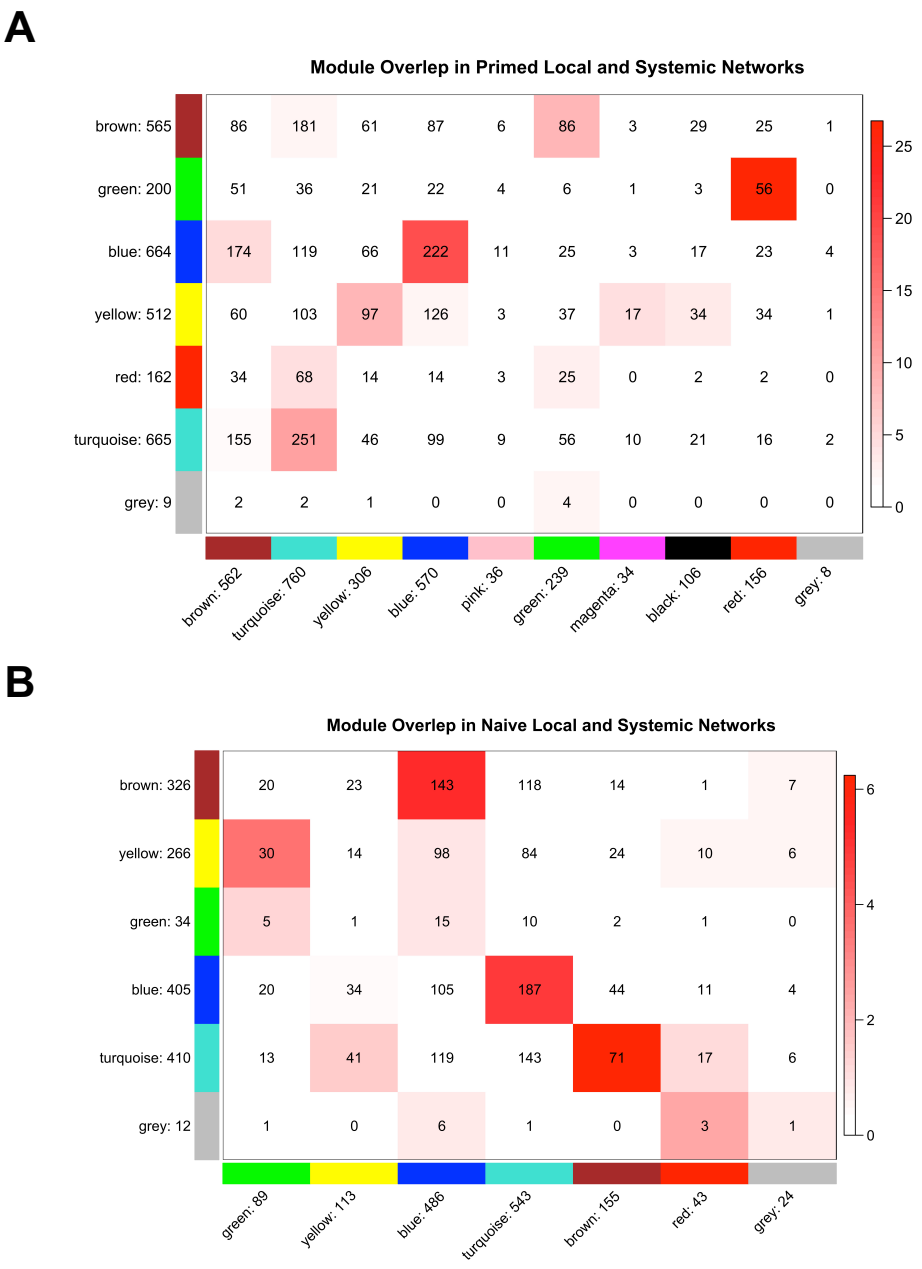

Figure S2.8. Cross-tabulation for local and systemic modules (columns) in primed and naive vines. Primed (A) and Naive (B) corresponding intersecting cells indicate the number of DEGs shared by both local (rows) and systemic (columns) modules. These cells are color-coded for their -$\log_{10}$(P-value) generated by the Fisher's exact test. A darker red color signifies a more significant overlap.

Module Overlap	Modulation			
Local-Systemic (gene number)	Local	Systemic	Enriched functional category	*P-value*
Blue-Turquoise (187)	↑ 4 hpi	↑ 4 hpi	Water transport	9.08E-08
			Aquaporins	9.08E-08
			A-Type channels-Major Intrinsic Protein	1.27E-07
			Aquaporins-PIP	1.97E-05
			Shikimate metabolism	2.67E-05
			Secondary metabolism	1.82E-04
			Aromatic amino acid biosynthesis	2.87E-04
			Terpenoid metabolism	8.36E-04
			K+ Transporter	1.06E-03
			Aquaporins-TIP	1.06E-03
			Aromatic amino acid metabolism	1.09E-03
			Channels and pores-A-Type channels	1.18E-03
			Terpenoid biosynthesis	2.11E-03
			Channels and pores	2.48E-03
			Zinc finger B-box family transcription factor	3.85E-03
			Thylakoid targeting pathway	3.99E-03
			Auxin transport	4.22E-03
			Cellular metabolism	4.36E-03
			Lipid metabolism	5.48E-03
			Amino acid biosynthesis	7.28E-03
			Steroid biosynthesis	9.06E-03
Yellow-Blue (98)	↑ 24 hpi	↑ 24 hpi	Ion transport	1.24E-05
			Anion transport	4.06E-05
			Proton-dependent Oligopeptide Transporter	7.03E-05
			Porters	7.34E-05
			Electrochemical Potential-driven Transporters	7.48E-05
			Hormone Signaling	6.23E-04
			Transport overview	7.66E-04
			Orphans Response reg family transcription factor	9.39E-04
			Oligopeptide transport	2.16E-03
			Circadian clock Signaling	2.24E-03
			Nitrate transport	2.34E-03
			RCC1 superfamily protein	2.79E-03
			Plasma membrane H+ ATPase	3.02E-03
			P-type ATPase (P-ATPase)	3.56E-03
			Regulation of transcription	5.01E-03
			Regulation of gene expression	6.35E-03
			Tetraterpenoid metabolism	9.16E-03
			Tetraterpenoid biosynthesis	9.16E-03
			Carotenoid biosynthesis	9.16E-03
			Transcription factor	9.21E-03
			Glycolysis Gluconeogenesis-Activator	9.78E-03
			Proton transport	9.96E-03
Turquoise-Brown (71)	↓ 48 hpi	↓ 48 hpi	HSP-mediated protein folding	2.30E-05
			NAC family transcription factor	3.09E-05
			Chaperone-mediated protein folding	8.08E-05
			PseudoARR-B family transcription factor	1.54E-04
			Transcription factor	2.81E-04
			Regulation of transcription	3.64E-04
			Regulation of gene expression	4.75E-04
			Oligopeptide transport	8.53E-04
			Regulation overview	8.65E-04
			Circadian clock Signaling	8.85E-04
			Amino Acid/Auxin Permease	1.06E-03
			Protein folding	1.12E-03
			Amino acid transport	1.51E-03
			Oligopeptide Transporter	1.87E-03
			Porters	1.98E-03
			Electrochemical Potential-driven Transporters	2.00E-03
			Solute:Sodium Symporter	2.37E-03
			Transcription factor-MBF	7.09E-03

Table S2.1. Enriched grape functional categories among the intersecting co-expressed genes in naive local and systemic modules during early *X. fastidiosa* infection. For each local-systemic module overlap, the number of shared genes and their corresponding modulation is indicated. Only functional categories with a P-value < 0.01 are listed. The analysis detected only three significant overlaps that occurred at the same

time in naive vines: one module overlap up-regulated at 4 hpi, one group up-regulated at 24 hpi, and another down-regulated at 48 hpi. The largest module overlap occurring at the same time was “Blue-Turquoise” with 187 up-regulated genes that showed enrichment of functional categories related to water transport and secondary metabolism. At 24 hpi, most enriched functional categories were associated with ion and peptide transporters, with the exception of a single “Hormone signaling” category (Table S1). The overlapping genes under this category like *VvERF064*, Dehydration-induced protein, and *VvNCED2* participate in ethylene and ABA signaling and are known to engage in drought stress tolerance [64–67].These drought stress responses, especially ethylene signaling, are commonly induced in PD-infected vines[15,16]. Additionally, SA-biosynthesis gene, *enhanced disease susceptibility 5* or *EDS5* (*VIT_03s0038g00410*), was up-regulated under the same category suggesting naive vines perceived X. fastidiosa as a biotic stress at this point. By 48 hpi, naive vines displayed down-regulation of overlapping modules “Turquoise-Brown” for local and systemic tissues that were generally enriched in transcription factors and protein folding genes.

Sample ID	Tissue	Time	File name	Raw reads	Parsed reads	%	Unambiguously mapped	%
H2O_PBS_4H_P_1	Point of inoculation	4 h	1P_S287_L007_R1_001.fastq.gz	12,654,984	12,629,071	99.80	9,841,360	77.9
H2O_PBS_4H_P_2	Point of inoculation	4 h	25P_S306_L008_R1_001.fastq.gz	20,582,144	20,513,412	99.67	16,260,146	79.3
H2O_PBS_4H_P_3	Point of inoculation	4 h	49P_S311_L008_R1_001.fastq.gz	15,387,134	15,346,393	99.74	12,090,047	78.8
H2O_PBS_24H_P_1	Point of inoculation	24 h	3P_S289_L007_R1_001.fastq.gz	12,673,475	12,646,993	99.79	10,026,129	79.3
H2O_PBS_24H_P_2	Point of inoculation	24 h	27P_S308_L008_R1_001.fastq.gz	13,664,131	13,623,900	99.71	10,792,799	79.2
H2O_PBS_24H_P_3	Point of inoculation	24 h	51P_S313_L008_R1_001.fastq.gz	16,246,682	16,205,181	99.74	12,860,118	79.4
H2O_PBS_48H_P_1	Point of inoculation	48 h	5P_S291_L007_R1_001.fastq.gz	13,110,729	13,070,242	99.69	10,329,139	79.0
H2O_PBS_48H_P_2	Point of inoculation	48 h	29P_S310_L008_R1_001.fastq.gz	14,328,241	14,289,331	99.73	11,261,597	78.8
H2O_PBS_48H_P_3	Point of inoculation	48 h	53P_S315_L008_R1_001.fastq.gz	15,522,221	15,490,628	99.80	12,273,612	79.2
H2O_PBS_4H_S_1	Systemic	4 h	2P_S288_L007_R1_001.fastq.gz	13,385,557	13,356,313	99.78	10,648,375	79.7
H2O_PBS_4H_S_2	Systemic	4 h	26P_S307_L008_R1_001.fastq.gz	13,318,502	13,279,537	99.71	10,426,466	78.5
H2O_PBS_4H_S_3	Systemic	4 h	50P_S312_L008_R1_001.fastq.gz	15,047,873	15,006,225	99.72	11,967,771	79.8
H2O_PBS_24H_S_1	Systemic	24 h	4P_S290_L007_R1_001.fastq.gz	14,862,867	14,831,498	99.79	11,719,833	79.0
H2O_PBS_24H_S_2	Systemic	24 h	28P_S309_L008_R1_001.fastq.gz	12,282,574	12,249,406	99.73	9,656,496	78.8
H2O_PBS_24H_S_3	Systemic	24 h	52P_S314_L008_R1_001.fastq.gz	17,376,759	17,336,264	99.77	13,758,768	79.4
H2O_PBS_48H_S_1	Systemic	48 h	6P_S292_L007_R1_001.fastq.gz	11,939,177	11,908,866	99.75	9,457,485	79.4
H2O_PBS_48H_S_2	Systemic	48 h	30P_S311_L008_R1_001.fastq.gz	18,032,341	17,979,927	99.71	14,113,780	78.5
H2O_PBS_48H_S_3	Systemic	48 h	54P_S316_L008_R1_001.fastq.gz	16,428,371	16,393,028	99.78	13,032,774	79.5
H2O_Xf_4H_P_1	Point of inoculation	4 h	7P_S293_L007_R1_001.fastq.gz	11,652,657	11,622,494	99.74	9,329,299	80.3
H2O_Xf_4H_P_2	Point of inoculation	4 h	31P_S312_L008_R1_001.fastq.gz	15,782,697	15,739,685	99.73	12,556,971	79.8
H2O_Xf_4H_P_3	Point of inoculation	4 h	55P_S317_L008_R1_001.fastq.gz	14,952,110	14,919,013	99.78	11,890,510	79.7
H2O_Xf_24H_P_1	Point of inoculation	24 h	9P_S295_L007_R1_001.fastq.gz	12,770,535	12,742,804	99.78	10,072,113	79.0
H2O_Xf_24H_P_2	Point of inoculation	24 h	33P_S314_L008_R1_001.fastq.gz	17,167,649	17,124,905	99.75	13,645,379	79.7
H2O_Xf_24H_P_3	Point of inoculation	24 h	57P_S319_L008_R1_001.fastq.gz	14,852,917	14,817,022	99.76	11,821,253	79.8
H2O_Xf_48H_P_1	Point of inoculation	48 h	11P_S297_L007_R1_001.fastq.gz	13,669,041	13,637,621	99.77	11,005,518	80.7
H2O_Xf_48H_P_2	Point of inoculation	48 h	35P_S316_L008_R1_001.fastq.gz	13,727,503	13,682,466	99.67	10,880,663	79.5
H2O_Xf_48H_P_3	Point of inoculation	48 h	59P_S321_L008_R1_001.fastq.gz	17,729,131	17,692,032	99.79	14,257,462	80.6
H2O_Xf_4H_S_1	Systemic	4 h	8P_S294_L007_R1_001.fastq.gz	12,321,377	12,300,090	99.83	9,860,788	80.2
H2O_Xf_4H_S_2	Systemic	4 h	32P_S313_L008_R1_001.fastq.gz	16,353,509	16,311,121	99.74	12,941,916	79.3
H2O_Xf_4H_S_3	Systemic	4 h	56P_S318_L008_R1_001.fastq.gz	13,481,898	13,455,134	99.80	10,711,831	79.6
H2O_Xf_24H_S_1	Systemic	24 h	10P_S296_L007_R1_001.fastq.gz	10,778,496	10,738,292	99.63	8,543,561	79.6
H2O_Xf_24H_S_2	Systemic	24 h	34P_S315_L008_R1_001.fastq.gz	12,760,463	12,732,117	99.78	10,072,992	79.1
H2O_Xf_24H_S_3	Systemic	24 h	58P_S320_L008_R1_001.fastq.gz	13,122,145	13,078,819	99.67	10,413,944	79.6
H2O_Xf_48H_S_1	Systemic	48 h	12P_S298_L007_R1_001.fastq.gz	13,040,203	13,017,231	99.82	10,414,940	80.0
H2O_Xf_48H_S_2	Systemic	48 h	36P_S317_L008_R1_001.fastq.gz	12,089,824	12,029,207	99.50	9,480,976	78.8
H2O_Xf_48H_S_3	Systemic	48 h	60P_S322_L008_R1_001.fastq.gz	15,715,508	15,683,693	99.80	12,451,475	79.4
LPS_PBS_4H_P_1	Point of inoculation	4 h	13P_S299_L007_R1_001.fastq.gz	13,317,209	13,289,285	99.79	10,533,932	79.3
LPS_PBS_4H_P_2	Point of inoculation	4 h	37P_S318_L008_R1_001.fastq.gz	18,754,601	18,708,505	99.75	14,890,642	79.6
LPS_PBS_4H_P_3	Point of inoculation	4 h	61P_S323_L008_R1_001.fastq.gz	14,961,510	14,911,821	99.67	11,829,703	79.3
LPS_PBS_24H_P_1	Point of inoculation	24 h	15P_S301_L007_R1_001.fastq.gz	12,991,594	12,965,292	99.80	10,305,685	79.5
LPS_PBS_24H_P_2	Point of inoculation	24 h	39P_S320_L008_R1_001.fastq.gz	17,829,917	17,785,987	99.75	14,200,166	79.8
LPS_PBS_24H_P_3	Point of inoculation	24 h	63P_S325_L008_R1_001.fastq.gz	14,316,490	14,272,446	99.69	11,360,128	79.6
LPS_PBS_48H_P_1	Point of inoculation	48 h	17P_S303_L007_R1_001.fastq.gz	14,230,728	14,203,736	99.81	11,427,706	80.5
LPS_PBS_48H_P_2	Point of inoculation	48 h	41P_S322_L008_R1_001.fastq.gz	20,720,750	20,667,279	99.74	16,515,596	79.9
LPS_PBS_48H_P_3	Point of inoculation	48 h	65P_S327_L008_R1_001.fastq.gz	13,906,943	13,867,920	99.72	11,007,840	79.4
LPS_PBS_4H_S_1	Systemic	4 h	14P_S300_L007_R1_001.fastq.gz	13,712,820	13,686,616	99.81	10,815,968	79.0
LPS_PBS_4H_S_2	Systemic	4 h	38P_S319_L008_R1_001.fastq.gz	16,118,151	16,074,409	99.73	12,774,429	79.5
LPS_PBS_4H_S_3	Systemic	4 h	62P_S324_L008_R1_001.fastq.gz	16,862,134	16,822,059	99.76	13,397,966	79.6
LPS_PBS_24H_S_1	Systemic	24 h	16P_S302_L007_R1_001.fastq.gz	13,810,822	13,784,451	99.81	11,043,558	80.1
LPS_PBS_24H_S_2	Systemic	24 h	40P_S321_L008_R1_001.fastq.gz	16,842,813	16,802,784	99.76	13,354,296	79.5
LPS_PBS_24H_S_3	Systemic	24 h	64P_S326_L008_R1_001.fastq.gz	16,180,097	16,145,467	99.79	12,814,944	79.4
LPS_PBS_48H_S_1	Systemic	48 h	18P_S304_L007_R1_001.fastq.gz	13,203,691	13,176,335	99.79	10,588,108	80.4
LPS_PBS_48H_S_2	Systemic	48 h	42P_S323_L008_R1_001.fastq.gz	11,725,610	11,685,919	99.66	9,211,800	78.8
LPS_PBS_48H_S_3	Systemic	48 h	66P_S328_L008_R1_001.fastq.gz	15,216,103	15,184,590	99.79	12,039,246	79.3
LPS_Xf_4H_P_1	Point of inoculation	4 h	19P_S305_L007_R1_001.fastq.gz	14,120,386	14,092,321	99.80	11,233,441	79.7
LPS_Xf_4H_P_2	Point of inoculation	4 h	43P_S324_L008_R1_001.fastq.gz	13,803,783	13,768,991	99.75	10,817,095	78.6
LPS_Xf_4H_P_3	Point of inoculation	4 h	67P_S329_L008_R1_001.fastq.gz	16,665,327	16,627,545	99.77	13,227,882	79.6
LPS_Xf_24H_P_1	Point of inoculation	24 h	21P_S307_L007_R1_001.fastq.gz	12,812,699	12,786,756	99.80	10,058,758	78.7
LPS_Xf_24H_P_2	Point of inoculation	24 h	45P_S326_L008_R1_001.fastq.gz	15,894,050	15,863,539	99.81	12,741,515	80.3
LPS_Xf_24H_P_3	Point of inoculation	24 h	69P_S331_L008_R1_001.fastq.gz	12,944,892	12,914,181	99.76	10,348,709	80.1
LPS_Xf_48H_P_1	Point of inoculation	48 h	23P_S309_L007_R1_001.fastq.gz	13,987,548	13,953,383	99.76	11,026,973	79.0
LPS_Xf_48H_P_2	Point of inoculation	48 h	47P_S328_L008_R1_001.fastq.gz	16,029,098	15,986,803	99.74	12,762,895	79.8
LPS_Xf_48H_P_3	Point of inoculation	48 h	71P_S333_L008_R1_001.fastq.gz	16,201,864	16,165,079	99.77	11,610,563	71.8
LPS_Xf_4H_S_1	Systemic	4 h	20P_S306_L007_R1_001.fastq.gz	14,840,938	14,813,253	99.81	11,831,789	79.9
LPS_Xf_4H_S_2	Systemic	4 h	44P_S325_L008_R1_001.fastq.gz	18,312,844	18,260,789	99.72	14,490,917	79.4
LPS_Xf_4H_S_3	Systemic	4 h	68P_S330_L008_R1_001.fastq.gz	15,436,355	15,404,061	99.79	12,292,227	79.8
LPS_Xf_24H_S_1	Systemic	24 h	22P_S308_L007_R1_001.fastq.gz	15,838,864	15,799,858	99.75	12,488,204	79.0
LPS_Xf_24H_S_2	Systemic	24 h	46P_S327_L008_R1_001.fastq.gz	18,506,462	18,449,922	99.69	14,694,746	79.6
LPS_Xf_24H_S_3	Systemic	24 h	70P_S332_L008_R1_001.fastq.gz	15,236,417	15,197,471	99.74	12,103,257	79.6
LPS_Xf_48H_S_1	Systemic	48 h	24P_S310_L007_R1_001.fastq.gz	13,002,070	12,976,855	99.81	10,339,789	79.7
LPS_Xf_48H_S_2	Systemic	48 h	48P_S329_L008_R1_001.fastq.gz	13,233,075	13,206,731	99.80	10,533,829	79.8
LPS_Xf_48H_S_3	Systemic	48 h	72P_S334_L008_R1_001.fastq.gz	15,276,198	15,236,151	99.74	12,148,030	79.7

Table S2.2. Summary of RNAseq data and mapping metrics. Reads were trimmed using Trimmomatic v.0.36 and trimmed single-end reads were mapped onto the predicted protein-coding sequences of V. vinifera 'PN40024' using Bowtie2 v.2.3.4.1. Counts of reads mapping uniquely onto the grape reference transcriptome (i.e., with Q > 30) were extracted using sam2counts.py v.0.91.

Chapter III

Xylella fastidiosa Utilizes a β-1,4-endoglucanase to Modulate Exopolysaccharide Production and the Dynamics of Biofilm Development

Abstract

Xylella fastidiosa is a Gram-negative bacterium that causes disease in many economically important crops. It colonizes the plant host xylem and the mouthparts of its insect vectors where it produces exopolysaccharide (EPS) and forms robust biofilms. Here we demonstrate that the *X. fastidiosa* EPS is a β-1,4-glucan backbone with alternating 3-linked side chains, one with terminal β-glucuronic acid and α-1,2-mannose residues, and the other with a terminal β-glucose and α-1,2-mannose residues. An endoglucanase mutant, Δ*engXCA2*, has a hypermucoid colony morphotype *in vitro* indicating that EngXCA2 is involved in EPS processing and/or turnover. Furthermore, Δ*engXCA2* was severely impaired in several key steps in biofilm development that included cell-cell aggregation, attachment to surface substrata and biofilm maturation. *In vitro*, Δ*engXCA2* biofilms were structurally compromised compared to wildtype biofilms. *In planta*, Δ*engXCA2* biofilms were encased in copious amounts of EPS compared to wild type biofilms which corroborates our *in vitro* findings of hypermucoidy. Recombinant EngXCA2 digested *X. fastidiosa* EPS confirming that EngXCA2 utilizes the EPS as a substrate. These results demonstrate that EngXCA2 plays an important role in regulating *X. fastidiosa* biofilm formation through enzymatic degradation of the β-1,4-glucan backbone of EPS.

Introduction

Xylella fastidiosa is a fastidious, Gram-negative bacterium that causes disease in many economically important crops including grape, olive, citrus, coffee, and almond. This plant-pathogenic bacterium resides exclusively in the foregut of its insect vectors and in the xylem of its plant hosts [1,2]. *X. fastidiosa* is endemic to the Americas and recently emerged in Europe in 2013 where it is severely impacting Italy's olive trees [3]. *X. fastidiosa* subsp. *fastidiosa*, the causal agent of Pierce's disease of grapevine (PD), was first observed in southern California in the 1800's and it still remains a significant problem for raisin, table, and wine grape growers in the U.S.

X. fastidiosa forms robust biofilms in the xylem and in the precibarial trough and cibarium of its insect vectors, *Graphocephala atropunctata* and *Homalodisca vitripennis* [1,3]. Biofilms are organized multicellular aggregates enclosed in a protective self-produced matrix. Biofilm formation begins with the attachment of planktonic cells to a surface and is mediated by fimbrial and afimbrial adhesins and cell surface charges. After attachment, cells will multiply and aggregate to each other to form microcolonies. Cells then begin secreting extracellular polymeric substances such as polysaccharides, extracellular DNA, proteins, and lipids to form the biofilm matrix. Once the biofilm is mature, it can be reconfigured and degraded to promote growth of the biofilm or initiate cell dispersal. The release from the biofilm allows cells to return to the planktonic state to explore and begin the colonization of a new niche [4,5]. *X. fastidiosa* resides in the xylem of grapevines under both planktonic and biofilm states [6].

Both the insect foregut and the plant xylem are environments where *X. fastidiosa* experiences extreme high shear stress making robust adherence to the xylem wall or insect cuticle an integral component of the *X. fastidiosa*-host interaction [7]. During insect acquisition, *X. fastidiosa* utilizes type I pili afimbrial adhesins and LPS for initial attachment to the foregut cuticle [8–11]. Exopolysaccharide (EPS) is also required for attachment to the insect cuticle [12–14]. *In planta*, EPS production is associated with biofilm maturation. Confocal images of mature biofilms showed that *X. fastidiosa* EPS is intercalated throughout the mature biofilm matrix indicating it is likely a critical structural component that contributes to the architecture of the biofilm [15]. The regulation of genes required for colonization is density-dependent through the diffusible signaling factor (DSF) molecule [16]. At high levels, the DSF molecule promotes the up-regulation of surface adhesins and EPS and the down-regulation of type IV twitching motility. It has been proposed that when cells are in high numbers in the xylem, the accumulation of DSF causes *X. fastidiosa* cells to become stickier allowing them to be easily acquired by the sharpshooter [2]. In addition, *X. fastidiosa* possesses several two-component regulatory systems and several response regulators that could promote fine-tuning of gene expression [17].

Because the *X. fastidiosa* EPS operon is homologous to *Xanthomonas campestris* EPS operon, the structure of *X. fastidiosa* EPS is predicted to be similar in structure and composition to xanthan gum. Genomic analysis predicted the EPS have a β-1,4-glucan backbone that links a side chain composed of one mannose which can be acetylated and one glucuronic acid residue [15,18]. However, the structure and composition was not

fully characterized due to the limitations of small amounts of EPS production by *X. fastidiosa in vitro*. However, with the advent of additional medium types that allow for growth of this fastidious organism, we have determined that XFM medium induces EPS production to levels that allow for sufficient EPS for purification and downstream carbohydrate analysis.

The glycoside hydrolase EngXCA2, is a type II secreted β-1,4-endoglucanase with a hydrolytic N-terminal domain and a C-terminal cellulose binding domain. This protein belongs to the glycoside hydrolase family 5 and can degrade carboxymethyl cellulose and xyloglucan *in vitro*. Moreover, in tandem with a polygalacturonase, EngXCA2 degrades grapevine pit membranes [15,19]. Glycoside hydrolases from this family can also degrade bacterial carbohydrate polymers and many of them harbor catalytic promiscuity, meaning they can cleave more than one substrate [20]. Interestingly, an *engXCA2* deletion mutant, *ΔengXCA2*, is hypervirulent in planta suggesting an secondary virulence mechanism for this endoglucanase in addition to its role in dismantling pit membranes [21]. Biofilm formation is commonly correlated with virulence in pathogenic bacteria. However, non-aggregating mutant strains of *X. fastidiosa* are typically hypervirulent in planta [16,22–24]. Thus, it's hypothesized that *X. fastidiosa* attenuates its virulence through autoaggregation in the xylem of grapevines to prevent killing its plant host too quickly. In this study, we investigate *X. fastidiosa* EngXCA2's involvement in EPS biosynthesis and biofilm development.

Materials and Methods

Bacterial strains. *X. fastidiosa* subsp. *fastidiosa* Temecula1 wildtype and Δ*engXCA2* mutant strains were grown on solid PD3 medium at 28°C for five days. Repeated attempts to obtain transformant colonies for gene complementation of Δ*engXCA2* were previously unsuccessful and again during this study [21]. Because *X. fastidiosa* complementation tools are limited, attempts at *in trans* gene complementation are often not successful [39].

Exopolysaccharide extraction and quantification. *X. fastidiosa* cells were harvested from solid PD3 plates and adjusted to $OD_{600\ nm}$= 0.5 in XFM medium and cells were added to 15 mL XFM-pectin liquid cultures to a final $OD_{600\ nm}$=0.05 and grown at 28°C, 180 rpm for six days Killiny et al. (2009). After six days, the $OD_{600\ nm}$ was recorded and cultures were centrifuged at 7,000 rpm at 4°C for 20 minutes. 10 mL of the supernatant were collected and placed in a 50 mL conical tube, mixed with 30 mL cold 95% ethanol, and placed at -80°C for 30 min then centrifuged 7,000 rpm at 4°C for 20 min and supernatants were discarded. Pellets were washed 2X with 10 mL cold 70% ethanol. A steel grinding ball (size ⅜ in., BC Precision) and 10 mL water was added to the EPS pellet. Then, the tubes were placed inside a shaker (200-300 rpm) for 1 hr. to break up and resuspend the pellet.

To quantify total EPS, we performed a phenol-sulfuric acid assay to quantify total neutral sugar content. 500 µL EPS sample in water was added to a clean test tube with a cap. Then, 500 µL 5% phenol (Acros organics, Cat. No. 327105000) and 2.5 mL concentrated sulfuric acid (Fisher Scientific, Cat. No. S25894) were carefully added to

the sample and gently vortexed to mix solution. Samples were cooled on ice and the absorbance was then recorded at 488 nm. A dilution series of known concentrations of glucose were used to create a standard curve.

Cell surface attachment to glass assay. This assay was adapted from Espinosa-Urgel et al. (2000). Cells were harvested from solid PD3 plates and $OD_{600\ nm}$ was adjusted to 0.25 in liquid PD3 medium. 500 µL of this was sub-cultured into 5 mL of PD3 in a 13 x 100 mm glass tube. Cultures were incubated at 28°C, 100 rpm for 7 days. 500 µL of 1% crystal violet was added to the culture and allowed to incubate at room temperature for 20 min. The culture and stain mixture was carefully decanted to prevent biofilm disruption. The tube was then gently washed 3X with 1 mL water and allowed to dry overnight. 2 mL 30% acetic acid was used to dissolve the crystal violet-stained biofilm. Optical density was measured at 600nm using 30% acetic acid as a blank.

Cell-cell aggregation assay. Cells were harvested from solid PD3 plates and adjusted to $OD_{600\ nm}$ =0.25 in liquid PD3 medium. 500 µL culture was subcultured into 5 mL of PD3 in a 13 x 100 mm glass tube. Cultures were incubated at 28°C without agitation for 10 days. After incubation, cultures were gently agitated by hand and then left undisturbed for 20 min to promote settling of cell aggregates to the bottom of the tube. The top 1 mL of the cultured was collected (ODs) and its $OD_{540\ nm}$ was measured and returned to the culture tube. Then, the entire culture was vortexed thoroughly to disperse cell aggregates

and a1 mL aliquot was measured at $OD_{540\ nm}$ (ODt). The percent aggregation was calculated as [(ODt-ODs)/ODt]*100.

Antimicrobial sensitivity assay. This assay was adapted from Aldrich et al. (2015). Cells were harvested from solid PD3 plates and $OD_{600\ nm}$ was adjusted to 0.1 in liquid PD3 medium. 300 µL culture was mixed with 3 mL of PD3 top agar (0.8%) and gently overlaid on top of a 20 mL PD3 agar plate already solidified. Top agar plates were incubated at 28°C for 2 days and filter discs containing compound of interest, 20 µL of 100 mM H_2O_2 or 20 µL polymyxin B (1 mg/mL), were placed on the plate. Plates were incubated again until the zone of inhibition appeared.

Confocal laser scanning microscopy. Cells were harvested from solid PD3 plates and the $OD_{600\ nm}$ was adjusted to 0.25 in liquid PD3 medium. 200 µL of this culture was added to 20 mL of liquid PD3 in a 50 mL conical tube containing a glass slide and incubated at 28°C, 180 rpm. After four days, biofilms formed on both sides of the glass slide at the air-liquid interface, the glass slide was removed, and the biofilm on one side of the slide was removed with a Kimwipe. The intact biofilm on the other side of the slide was fixed with 4% paraformaldehyde for 15 min. The fixed biofilm was stained with 20 µM Syto 9 Green Fluorescent Nucleic Acid Stain (Invitrogen, Cat. No. S34854) for 15 min. in the dark. Slides were gently washed with 1X PBS and one drop of SlowFade Diamond Antifade Mountant (Invitrogen, Cat. No. S36967) was added to the biofilm before placing the cover slip. A Zeiss 880 inverted confocal scanning laser microscope

(UC Riverside Microscopy and Imaging Core Facility) with a 488 nm laser and a 63X oil immersion lens was used to acquire biofilm z-stack images. A total of 5 biological replicates were imaged with 5 images each taken for each biological replicate at random points along the length of the biofilm (beginning from one edge of the slide to the other) for a total of 25 data points.

BiofilmQ software analysis. Quantitative three-dimensional image analysis of biofilms was performed using BiofilmQ software developed by Hartmann et al. (2021). Biofilm z-stack images were denoised by convolution using the default parameters. Floating cells were removed from images and a threshold of 100 vox was used to remove small artifacts due to noise. The Top-hat filter was set to 15 to remove background fluorescence. Images were segmented automatically using the Otsu algorithm with a sensitivity of 1.75.

Scanning electron microscopy of in planta biofilms. *X. fastidiosa* subsp. *fastidiosa* Temecula1 wildtype and Δ*engXCA2* strains were grown on solid PD3 medium at 28°C for five days. Three grapevines were inoculated with 40 µL of *X. fastidiosa* wildtype inoculum in 1X PBS (10^8 CFU/mL) at the second true internode using the needle-inoculation method described by Hill and Purcell. Three grapevines were inoculated with 1X PBS as negative controls. At 15 weeks post-inoculation, the internode located 20 nodes above the point of inoculation and the three petioles closest to it were collected, cut into three equal length pieces, and fixed in a 70% ethanol, 5% glacial acetic acid, and 5%

formalin solution. Samples were prepared for SEM and imaged according to Ingel et al. (2020).

Structural characterization of exopolysaccharide. EPS extraction was carried out as described above. The removal of contaminating protein in the *X. fastidiosa* EPS preparation was accomplished by enzymatic digestion using proteinase K (Sigma) (20 U Proteinase/mL) in 50 mM MgCl buffer (pH 7.5) overnight at 50°C (10 mg of EPS /mL solution). After overnight digestion, 10 U Pronase (Roche)/ml solution was added, and digestion was carried out as above for an additional 12 hours. After the second round of digestion was complete, the sample was dialyzed against deionized water using a 50 kDa dialysis membrane (SpectraPor®) at 4°C for 3 days, with the water being exchanged each day.

Nuclear magnetic resonance (NMR) data were acquired on a Bruker 600 MHz spectrometer equipped with a 5 mm TXI cryo-probe at probe temperature 45 0C, except otherwise stated. Between 5 - 10 mg of the samples were permethylated and dissolved in 550 µL chloroform-d prior to NMR acquisition. The following general parameters were used for NMR data acquisition: ^{1}H NMR experiment (600 Hz spectral width, 8,192 t1 points and 4 scans); COSY experiment (5144.0*5144.0 F1*F2 spectral width, 1024*512 t2*t1 points and 4 scans); HSQC experiment (5144.0*10570.8 F1*F2 spectral width, 1024*512 t2*t1 points, 145 Hz 1JCH delay and 10 scans); HSQC_TOCSY experiment (5208.3*10570.8 F1*F2 spectral width, 1024*512 t2*t1 points, 145 Hz 1JCH delay, 18 ms mixing time and 24 scans); HMQC_NOESY experiment (5208.3*10570.8 F1*F2

spectral width, 1024*512 t2*t1 points, 145 Hz 1JCH delay, 60 ms mixing time and 182 scans); HMBC experiment (5319.1*10570.8 F1*F2 spectral width, 1536*512 t2*t1 points at 50 % non-uniform sampling in the indirect dimension, 8 Hz 1JCH delay and 540 scans); TOCSY experiment (6250.0*6250.0 F1*F2 spectral width, 1536*512 t2*t1 points, 60 ms spin-lock time and 8 scans); ROESY experiment (6250.0*6250.0 F1*F2 spectral width, 1536*512 t2*t1 points, 70 ms mixing time and 24 scans).

EPS extraction and recombinant EngXCA2 expression for reducing sugar assay. EPS was extracted from Δ*engXCA2* cultures in XFM liquid medium that was slightly modified from Killiny et al. (2009) to increase EPS production. In brief, 5 mL hemin chloride (0.05% in NaOH 0.5 μM), 1.5 g casamino acids (Acros Organics, Cat. No. 61204-1000), 0.25 g bovine serum albumin (Sigma-Aldrich, Cat. No. A4503-100G), and 0.1 g Galacturonic acid sodium salt (Sigma-Aldrich, Cat. No. 73960-5G-F) were added to 200 mL water and filter sterilized (0.22 μm filter). This was then added to 800 mL of autoclaved XFM medium. *X. fastidiosa* was grown and EPS was extracted as described above. After six days of growth, cultures were centrifuged at 7,000 rpm at 4°C for 20 minutes. Ten mL of the supernatant were collected and placed in a 50 mL conical tube, mixed with 30 mL cold 95% ethanol, and stored in a -80°C freezer for 30 min. The solution mixture was centrifuged at 7,000 rpm at 4°C for 20 min and the supernatant discarded. The remaining pellet was resuspended in 5 mL water and 500 μL Proteinase K (Qiagen, Cat. No. 19133) and was incubated at room temperature on an orbital shaker overnight. Following this, the complete EPS extraction protocol described above was

repeated and the resulting pellet was resuspended in 2 mL sodium acetate buffer (100 mM, pH9). The EPS sample was heated at 95°C for 10 min. to deactivate the proteinase K and then dialysed overnight at 4°C against two changes of 1 L sodium acetate buffer using regenerated cellulose dialysis tubing with a 50 kDa molecular weight cutoff (Spectrum, Cat. No. 132542). EPS was quantified using the phenol-sulfuric acid method and stored at -20°C. Recombinant EngXCA2 expression was performed according to Ingel et al. (2019).

Reducing sugar assay. We performed this assay based on the protocol from Gross 1982. In brief, 650 µL of substrate (EPS or carboxymethylcellulose, 0.4 mg/mL) and 650 µL of *E. coli* cell lysate (harboring pMCR7 or pET20b(+) empty vector) were added to a small glass vial and incubated at 37°C, 120 rpm. A 200 µL aliquot was removed for each timepoint and added to 1 mL Na-borate and 200 µL 1% 2-cyanoacetamide in a new glass vial. The sample was vortexed and boiled for 10 min. After cooling to room temperature, absorbance was measured at 276 nm using a spectrophotometer. Absorbances were normalized to total protein in lysates from E. coli harboring pET20b(+) empty vector or pMCR7. Empty vector absorbance 276 nm/mg protein totals were subtracted from pMCR7. Protein from cell lysates were subjected to SDS-PAGE using a 10% polyacrylamide gel to confirm recombinant EngXCA2 expression. This experiment was performed with three technical replicates and repeated three times.

Results

Δ*engXCA2* is hypermucoid *in vitro.* Qualitatively**,** Δ*engXCA2* has a hypermucoid phenotype with a loose slime layer when propagated on solid XFM medium supplemented with pectin as compared to wildtype *X. fastidiosa*. Quantitatively, Δ*engXCA2* cells produced significantly more EPS when propagated in liquid XFM medium supplemented with pectin as compared to wildtype (Figure 3.1A).

Δ*engXCA2* is defective in the early steps of biofilm formation: cell-surface attachment and cell-cell aggregation. A critical early step of biofilm formation is the ability of cells to attach to a surface. When grown upright in glass tubes in liquid medium, *X. fastidiosa* forms biofilms at the air-liquid interface. We quantified cell-surface attachment using glass as the surface substrate using a colorimetric crystal violet assay. Wildtype biofilms formed a thicker cell surface attachment ring and, thus, retained more crystal violet than Δ*engXCA2* biofilms indicating that Δ*engXCA2* was significantly impaired in attachment to the glass substrate (Figure 3.1B and C). Cell-cell aggregation, or auto-aggregation, is a critical early step in forming a biofilm [11,25]. *X. fastidiosa* is particularly adept at cell-cell aggregation, particularly when propagated in liquid medium. *X. fastidiosa* has a high propensity to self-aggregate and forms large, visible aggregates in culture that are very difficult to disperse via agitation or vortexing. Quantitatively, Δ*engXCA2* aggregates significantly less than wildtype (Figure 3.1D). In addition, this lack of aggregation phenotype can also be observed visually because Δ*engXCA2* appears turbid in liquid culture rather than in aggregates like the wildtype parent (Figure 3.1E).

Δ*engXCA2 in vitro* biofilms have altered 3-dimensional biofilm architecture. To determine how overproduction of EPS affected Δ*engXCA2* biofilm architecture, we examined Δ*engXCA2* biofilms grown on a glass surface using confocal laser scanning microscopy. After four days of incubation in liquid medium, both wildtype and Δ*engXCA2* cells had formed biofilms on the glass slide. However, Δ*engXCA2* biofilms colonized less glass surface area than wildtype and localized thickness measurements obtained using BiofilmQ software indicated that Δ*engXCA2* biofilms were thinner than wildtype biofilms [27]. Specifically, Δ*engXCA2* and wild type biofilms were 5.68 μm and 14.58 μm in thickness, respectively (Figures 3.3A-D). Furthermore, we used BiofilmQ software to segment the z-stack images and measure each point from the glass substrate to the highest point of the biofilm (Figure 3.3B and D). From this, we determined that the highest peaks in the wild type biofilms had a median height of 15.03 μm and the highest peaks in the Δ*engXCA2* biofilms had a median height of 8.32 μm (Figure 3.4B). Overall, Δ*engXCA2* had significantly less biomass with an average of 5.02 mm^3 in comparison to wildtype that had an average biomass volume of 8.47 mm^3. Finally, average roughness coefficients for the two strains indicate that Δ*engXCA2* biofilms had a more uneven or rougher surface than wildtype which had a smoother surface, 0.221 and 0.149 respectively. Taken together, these assay results show that *ΔengXCA2* biofilms are compromised in their capacity to construct a mature biofilm architecture.

Deletion of *engXCA2* sensitizes cells to membrane disrupting antimicrobials

hydrogen peroxide and polymyxin B. In addition to playing a role in early biofilm formation, autoaggregation can also protect bacteria from exposure to antimicrobial host responses and/or environmental stresses [25]. Because Δ*engXCA2* cells are impaired in cell-cell aggregation, we hypothesized this strain was more sensitive to antimicrobials. After treating wildtype and Δ*engXCA2* with hydrogen peroxide or polymyxin b, we measured the zones of inhibition and found that Δ*engXCA2* cells are more susceptible to these antimicrobials suggesting that cell-cell aggregation is an important mechanism for *X. fastidiosa* resistance against antimicrobial compounds in the xylem, as well as for biofilm formation (Figure 3.2).

***In vivo,* Δ*engXCA2* biofilms are encased in copious amounts of EPS.** Because Δ*engXCA2* biofilm formation was impaired *in vitro*, we investigated if this phenotype was recapitulated *in vivo*. Using Scanning electron microscopy (SEM), we analyzed Δ*engXCA2* and wildtype biofilms that were formed in the xylem of grapevines stems and petioles. Δ*engXCA2* bacterial cells were encased in large amounts of EPS as compared to wildtype (Figure 3.5A-F), which corroborated our *in vitro* findings. However, contrary to our observations *in vitro,* these biofilms were more dense than wildtype biofilms in both stems and petioles. Specifically, in petioles, the majority of Δ*engXCA2* cells were part of biofilms that extensively colonized the xylem, whereas wildtype cells were rarely present in petiole samples. Stem samples were colonized by both wildtype and Δ*engXCA2,* but both were at different stages of biofilm development. Wildtype cells were observed as single cells attached to the xylem wall, as microcolonies, and in mature biofilms. In

contrast, Δ*engXCA2* was not frequently observed as individual cells or microcolonies but rather were frequently present in mature biofilms that filled the vessel lumen. No bacterial cells were observed in PBS mock-inoculated vines (Figure 3.5G-I).

Structural characterization of *X. fastidiosa* EPS. EPS plays a major role in vector transmission and disease development in grapevines, but its structure has not been fully elucidated [12]. The *X. fastidiosa* genome contains an operon that is similar to the well characterized xanthan gum biosynthetic operon produced by the phylogenetically related *Xanthomonas campestris* [18]. The composition of the EPS was predicted to consist of a tetrasaccharide subunit with a β-1,4-glucan backbone and a single sidechain composed of a terminal β-glucuronic acid and an acetylated α-1,2-mannose linked at the 3-position, which is structurally similar to but not exactly like xanthan gum [18]. Our compositional and structural analyses indicated that, indeed, *X. fastidiosa* EPS is similar to xanthan, but with notable differences. Specifically, *X. fastidiosa* EPS consists of octasaccharide repeating units composed of a β-1,4-glucan backbone with two different alternating 3-linked side chains, one with terminal β-glucuronic acid and α-1,2-mannose residues, and the other with terminal β-glucose and α-1,2-mannose residues (Figure 3.6). We did not detect any acetylation on the EPS side chain as predicted by the genomic analysis [18].

Recombinant EngXCA2 cleaves Δ*engXCA2X. fastidiosa* EPS. Because Δ*engXCA2* had a hypermucoid phenotype that affected biofilm development, we hypothesized that EngXCA2 modulates EPS turnover and/or biosynthesis through enzymatic degradation of

the β-1,4-glucan backbone of EPS. We performed a reducing sugar assay to test EPS as a potential substrate for recombinant *X. fastidiosa* EngXCA2 protein expressed in *Escherichia coli*. Recombinant EngXCA2 can cleave carboxymethylcellulose (CMC) and xyloglucan *in vitro* and here we used CMC as a positive control in the reducing sugar assay [19]. Indeed, recombinant EngXCA2 cleaved EPS from Δ*engXCA2* as indicated by the production of reducing ends over time (Figure 3.8). Similarly, our collaborators used this recombinant protein to break down wildtype EPS for its structural characterization via MALDI-TOF-MS analysis (*data not shown*), showing again this endoglucanase can degrade EPS. These data confirm that EngXCA2 can utilize EPS as a substrate supporting our hypothesis that EngXCA2 plays a role in maintenance of the biofilm EPS matrix by enzymatic processing of the EPS polymer.

Discussion

The developmental regimen that leads to mature biofilm formation is a sequence of events that enables the transition from the planktonic lifestyle to a surface-attached multicellular community. Specifically, planktonic cells attach to a surface and these surface-attached founder cells undergo cell division, recruit cells and produce an extracellular matrix that encases their progeny and cell recruits to form microcolonies that develop into mature biofilms. A major component of the matrix is EPS. EPS is critical for building and maintaining the architecture of a mature biofilm but the mechanisms that underlie EPS processing and turnover in a developing biofilm is an active area of research.

Compositional and structural analysis indicated that the EPS of *X. fastidiosa* consists of a β-1,4-glucan backbone and recombinant *X. fastidiosa* EngXCA2 enzymatically cleaved the *X. fastidiosa* EPS confirming that EngXCA2 can use *X. fastidiosa* EPS as a substrate. In the human pathogen, *Pseudomonas aeruginosa*, enzymatic digestion of one its major EPS polymers, Pel EPS, by the endogenous PelA glycoside hydrolase is implicated in the dissolution stage of biofilm development when communal cells leave the biofilm and return to the planktonic state to explore a new environment [31–33]. This stage is considered to be the last stage of the biofilm development cycle as the cells transition to re-enter the exploratory state. However, little is known about the mechanistic role of endogenous, self-produced EPS degradative enzymes in modulating biofilm structural integrity as a nascent biofilm matures. Deletion of the *engXCA2* gene in *X. fastidiosa* resulted in a hypermucoid phenotype and quantitative overproduction of EPS as compared to the wildtype parent which effectively impaired the cells from entering the early stages of biofilm formation, surface attachment and cell-cell aggregation. This suggests a role for EngXCA2 in EPS processing and/or turnover that has an intrinsic role in initiating early biofilm establishment. Over the course of biofilm development Δ*engXCA2* biofilms were structurally impaired. They were significantly thinner and had lower biomass indicating they contain fewer cells. Moreover, Δ*engXCA2* biofilms had higher surface roughness. These data, taken together, indicate that Δ*engXCA2* cells are impaired in building upon themselves as the biofilm matures.

In planta, Δ*engXCA2* biofilms were associated with a larger amount of EPS than the wild type parental strain, which substantiates our *in vitro* findings. Interestingly, Δ*engXCA2* biofilms were more qualitatively more compacted and filled more of the vessel lumen in the xylem in comparison to wildtype. Moreover, Δ*engXCA2* cells were observed in both stems and petioles, whereas wild type cells were only observed in stems. Because the cells were originally inoculated into the stem, the cells first need to traverse the stem to get to the petioles. The Δ*engXCA2* more readily moved into the petioles likely because of its non-aggregative phenotype. Aggregation deficient strains of *X. fastidiosa* often move faster and have a hypervirulent phenotype in grapevines. Δ*engXCA2* is hypervirulent in grapevines [21, 26]. It has been hypothesized that autoaggregation allows *X. fastidiosa* to attenuate its virulence to prevent killing its plant host too quickly. Excessive EPS may block cell surface adhesins required for cell-cell adhesion that effectively locks Δ*engXCA2* in a planktonic, exploratory state. The concomitant non-aggregative and hypervirulent phenotypes of Δ*engXCA2* corroborates this hypothesis.

To the best of our knowledge this is the first report of an endogenous EPS glycoside hydrolase that targets the major EPS component of its own self-produced biofilm matrix in a phytopathogenic bacterium. We speculate that EngXCA2 may be involved in processing the EPS from a higher molecular weight precursor to a lower molecular weight end product and the lack of pruning of the EPS result in the observed hypermucoid phenotype. It is not clear if EngXCA2-mediated processing of EPS occurs extracellularly or in the periplasmic space prior to secretion out of the cell. However, following repeated attempts, EngXCA2 has not been detected in the *X. fastidiosa*

secretome suggesting it is localized internally. In *P. aeruginosa*, the alginate lyase, AlgL, is localized in the periplasm and degrades mislocalized alginate that is trapped in the periplasmic space [29,30] and overexpression of the periplasmic glycoside hydrolase PslG affects EPS (Psl) synthesis [31]. Further localization studies for *X. fastidiosa* EngXCA2 are warranted to determine if it is localized to the cell surface, periplasm or cytoplasm. An imbalance of biofilm structural components (*i.e.* EPS, eDNA, adhesins) can lead to an architecturally unstable biofilm [28] and alteration of the quantity of matrix had clear negative impacts on overall biofilm thickness and structure.

Literature Cited

1. Hill BL, Purcell AH. Acquisition and retention of Xylella fastidiosa by an efficient vector, Graphocephala atropunctata. Phytopathology. 1995. Available: https://www.apsnet.org/publications/phytopathology/backissues/Documents/1995Articles/Phyto85n02_209.PDF

2. Chatterjee S, Almeida RPP, Lindow S. Living in two Worlds: The Plant and Insect Lifestyles of Xylella fastidiosa. Annu Rev Phytopathol. 2008;46: 243–271.

3. Rapicavoli J, Ingel B, Blanco-Ulate B. Xylella fastidiosa: An examination of a re-emerging plant pathogen. Mol Plant. 2017. Available: http://onlinelibrary.wiley.com/doi/10.1111/mpp.12585/full

4. Flemming H-C, Wingender J, Szewzyk U, Steinberg P, Rice SA, Kjelleberg S. Biofilms: an emergent form of bacterial life. Nat Rev Microbiol. 2016;14: 563–575.

5. Boyd A, Chakrabarty AM. Role of alginate lyase in cell detachment of Pseudomonas aeruginosa. Appl Environ Microbiol. 1994;60: 2355–2359.

6. Newman KL, Almeida RPP, Purcell AH, Lindow SE. Use of a green fluorescent strain for analysis of Xylella fastidiosa colonization of Vitis vinifera. Appl Environ Microbiol. 2003;69: 7319–7327.

7. Rapicavoli JN, Kinsinger N, Perring TM, Backus EA, Shugart HJ, Walker S, et al. O antigen modulates insect vector acquisition of the bacterial plant pathogen Xylella fastidiosa. Appl Environ Microbiol. 2015;81: 8145–8154.

8. Li Y, Hao G, Galvani CD, Meng Y, De La Fuente L, Hoch HC, et al. Type I and type IV pili of Xylella fastidiosa affect twitching motility, biofilm formation and cell-cell aggregation. Microbiology. 2007;153: 719–726.

9. Feil H, Feil WS, Lindow SE. Contribution of Fimbrial and Afimbrial Adhesins of Xylella fastidiosa to Attachment to Surfaces and Virulence to Grape. Phytopathology. 2007;97: 318–324.

10. Guilhabert MR, Kirkpatrick BC. Identification of Xylella fastidiosa Antivirulence Genes: Hemagglutinin Adhesins Contribute to X. fastidiosa Biofilm Maturation and Colonization …. Mol Plant Microbe Interact. 2005. Available: http://apsjournals.apsnet.org/doi/abs/10.1094/MPMI-18-0856

11. De La Fuente L, Montanes E, Meng Y, Li Y, Burr TJ, Hoch HC, et al. Assessing adhesion forces of type I and type IV pili of Xylella fastidiosa bacteria by use of a microfluidic flow chamber. Appl Environ Microbiol. 2007;73: 2690–2696.

12. Killiny N, Martinez RH, Dumenyo CK, Cooksey DA, Almeida RPP. The

exopolysaccharide of Xylella fastidiosa is essential for biofilm formation, plant virulence, and vector transmission. Mol Plant Microbe Interact. 2013;26: 1044–1053.

13. Roper MC, Greve LC, Labavitch JM, Kirkpatrick BC. Detection and Visualization of an Exopolysaccharide Produced by Xylella fastidiosa In Vitro and In Planta. Appl Environ Microbiol. 2007;73: 7252–7258.

14. Sahoo PK, Janissen R, Monteiro MP, Cavalli A, Murillo DM, Merfa MV, et al. Nanowire Arrays as Cell Force Sensors To Investigate Adhesin-Enhanced Holdfast of Single Cell Bacteria and Biofilm Stability. Nano Lett. 2016;16: 4656–4664.

15. Roper MC. The characterization and role of Xylella fastidiosa plant cell wall degrading enzymes and exopolysaccharide in Pierce's disease of grapevine. ProQuest. 2006.

16. Newman KL, Almeida RPP, Purcell AH, Lindow SE. Cell-cell signaling controls Xylella fastidiosa interactions with both insects and plants. Proc Natl Acad Sci U S A. 2004;101: 1737–1742.

17. Voegel TM, Doddapaneni H, Cheng DW, Lin H, Stenger DC, Kirkpatrick BC, et al. Identification of a response regulator involved in surface attachment, cell-cell aggregation, exopolysaccharide production and virulence in the plant pathogen Xylella fastidiosa. Mol Plant Pathol. 2013;14: 256–264.

18. da Silva FR, Vettore AL, Kemper EL, Leite A, Arruda P. Fastidian gum: the Xylella fastidiosa exopolysaccharide possibly involved in bacterial pathogenicity. FEMS Microbiol Lett. 2001;203: 165–171.

19. Pérez-Donoso AG, Sun Q, Roper MC, Greve LC, Kirkpatrick B, Labavitch JM. Cell wall-degrading enzymes enlarge the pore size of intervessel pit membranes in healthy and Xylella fastidiosa-infected grapevines. Plant Physiol. 2010;152: 1748–1759.

20. Aspeborg H, Coutinho PM, Wang Y, Brumer H 3rd, Henrissat B. Evolution, substrate specificity and subfamily classification of glycoside hydrolase family 5 (GH5). BMC Evol Biol. 2012;12: 186.

21. Ingel B, Jeske DR, Sun Q, Grosskopf J, Roper MC. Xylella fastidiosa Endoglucanases Mediate the Rate of Pierce's Disease Development in Vitis vinifera in a Cultivar-Dependent Manner. Mol Plant Microbe Interact. 2019; MPMI04190096R.

22. Gouran H, Gillespie H, Nascimento R, Chakraborty S, Zaini PA, Jacobson A, et al. The Secreted Protease PrtA Controls Cell Growth, Biofilm Formation and Pathogenicity in Xylella fastidiosa. Sci Rep. 2016;6: 31098.

23. Burbank LP, Stenger DC. The DinJ/RelE Toxin-Antitoxin System Suppresses Bacterial Proliferation and Virulence of Xylella fastidiosa in Grapevine. Phytopathology. 2017;107: 388–394.

24. Guilhabert MR, Hoffman LM, Mills DA, Kirkpatrick BC. Transposon mutagenesis of Xylella fastidiosa by electroporation of Tn5 synaptic complexes. Mol Plant Microbe Interact. 2001;14: 701–706.

25. Trunk T, Khalil HS, Leo JC. Bacterial autoaggregation. AIMS Microbiol. 2018;4: 140–164.

26. Roper C, Castro C, Ingel B. Xylella fastidiosa: bacterial parasitism with hallmarks of commensalism. Curr Opin Plant Biol. 2019;50: 140–147.

27. Hartmann R, Jeckel H, Jelli E, Singh PK, Vaidya S, Bayer M, et al. Quantitative image analysis of microbial communities with BiofilmQ. Nat Microbiol. 2021. doi:10.1038/s41564-020-00817-4

28. Reichhardt C, Wong C, Passos da Silva D, Wozniak DJ, Parsek MR. CdrA Interactions within the Pseudomonas aeruginosa Biofilm Matrix Safeguard It from Proteolysis and Promote Cellular Packing. MBio. 2018;9. doi:10.1128/mBio.01376-18

29. Farrell EK, Tipton PA. Functional characterization of AlgL, an alginate lyase from Pseudomonas aeruginosa. Biochemistry. 2012;51: 10259–10266.

30. Zhu B, Yin H. Alginate lyase: Review of major sources and classification, properties, structure-function analysis and applications. Bioengineered. 2015;6: 125–131.

31. Baker P, Whitfield GB, Hill PJ, Little DJ, Pestrak MJ, Robinson H, et al. Characterization of the Pseudomonas aeruginosa Glycoside Hydrolase PslG Reveals That Its Levels Are Critical for Psl Polysaccharide Biosynthesis and Biofilm Formation. J Biol Chem. 2015;290: 28374–28387.

32. Cherny KE, Sauer K. Untethering and Degradation of the Polysaccharide Matrix Are Essential Steps in the Dispersion Response of Pseudomonas aeruginosa Biofilms. J Bacteriol. 2020;202. doi:10.1128/JB.00575-19

33. Yu S, Su T, Wu H, Liu S, Wang D, Zhao T, et al. PslG, a self-produced glycosyl hydrolase, triggers biofilm disassembly by disrupting exopolysaccharide matrix. Cell Res. 2015;25: 1352–1367.

34. Mazur O, Zimmer J. Apo- and cellopentaose-bound structures of the bacterial cellulose synthase subunit BcsZ. J Biol Chem. 2011;286: 17601–17606.

35. Köseoğlu VK, Heiss C, Azadi P, Topchiy E, Güvener ZT, Lehmann TE, et al. Listeria monocytogenes exopolysaccharide: origin, structure, biosynthetic machinery and c-di-GMP-dependent regulation. Mol Microbiol. 2015;96: 728–743.

36. Köseoğlu VK, Agaisse H. Evolutionary Perspectives on the Moonlighting Functions of Bacterial Factors That Support Actin-Based Motility. MBio. 2019;10. doi:10.1128/mBio.01520-19

37. Singh N, Bhalla N. Moonlighting Proteins. Annu Rev Genet. 2020;54: 265–285.

38. Henderson B, Martin A. Bacterial virulence in the moonlight: multitasking bacterial moonlighting proteins are virulence determinants in infectious disease. Infect Immun. 2011;79: 3476–3491.

39. Kandel PP, Chen H, De La Fuente L. A Short Protocol for Gene Knockout and Complementation in Xylella fastidiosa Shows that One of the Type IV Pilin Paralogs (PD1926) Is Needed for Twitching while Another (PD1924) Affects Pilus Number and Location. Appl Environ Microbiol. 2018;84. doi:10.1128/AEM.01167-18

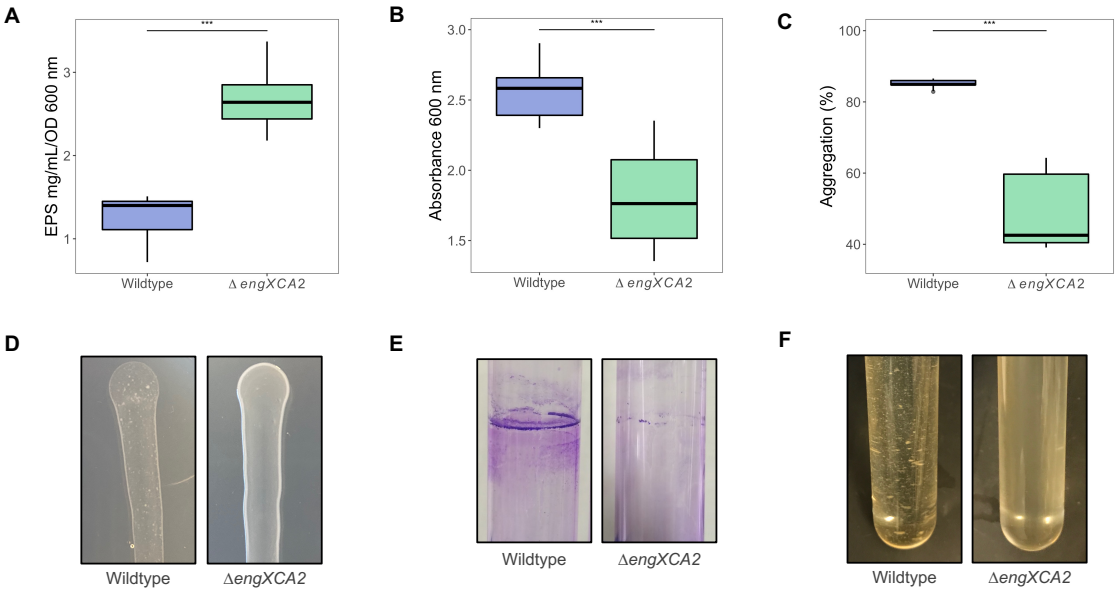

Figure 3.1. Δ*engXCA2* produces significantly more exopolysaccharide (EPS) and has impaired cell-cell aggregation and cell-surface attachment. (A) Quantification of EPS production in wildtype and ΔengXCA2 liquid culture (n = 9, ANOVA followed by Tukey's Honest Significant Difference test). (B) Quantification of cell-glass surface attachment at the air-liquid interphase (n = 9, ANOVA followed by Tukey's Honest Significant Difference test, asterisks indicate level of significance: * $P < 0.05$, ** $P < 0.01$, *** $P < 0.001$). (C) Cell-cell aggregation percentage in wildtype and ΔengXCA2 liquid cultures (n = 9, ANOVA followed by Tukey's Honest Significant Difference test). (D) Representative photographs of Δ*engXCA2* and wildtype growth on PD3 solid medium. (E) Representative photographs of crystal violet stained biofilm cells attached to glass at the air-liquid interphase. (F) Representative photographs of wildtype cell aggregates and Δ*engXCA2* cells showing significantly decreased aggregation in liquid culture.

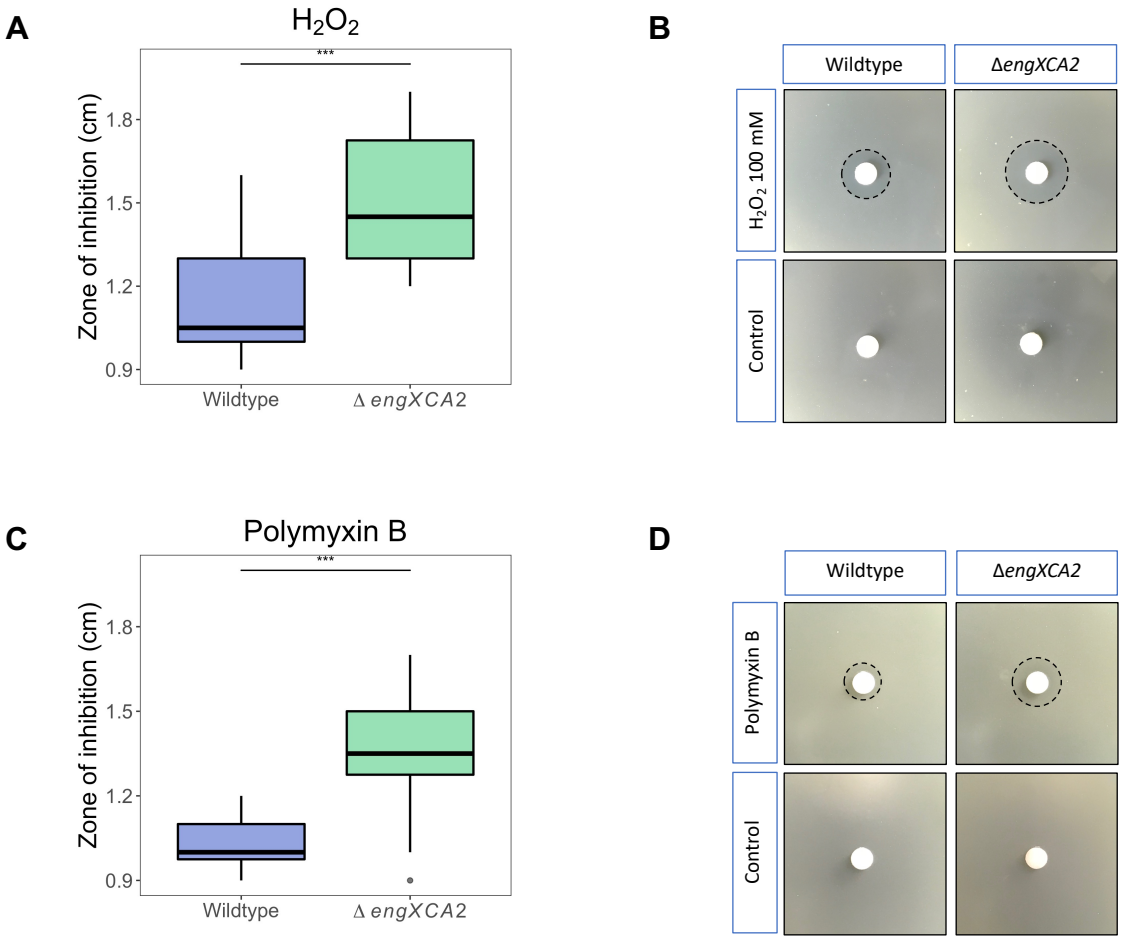

Figure 3.2. Δ*engXCA2* is more sensitive to hydrogen peroxide and polymyxin B. (A) Measurements of wildtype and Δ*engXCA2* inhibition zones after treatment with H_2O_2. (B) Images of inhibition zones after treatment with H_2O_2 and water negative control. (C) Measurements of wildtype and Δ*engXCA2* inhibition zones after treatment with polymyxin B. (D) Images of inhibition zones after treatment with polymyxin B and water negative control (n = 13, Kruskal-Wallis test followed by Dunn's test with Bonferroni's method for multiple-comparison correction, asterisks indicate level of significance: * $P < 0.05$, ** $P < 0.01$, *** $P < 0.001$).

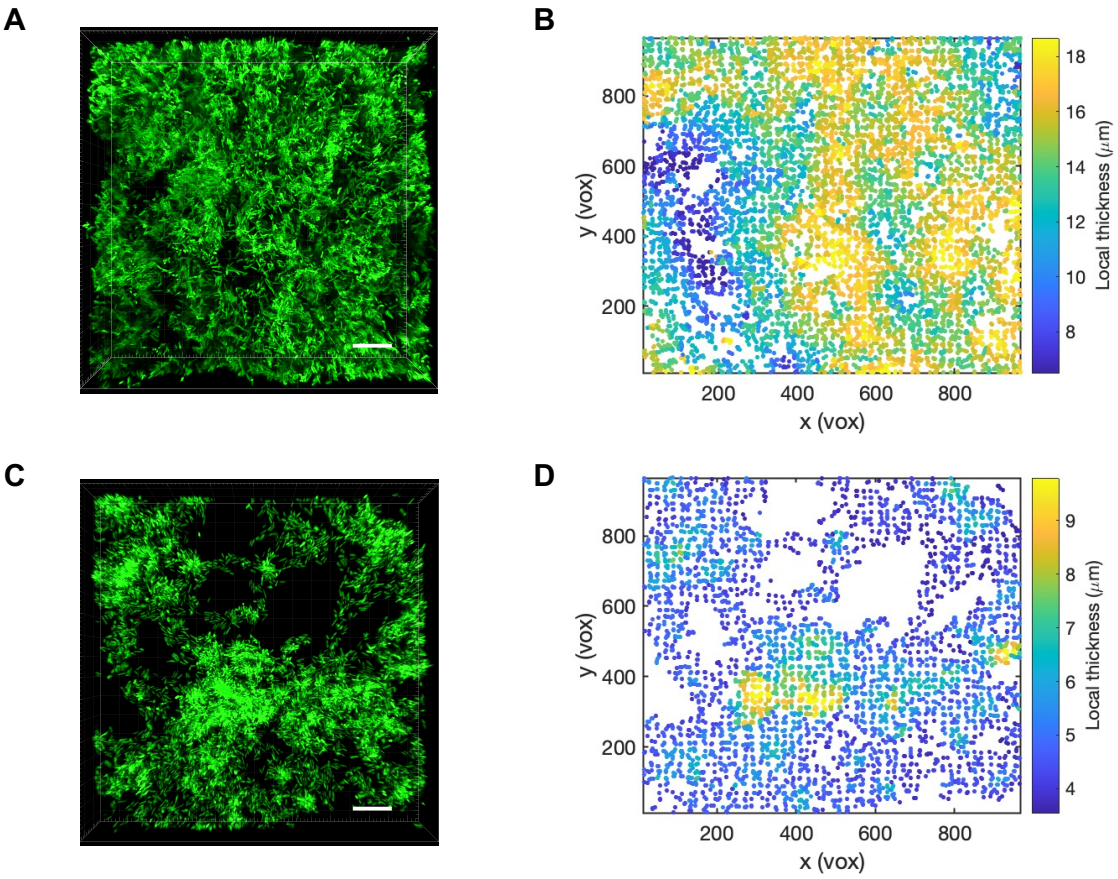

Figure 3.3. Δ*engXCA2 in vitro* biofilms are structurally impaired. Representative confocal laser scanning microscopy images of (A) wildtype and (C) Δ*engXCA2 in vitro* biofilms stained with SYTO 9 green. Localized thickness measurements (μm) of (B) wildtype and (D) Δ*engXCA2 in vitro* biofilms. Scale bar is 10 μm for (A) and (C).

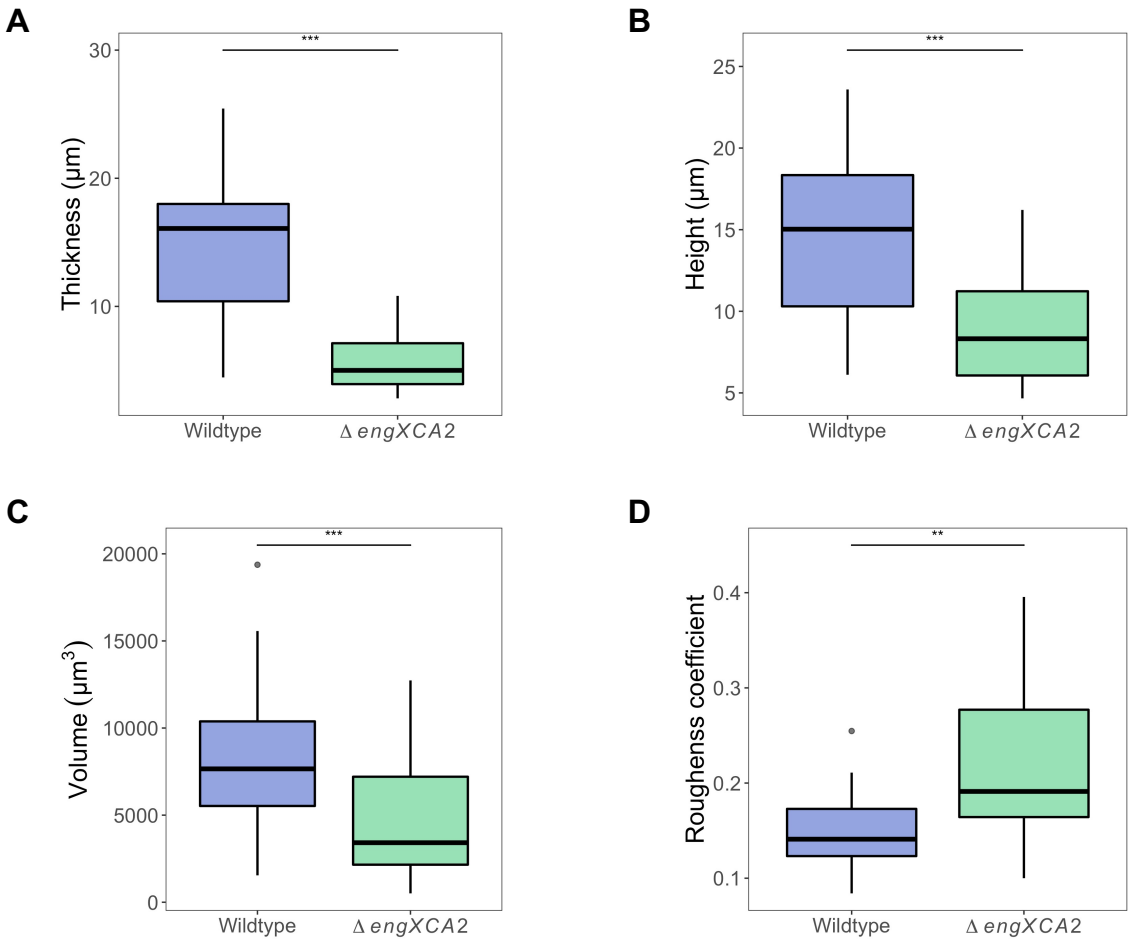

Figure 3.4. Δ*engXCA2 in vitro* biofilms are thinner, have lower biomass, and a higher roughness coefficient. (A) Average thickness, (B) height (highest peak), (C) average volume, and (D) roughness coefficient for wildtype and ΔengXCA2 *in vitro* biofilms. (n = 25, ANOVA followed by Tukey's Honest Significant Difference test, asterisks indicate level of significance: * $P < 0.05$, ** $P < 0.01$, *** $P < 0.001$)

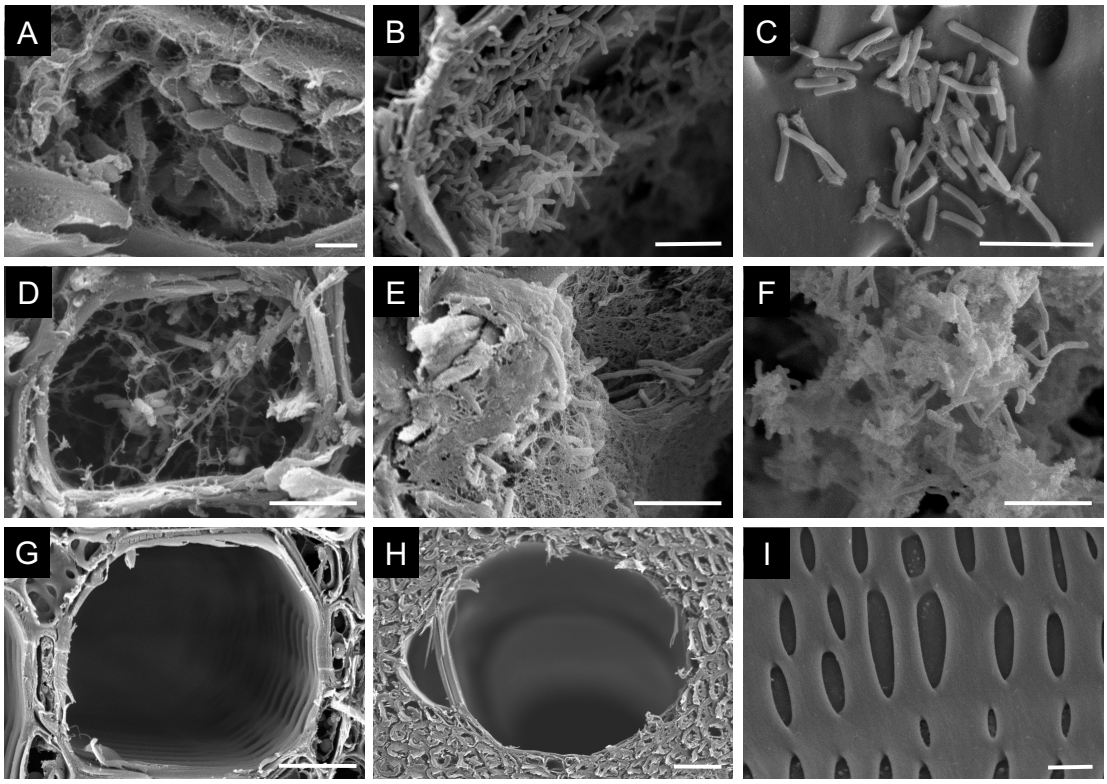

Figure 3.5. Δ*engXCA2* biofilms in the xylem of *Vitis vinifera* 'Cabernet Sauvignon' plants are associated with larger amounts of exopolysaccharide (EPS) and are larger in size. Δ*engXCA2* extensively colonized xylem vessels compared to wildtype biofilms. Transmission electron micrographs of vines inoculated with (A-C) wildtype, (D-F) Δ*engXCA2*, and (G-I) PBS. First column from the left, petiole transverse sections. Second column, stem transverse sections. Third column, stem longitudinal sections. (A-C) *X. fastidiosa* wildtype biofilms are associated with varying amounts of EPS. (D-F) Δ*engXCA2* cells develop larger biofilms that are associated with higher amounts of EPS. (G, H) Empty xylem vessels of PBS-inoculated vines are free of biofilms. (I) Secondary xylem pit membranes are intact in PBS-inoculated vines. Scale bar is 1 µm in (A), 5 µm in (B-F, and I), 10 µm in (G), 30 µm in (H).

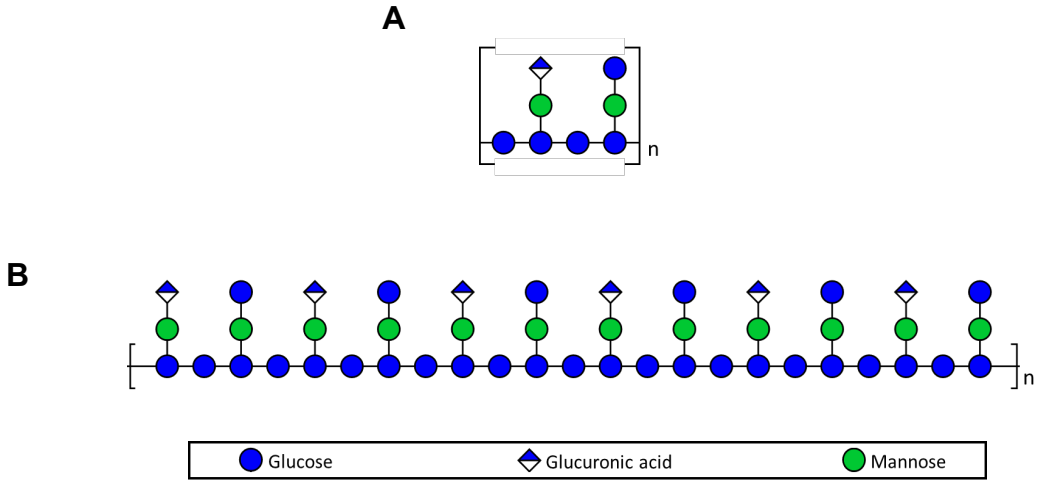

Figure 3.6. *X. fastidiosa* exopolysaccharide is comprised of octasaccharide subunits with a β-1,4-glucan backbone. (A) EPS octasaccharide subunit composed of a β-1,4-glucan backbone with two slightly different alternating 3-linked side chains, one with terminal β-glucuronic acid and α-1,2-mannose residues, and the other with terminal β-glucose and α-1,2-mannose residues. (B) EPS octasaccharide subunits linked to form a long chain.

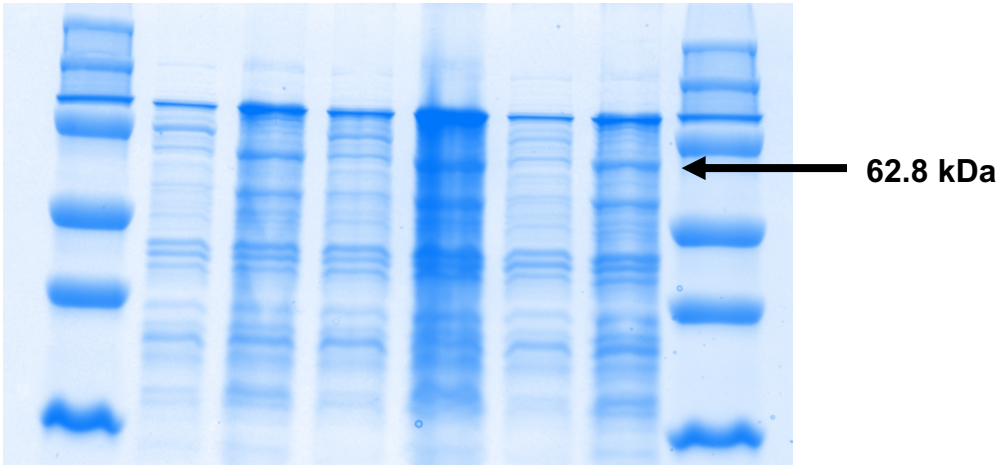

Figure 3.7. SDS-PAGE analysis of *E. coli* cell lysates transformed with pMCR7 or pET20b(+) empty vector. Lanes 1 and 10, M.W. standard ladder, Lanes 2, 4, and 6, cell lysates from *E. coli* pET20b(+) empty vector after IPTG induction (three replicates), Lanes 3, 5, and 7, cell lysates from *E. coli* pMCR7 after IPTG induction (three replicates). 62.8kd

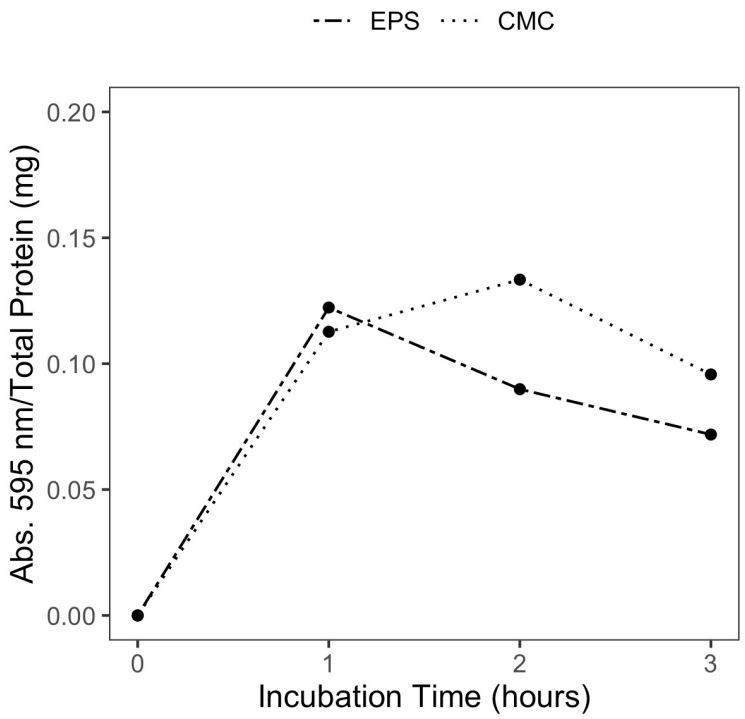

Figure 3.8. Recombinant *X. fastidiosa* EngXCA2 expressed in *E. coli* cleaves Δ*engXCA2* exopolysaccharide. *E. coli* BL21 (DE3) lysates containing recombinant *X. fastidiosa* EngXCA2 were incubated with carboxymethyl cellulose (CMC) or *X. fastidiosa* exopolysaccharide (EPS). CMC was used as a positive control. Total lysates from *E. coli* carrying pET-20(b)+ empty vector incubated with CMC or EPS were subtracted from lysates from *E. coli* containing recombinant *X. fastidiosa* EngXCA2 with CMC or EPS. Line graph data points represent the average of three independent experiments (n = 9).

Chapter IV

Xylella fastidiosa Type IV Pili System Components PilB and PilA1 are Necessary for Pierce's Disease Symptom Development and Grapevine Colonization

Abstract

Xylella fastidiosa is a plant-pathogenic, Gram-negative bacterium with an extremely wide host range that includes economically important crops like grapes, olive, and citrus. *X. fastidiosa* subsp. *fastidiosa* is the causal agent of Pierce's disease of grapevine, a significant problem for the grape industry in the United States. This xylem-limited bacterium is nonflagellated and relies upon its type IV pili for movement. Type IV pili are filamentous appendages that quickly polymerize and depolymerize to pull and drag the cell along a surface. These structures are also involved in biofilm formation by linking cells to each other. To explore the role of T4P in *X. fastidiosa* pathogenesis in grapevines, we created three mutant strains in genes involved in the T4P machinery: pilB, pilA1, and pilA2. Δ*pilB* and Δ*pilA1* strains were deficient in cell-cell aggregation compared to wildtype and Δ*pilA2* strains. Moreover, Δ*pilB*- and Δ*pilA1*-inoculated grapevines had significantly less overall disease and lower *X. fastidiosa* titer while Δ*pilA2* behaved similarly to wildtype. Our results indicate that PilB, a putative ATPase that drives pili extension, and PilA1, a putative pilin subunit, are necessary for PD symptom development and grapevine colonization.

Introduction

Xylella fastidiosa is a Gram-negative, xylem-limited bacterium that causes severe diseases in many economically important plants such as grapevine, olive, and citrus[1]. *Vitis vinifera* grapevines are the most economically-valued fruit crop in California at $6.25 billion in 2018[2]. Pierce's disease of grapevine (PD) is caused by *X. fastidiosa* subsp. *fastidiosa* and leads to losses of $104.4 million a year in the California grape industry[3,4]. PD symptoms include leaf marginal necrosis, leaf abscission, stunting, and fruit desiccation. Moreover, *X. fastidiosa* infection elicits a damaging amount of tyloses that result in occlusions and impaired water transport. Disease progression ultimately ends in vine death. *X. fastidiosa* is vector-transmitted by xylem-feeding insects such as sharpshooters. These insects acquire *X. fastidiosa* in their foregut as the feed on the xylem sap of infected vines where bacterial cells attach, proliferate, and create robust biofilms. Currently, there is no cure for PD and efforts to control this disease rely on pesticide use to control the vector population, eradication of the plant, or severe pruning[1].

Pili are found in a wide and diverse range of bacteria[5–7]. *X. fastidiosa* has two types of pili, type I and type IV, that are polarly attached to one end of the cell[8,9]. *X. fastidiosa* type I pili are short, approximately 0.4 to 1 μm in length, and they are involved in individual cell attachment and biofilm formation. T4P are much longer than type I, approximately 1 to 6 μm in length[9]. *X. fastidiosa* is nonflagelleted and relies upon its type IV pili (T4P) for twitching motility[8,9]. The T4P machinery extends, binds, and

retracts long filamentous appendages to pull the bacterial cell along a surface. PilB, an ATPase, drives the quick polymerization of thousands of pilin subunits called PilA to form and extend the T4P filaments while PilT, a different ATPase, drives the depolymerization of the filaments pulling the cell in a retracting movement. Besides movement, T4P can pick up free floating DNA from the environment and participate in cell-cell aggregation, a key process for biofilm formation[5–7].

In nature, most bacteria exist attached to a surface as a part of a biofilm where cells are continually exposed to physical forces such as fluid shear force. Recent advances in bacterial sensing have incorporated mechanistic studies on the biophysical interactions of bacteria with their environment through their T4P and how this affects bacterial gene expression networks[7,10–12]. Meng et al. previously showed *X. fastidiosa* responds to unidirectional liquid flow in a microfluidic flow cell, causing the bacterium to move upstream against flow via type IV pili-mediated motility[8]. *X. fastidiosa* resides exclusively in the xylem and in the mouthparts of its vector where both environments expose *X. fastidiosa* to fluid shear stress that could potentially be perceived by T4P. We hypothesize that T4P are critical for disease development and the colonization of grapevines. In this study, we created three mutant strains in genes involved in the T4P assembly: *pilB, pilA1,* and *pilA2*. We expect that the deletion of these genes will result in the absence of T4P filaments.

Materials and Methods

Bacterial strains. *X. fastidiosa* subsp. *fastidiosa* Temecula1 wildtype, Δ*pilB*, Δ*pilA1*, and Δ*pilA2* mutant strains were used in our studies. All strains were grown on solid PD3 medium at 28°C for five days. Repeated attempts to obtain transformant colonies for gene complementation in these mutant strains were previously unsuccessful and again during this study. Protocols for genetic manipulation in *X. fastidiosa*, especially for gene complementation, are often ineffective[20].

Growth curve. Five mL liquid PD3 cultures were grown in glass tubes (13 x 100 mm) with starting $OD_{600\ nm}$ of 0.01 at 28°C, 180 rpm for 12 days. $OD_{600\ nm}$ were measured every 24 hours using a spectrophotometer.

Construction and confirmation of the Δ*pilB*, Δ*pilA1*, Δ*pilA2* mutants. Overlap extension PCR was used to link 5' and 3' flanking regions of the gene of interest with the kanamycin resistance gene to create a construct for homologous recombination and deletion of the gene of interest (i.e. *pilB*, *pilA1*, or *pilA2*). Primer pairs 1pilB and 2pilB and 5pilB and 6pilB were used to obtain the 5' and 3' flanking regions of pilB. The kanamycin resistance gene was amplified from pCR2.1 TOPO with primers 3pilB and 4pilB. Primer pairs 1pilA1 and 2pilA1 and 5pilA1 and 6pilA1 were used to obtain the 5' and 3' flanking regions of pilA1. The kanamycin resistance gene was amplified from pCR2.1 TOPO with primers 3pilA1 and 4pilA1. Primer pairs 1pilA2 and 2pilA2 and 5pilA2 and 6pilA2 were used to obtain the 5' and 3' flanking regions of pilA2. The

kanamycin resistance gene was amplified from pCR2.1 TOPO with primers 3pilA2 and 4pilA2. The resulting PCR products from overlap PCR were cloned into pCR8/GW/TOPO (Invitrogen). To create pASG1, pASG2, and pASG3. Insertion of the PCR products was verified by sanger sequencing with primers GW1 and GW2 (Invitrogen). Electroporation of *X. fastidiosa* cells and positive transformant colony screening was performed according to Ingel et al.[22]

Cell surface attachment to glass assay. This assay was adapted from Espinosa-Urgel et al. (2000). Cells were harvested from solid PD3 plates and $OD_{600\ nm}$ was adjusted to 0.25 in liquid PD3 medium. 500 µL culture was added to 5 mL PD3 in a 13 x 100 mm glass tube. Cultures were incubated at 28°C, 100 rpm for 7 days. 500 µL 1% crystal violet was added to the culture and allowed to incubate at room temperature for 20 min. The culture and stain mixture was carefully discarded to prevent biofilm damage at the air-liquid interface. The tube was gently washed 3X with 1 mL water and allowed to dry overnight. 2 mL 30% acetic acid was used to dissolve the crystal violet-stained biofilm. Optical density was measured at 600 nm using 30% acetic acid as a blank.

Cell-cell aggregation assay. Cells were harvested from solid PD3 plates and $OD_{600\ nm}$ was adjusted to 0.25 in liquid PD3 medium. 500 µL culture was added to 5 mL PD3 in a 13 x 100 mm glass tube. Cultures were incubated at 28°C without agitation for 10 days. After incubation, cultures were gently agitated by hand and undisturbed for 20 min. to promote settling of cell aggregates at the bottom of the tube. The top 1 mL of the cultured

was collected (ODs) and its $OD_{540\ nm}$ was measured and returned to the culture tube. Then, the entire culture was vortexed thoroughly to disperse cell aggregates and 1 mL of it (ODt) was measured at $OD_{540\ nm}$. The percent aggregation was calculated as [(ODt-ODs)/ODt]*100.

Virulence assay. A total of 30 *Vitis vinifera* Cabernet Sauvignon grapevines per treatment were used for disease progression studies. Grapevines were inoculated with 40 µL *X. fastidiosa* in 1X PBS (10^8 CFU/mL) using the needle-inoculation method described by Hill and Purcell. For controls, grapevines were inoculated with 1X PBS. PD symptom development was evaluated over 20 weeks post-inoculation using a standard Pierce's disease rating scale of 0 to 5 (Guilhabert & Kirkpatrick, 2005).

AUDPC analysis. AUDPC analysis was performed using the R scripts provided by Schandry (2017).

Bacterial titer quantification. To prepare tissue for *X. fastidiosa* quantification via qPCR, two petioles were collected from the point of inoculation and 20 nodes above in grapevines. Sample petioles were prepared similarly to citrus tissue in Ginnan et al. 2020 with some adaptations. Petioles were lyophilized for about 24 hrs. and transferred to a 5 mL tube with a steel grinding ball (size ⅜ in., BC Precision). Samples were pulverized using a Geno/Grinder machine (2010 model, SPEX SamplePrep) at 1680 rpm for 40 s. Then, 2 mL of guanidine buffer (4M guanidine thyocyanate, 0.2 M NaOAc, 25 mM

EDTA, 2.5% w/v PVP-40, pH 5) were added to each sample and mixed thoroughly. Samples were incubated at 4°C for 15 min. and centrifuged at 4°C for 45 min., 20,000xg. 300 µL of the supernatant was collected for DNA extraction using MagMAX™-96 DNA Multi-Sample Kit and MagMAX Express-96 Deep Well Magnetic Particle Processor with the "441302ForPlants" protocol (Invitrogen™, Cat. No. 4413021). Total DNA was quantified using a Qubit™ 4 Fluorometer (Invitrogen™, Cat. No. Q33226) and Qubit™ dsDNA HS Assay Kit (Invitrogen™, Cat. No. Q32854). The extracted DNA was used for absolute quantification qPCR to determine *X. fastidiosa* titer using the protocol described in Deyett et al. 2019.

Results

Type IV pili ATPase PilB and pilin subunit PilA1 are required for cell-cell aggregation but not cell-surface attachment to glass. To confirm gene deletions in *X. fastidiosa* Δ*pilB*, Δ*pilA1*, and Δ*pilA2* mutant strains did not affect their growth rate, we measured $OD_{600\ nm}$ of cultures grown in liquid PD3 medium every 24 hours over the course 12 days. The growth rates for these mutant strains were the same as wildtype (ANOVA followed by Tukey's Honest Significant Difference test) confirming the deletion of *pilB*, *pilA1*, and *pilA2* genes in the *X. fastidiosa* genome did not cause defects in the ability to metabolize nutrients and grow(Figure 1).

X. fastidiosa develops many cell-aggregates as well as planktonic cells in liquid culture. Cell-cell aggregation is a critical step for forming a biofilm[13,14]. Quantification of cell-cell aggregation of strains grown in liquid cultures showed Δ*pilB* and Δ*pilA1* cells significantly aggregate less compared to wildtype. The Δ*pilA2* strain showed no significant difference for this phenotype (Figure 2). This indicates that the putative ATPase PilB and pilin subunit protein PilA1 contribute to cell-cell aggregation.

Additionally, we performed a cell attachment assay to investigate if T4P are involved in cell-surface attachment, another critical step for biofilm formation[14]. We indirectly measured cell attachment at the air-liquid interface of liquid cultures grown in glass tubes by staining these cells with crystal violet and measuring its absorbance. Our results suggest that T4P system components pilB, pilA1, and pilA2 do not participate in cell attachment to glass. Their perspective absorbance (600 nm) values were not significantly different from the wildtype values (Kruskal-Wallis test, Figure 3).

Type IV pili machinery components PilB and PilA1 are required for full virulence in grapevines. We inoculated *Vitis vinifera* 'Cabernet Sauvignon' plants with 40 μL of 10^8 CFU/mL *Xylella fastidiosa* wildtype, Δ*pilB,* Δ*pilA1,* Δ*pilA2,* or PBS as a control and monitored PD symptoms over the course of 20 weeks using a disease rating scale of 0 to 5, where 0 indicates a healthy vine and 5 indicates the death of the vine[15]. At 13 weeks post-inoculation, plants inoculated with wildtype and Δ*pilA2* cells showed heavy leaf scorching and leaf abscission leaving behind "matchstick petioles" attached to the stem of

the plant. Meanwhile, plants inoculated with Δ*pilB* and Δ*pilA1* cells displayed marginal chlorosis on the lower leaves that would later develop into scorched tissue. We calculated the area under the disease progress curve (AUDPC) to quantify total disease severity over time which determined that Δ*pilB*- and Δ*pilA1*-inoculated grapevines had significantly less overall disease over the course of the entire experiment (Figure 4B). There was no significant difference in total disease severity between the wildtype and Δ*pilA2* treatments (Kruskal-Wallis test followed by Dunn's test with Bonferroni's method for multiple-comparison correction). Also, Δ*pilB*- and Δ*pilA1*-inoculated vines did not show clear PD symptoms until 11 weeks post-inoculation compared to 7 weeks post-inoculation in wildtype- and Δ*pilA2*-inoculated vines (Figure 4A). We did not observe any PD symptoms in PBS-treated plants over the course of the bioassay (Figure 5). Taken together, these data indicate that ATPase PilB and pilin subunit PilA1 are critical virulence factors in *X. fastidiosa* pathogenesis in grapevine.

PilB and PilA1 are necessary for local and systemic bacterial colonization in the xylem. To investigate if *pilB, pilA1,* and *pilA2* T4P genes are important for plant host colonization of local (point of inoculation) and systemic (20 nodes above the point of inoculation) tissues, we quantified *X. fastidiosa* titer via qPCR in grapevine petioles for all five treatments: wildtype, Δ*pilB,* Δ*pilA1,* Δ*pilA2,* and PBS. We found that grapevines inoculated with Δ*pilB* and Δ*pilA1* harbored significantly less *X. fastidiosa* DNA in local and systemic petioles compared to wildtype, with *P*-values of $P < 0.001$ (Kruskal-Wallis test followed by Dunn's test with Bonferroni's method for multiple-comparison

correction, Figure 6). Δ*pilA2*-inoculated vines contained significantly less pathogen at the point of inoculation but significantly more in systemic petioles ($P < 0.05$). We did not detect any *X. fastidiosa* DNA in PBS-inoculated plants.

Discussion

To explore the role of T4P in *X. fastidiosa* pathogenesis in grapevines, we created three mutant strains in genes involved in the T4P machinery: *pilB*, *pilA1*, and *pilA2*. T4P are dynamic, mechanical filaments used by many bacteria for movement and exploring surfaces[7]. We expected that these gene mutations would result in the absence of T4P filaments. Grapevines inoculated with Δ*pilB* and Δ*pilA1* mutant strains developed fewer symptoms, less overall disease, and contained lower *X. fastidiosa* titer indicating that T4P components PilB and PilA1 are required for full virulence and colonization in grapevines. *X. fastidiosa* follows the canonical biofilm development cycle in both its insect vector and plant host[14,16]. In order to form a biofilm, *X. fastidiosa* must first explore and interact with surfaces like the xylem wall and the cuticle of the insect mouthparts. *X. fastidiosa* uses its T4P for movement and presumably as a tool to explore surfaces during the reversible attachment phase of biofilm formation like other Gram-negative bacteria[7,8,17,18].

T4P mutants in *X. fastidiosa* are typically deficient in twitching motility and in basipetal movement in grapevines, but their virulence *in planta* has not been studied

(pilA1, pilA2, pilB, pilQ). Recent studies revealed *P. aeruginosa* uses T4P as mechanosensors to "feel" surfaces, triggering the production of cyclic-di-GMP(C-di-GMP) via the Chp system that interacts with the T4P machinery. C-di-GMP is an intracellular signal that initiates the transition from the planktonic to the biofilm phenotype and induces the expression of other virulence genes[10,12]. Furthermore, the production of c-di-GMP increased when the shear force created by liquid flow was applied to cells[12]. *X. fastidiosa's* Pil-Chp and a T4P system highly resemble the Chp and T4P systems in *P. aeruginosa[19]*. If *X. fastidiosa* also used its T4P and Pil-Chp for mechanosensing like *P. aeruginosa,* then the lack of T4P in the Δ*pilB* and Δ*pilA1* mutants would result in lower expression of virulence genes. This could explain why fewer PD symptoms and lower *X. fastidiosa* titer is observed in Δ*pilB*- and Δ*pilA1*-inoculated vines.

Kandel et al. previously reported the presence of at least four gene paralogs of *pilA* in *X. fastidiosa* strains WM1-1 and TemeculaL[20]. We found three *pilA* gene paralogs in the genome of the Temecula1 strain. Based on their findings, this study concluded that PilA2 is critical for twitching motility and that it is the major pilin for T4P in the WM1-1 and TemeculaL strains[20]. Our data show PilA1 is integral for cell-cell aggregation and virulence in grapevines indicating that this is the major pilin in the Temecula1 strain. Moreover, the Δ*pilA2* strain did not lose virulence or cell-cell aggregation. This strain also had the same phenotypic characteristics as the wildtype strain. This suggests that PilA2 is not a major player in the T4P machinery in the

Temecula1 strain. The difference in major pilin subunits between strains could be due to strain genotypic differences.

Δ*pilB* and Δ*pilA1* cells were significantly impaired in cell-cell aggregation indicating that T4P contribute to the formation of cell aggregates. Many bacterial systems have shown that T4P have been implicated in this process during biofilm formation. For example, *Neisseria meningitidis* utilizes its T4P to promote dynamic cell-cell aggregation by linking pili to pili. By altering the tension of their T4P during colonization, *N. meningitidis* cell aggregates become fluid and can change their shape to adjust to the diverse dimensions of the blood vessel network in mammals [7,21,22]. *X. fastidiosa* T4P could potentially allow cell aggregates inside the xylem to become fluid to adjust to the varying flow rates and dimensions of xylem vessels.

No significant difference was observed in cell-surface attachment between wildtype and all three mutant strains. Because T4P are involved in cell-cell aggregation, an important step of biofilm formation that contributes to cohesiveness, we suspect that there were differences in attachment to glass that our crystal violet assay was not able to detect. Further biofilm attachment analyses like confocal laser scanning microscopy would allow us to make a 3D comparison of cell attachment and biofilm architectures. Z-stack images would further allow us to quantify biofilm characteristics like average height, biovolume and substrate colonization of the biofilms.

T4P are dynamic tools used for bacterial movement on a surface and cell-cell aggregation during biofilm formation[7,9]. Recent studies have revealed that bacteria use these appendages to sense the physical environment around them[10,12,23]. *X. fastidiosa* is exposed to physical forces such as the xylem wall, the insect cuticle, and the constant shear stress created by the xylem flow and the ingestion of xylem sap during insect feeding[1]. Further investigation could reveal if *X. fastidiosa* can sense such forces via its T4P and if this mechanosensing leads to transcriptional changes that are important for virulence in its plant hosts.

Literature Cited

1. Rapicavoli J, Ingel B, Blanco-Ulate B. Xylella fastidiosa: An examination of a re-emerging plant pathogen. Mol Plant. 2017. Available: http://onlinelibrary.wiley.com/doi/10.1111/mpp.12585/full

2. California Department of Food, Agriculture. CDFA - Statistics. [cited 22 Nov 2019]. Available: https://www.cdfa.ca.gov/statistics/

3. Tumber K, Alston J, Fuller K. Pierce's disease costs California $104 million per year. Calif Agric. 2014. Available: http://calag.ucanr.edu/Archive/?article=ca.v068n01p20

4. Alston JM, Fuller KB, Kaplan JD, Tumber KP. Assessing the returns to R&D on perennial crops: the costs and benefits of Pierce's disease research in the California winegrape industry. Aust J Agric Resour Econ. 2015;59: 95–115.

5. Burdman S, Bahar O, Parker JK, De La Fuente L. Involvement of Type IV Pili in Pathogenicity of Plant Pathogenic Bacteria. Genes . 2011;2: 706–735.

6. Chang Y-W, Rettberg LA, Treuner-Lange A, Iwasa J, Søgaard-Andersen L, Jensen GJ. Architecture of the type IVa pilus machine. Science. 2016;351: aad2001.

7. Craig L, Forest KT, Maier B. Type IV pili: dynamics, biophysics and functional consequences. Nat Rev Microbiol. 2019;17: 429–440.

8. Meng Y, Li Y, Galvani CD, Hao G, Turner JN, Burr TJ, et al. Upstream migration of Xylella fastidiosa via pilus-driven twitching motility. J Bacteriol. 2005;187: 5560–5567.

9. Li Y, Hao G, Galvani CD, Meng Y, Fuente LDL, Hoch HC, et al. Type I and type IV pili of Xylella fastidiosa affect twitching motility, biofilm formation and cell-cell aggregation. Microbiology. 2007;153: 719–726.

10. Persat A, Inclan YF, Engel JN, Stone HA, Gitai Z. Type IV pili mechanochemically regulate virulence factors in Pseudomonas aeruginosa. Proc Natl Acad Sci U S A. 2015;112: 7563–7568.

11. Lee CK, de Anda J, Baker AE, Bennett RR, Luo Y, Lee EY, et al. Multigenerational memory and adaptive adhesion in early bacterial biofilm communities. Proc Natl Acad Sci U S A. 2018;115: 4471–4476.

12. Rodesney CA, Roman B, Dhamani N, Cooley BJ, Katira P, Touhami A, et al. Mechanosensing of shear by Pseudomonas aeruginosa leads to increased levels of the

cyclic-di-GMP signal initiating biofilm development. Proceedings of the National Academy of Sciences. 2017;114: 5906–5911.

13. Trunk T, Khalil HS, Leo JC. Bacterial autoaggregation. AIMS Microbiol. 2018;4: 140–164.

14. Feil H, Feil WS, Lindow SE. Contribution of Fimbrial and Afimbrial Adhesins of Xylella fastidiosa to Attachment to Surfaces and Virulence to Grape. Phytopathology. 2007;97: 318–324.

15. Guilhabert MR, Hoffman LM, Mills DA, Kirkpatrick BC. Transposon mutagenesis of Xylella fastidiosa by electroporation of Tn5 synaptic complexes. Mol Plant Microbe Interact. 2001;14: 701–706.

16. Roper MC, Greve LC, Labavitch JM, Kirkpatrick BC. Detection and Visualization of an Exopolysaccharide Produced by Xylella fastidiosa In Vitro and In Planta. Appl Environ Microbiol. 2007;73: 7252–7258.

17. Treuner-Lange A, Chang Y-W, Glatter T, Herfurth M, Lindow S, Chreifi G, et al. PilY1 and minor pilins form a complex priming the type IVa pilus in Myxococcus xanthus. Nat Commun. 2020;11: 5054.

18. Li YL, Yan YC, Deng SG, Zhang CP, Haq F, Chen T, et al. The Xanthomonas oryzae pv. oryzae type IV pilus alignment subcomplex protein PilN contributes to regulation of bacterial surface-associated behaviors and T3SS system. Plant Pathol. 2020. doi:10.1111/ppa.13157

19. Cursino L, Galvani CD, Athinuwat D, Zaini PA, Li Y, De La Fuente L, et al. Identification of an operon, Pil-Chp, that controls twitching motility and virulence in Xylella fastidiosa. Mol Plant Microbe Interact. 2011;24: 1198–1206.

20. Kandel PP, Chen H, De La Fuente L. A Short Protocol for Gene Knockout and Complementation in Xylella fastidiosa Shows that One of the Type IV Pilin Paralogs (PD1926) Is Needed for Twitching while Another (PD1924) Affects Pilus Number and Location. Appl Environ Microbiol. 2018;84. doi:10.1128/AEM.01167-18

21. Bonazzi D, Lo Schiavo V, Machata S, Djafer-Cherif I, Nivoit P, Manriquez V, et al. Intermittent Pili-Mediated Forces Fluidize Neisseria meningitidis Aggregates Promoting Vascular Colonization. Cell. 2018;174: 143–155.e16.

22. Welker A, Cronenberg T, Zöllner R, Meel C, Siewering K, Bender N, et al. Molecular Motors Govern Liquidlike Ordering and Fusion Dynamics of Bacterial Colonies. Phys Rev Lett. 2018;121: 118102.

23. Persat A, Nadell CD, Kim MK, Ingremeau F, Siryaporn A, Drescher K, et al. The mechanical world of bacteria. Cell. 2015;161: 988–997.

24. Ingel B, Jeske DR, Sun Q, Grosskopf J, Roper MC. Xylella fastidiosa Endoglucanases Mediate the Rate of Pierce's Disease Development in Vitis vinifera in a Cultivar-Dependent Manner. Mol Plant Microbe Interact. 2019; MPMI04190096R.

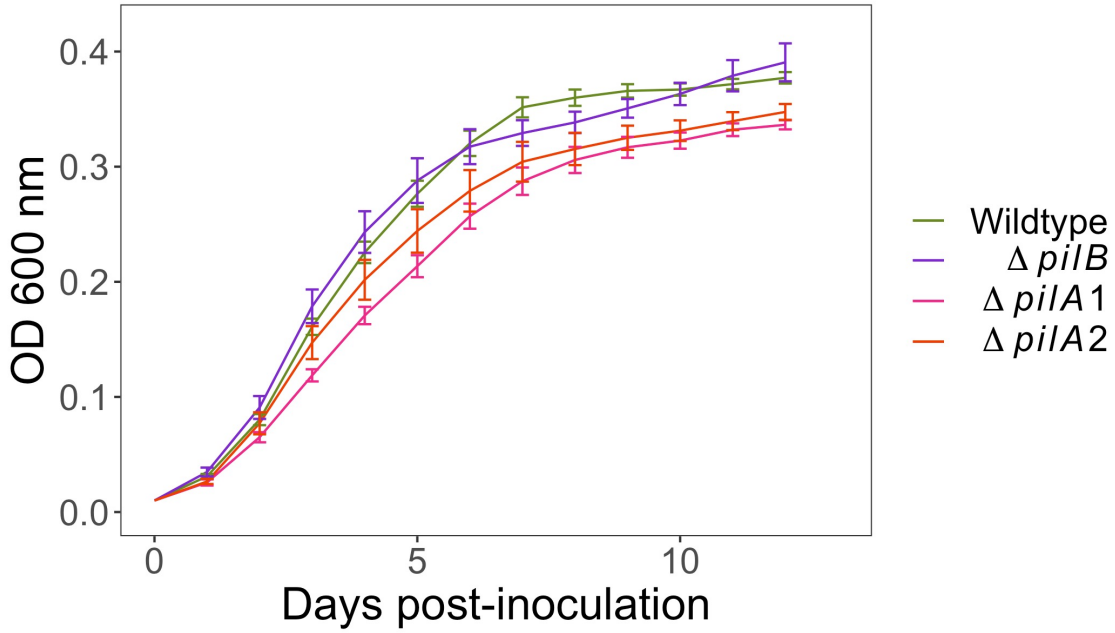

Figure 4.1. *Xylella fastidiosa* Δ*pilB*, Δ*pilA1*, Δ*pilA2* mutant strains grow at the same rate as wildtype in liquid PD3 medium. Starting $OD_{600\ nm}$ was 0.01. OD was measured every 24 hrs. using a spectrophotometer for 12 days. Mutant strains growth was not significantly different than wildtype (n = 12, ANOVA followed by Tukey's Honest Significant Difference test).

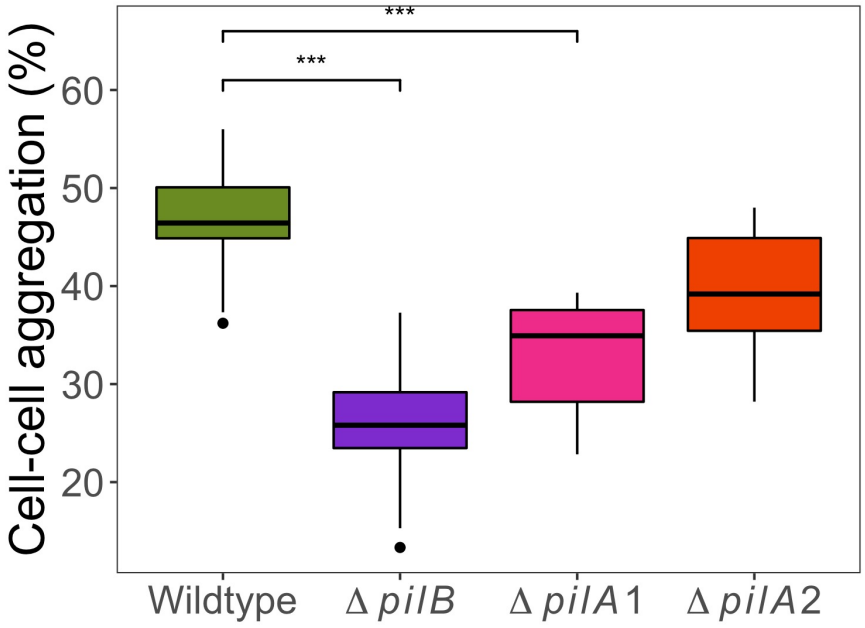

Figure 4.2. Δ*pilB* and Δ*pilA1* have impaired cell-cell aggregation. Cell-cell aggregation percentage in wildtype and ΔengXCA2 liquid cultures (n = 12, ANOVA followed by Tukey's Honest Significant Difference test, asterisks indicate level of significance: * $P < 0.05$, ** $P < 0.01$, *** $P < 0.001$).

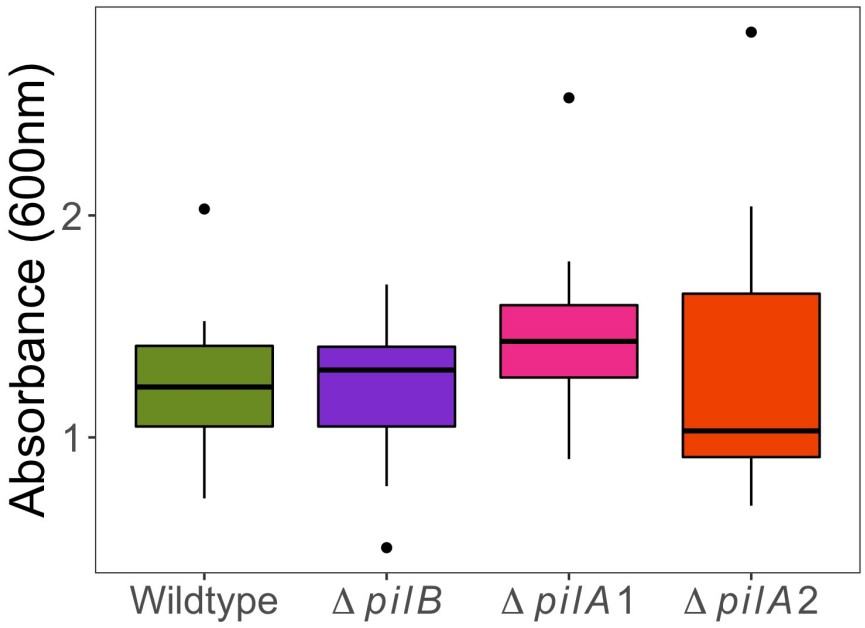

Figure 4.3. Gene deletions of type IV pilus machine genes *pilB*, *pilA1*, and *pilA2* do not affect cell attachment to glass at the air-liquid interface. Quantification of cell-glass surface attachment at the air-liquid interphase. Mutant strains were not significantly different than wildtype (n = 12, Kruskal-Wallis test).

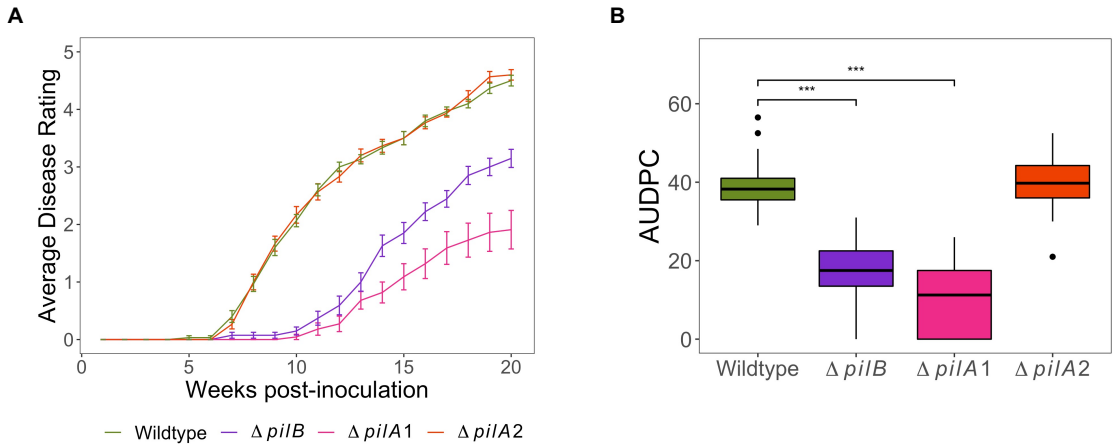

Figure 4.4. Type IV pili system components PilB and PilA1 are required for full virulence in grapevines. (A) Weekly average Pierce's disease symptom ratings observed over the course of 20 weeks for wildtype, Δ*pilB*, Δ*pilA1*, and Δ*pilA2* strains. Error bars represent standard error of the mean. (B) Area under the disease progress curve (AUDPC) values for grapevines inoculated with wildtype, ΔpilB, ΔpilA1, and ΔpilA2 based on disease rating scores over the course of 20 weeks post-inoculation. PBS-inoculated plants did not show any symptoms (n = 30, Kruskal-Wallis test followed by Dunn's test with Bonferroni's method for multiple-comparison correction, asterisks indicate level of significance: * $P < 0.05$, ** $P < 0.01$, *** $P < 0.001$).

Figure 4.5. *Vitis vinifera* 'Cabernet Sauvignon' plants inoculated with *Xylella fastidiosa* wildtype, Δ*pilB*, Δ*pilA1*, Δ*pilA2*, and PBS. Grapevines were inoculated with 40 µL of 10^8 CFU/mL bacterial suspension in PBS. Grapevines are shown at 13 weeks post-inoculation.

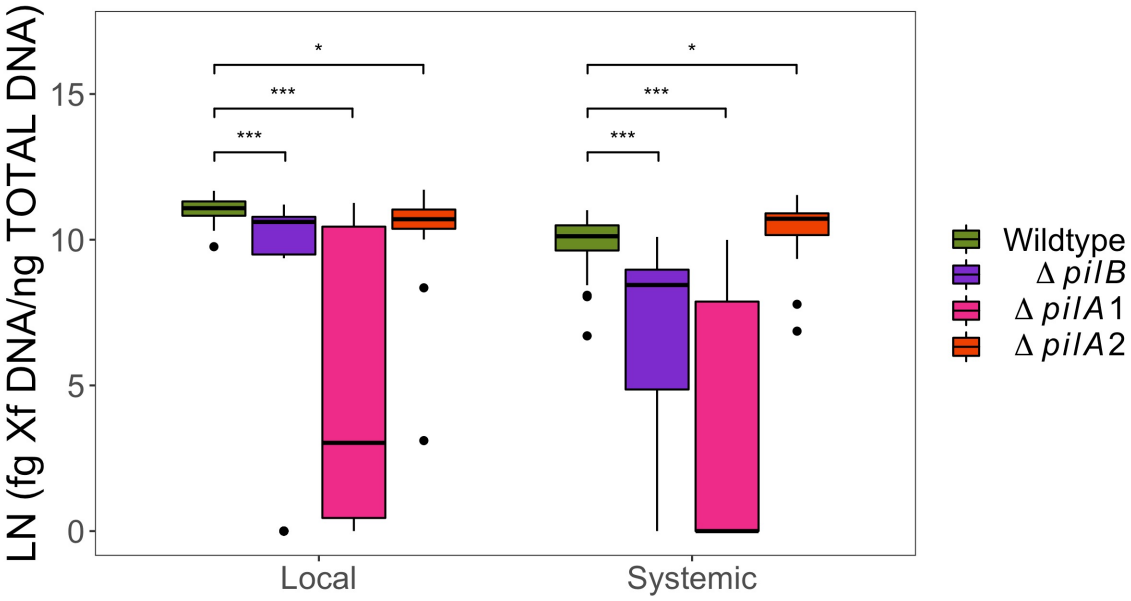

Figure 4.6. Type IV pili system components PilB and PilA1 are necessary for local and systemic colonization of the xylem. X. fastidiosa DNA quantification in local and systemic petioles for all treatments at 13 weeks post-inoculation via qPCR (n = 30, Kruskal-Wallis test followed by Dunn's test with Bonferroni's method for multiple-comparison correction, asterisks indicate level of significance: * $P < 0.05$, ** $P < 0.01$, *** $P < 0.001$).

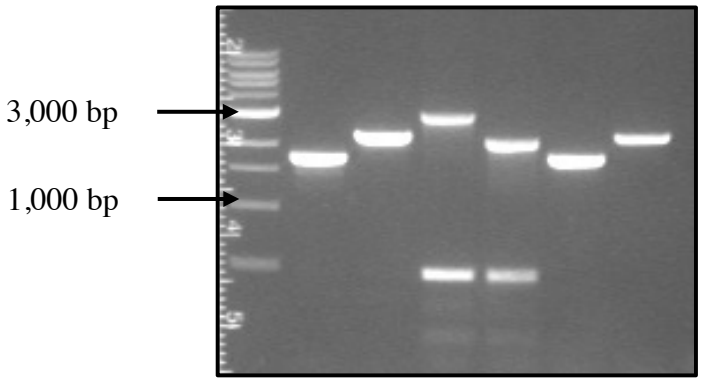

Figure 4.7. Confirmation of gene knockout deletion of *pilB, pilA1,* and *pilA2* and replacement with kanamycin resistance cassette. Lane 1, 1 kb ladder (New England Biolabs); Lane 2, PCR product using primers 1pilA1 and 6pilA1 and DNA from wildtype; Lane 3, PCR product using primers 1pilA1 and 6pilA1 and DNA from ΔpilA1; Lane 4, PCR product using primers 1pilB and 6pilB and DNA from wildtype; Lane 5, PCR product using primers 1pilB and 6pilB and DNA from ΔpilB; Lane 6, PCR product using primers 1pilA2 and 6pilA2 and DNA from wildtype; Lane 7, PCR product using primers 1pilA2 and 6pilA2 and DNA from ΔpilA2. 1.0% agarose gel was used to separate PCR products.

Strains, plasmids, and primers	Relevant characteristics or primer sequence	Source
Strain		
Escherichia coli TOP10	F- mcrA Δ(mrr-hsdRMS-mcrBC) Φ80lacZΔM15 ΔlacX74 recA1 araD139 Δ(araleu)7697 galU galK rpsL (StrR) endA1 nupG	Invitrogen
Xylella fastidiosa Temecula1		Temecula, CA, U.S.A.
Xylella fastidiosa	pilB deletion in Temecula1 background	This study
Xylella fastidiosa	pilA1 deletion in Temecula1 background	This study
Xylella fastidiosa	pilA2 deletion in Temecula1 background	This study
Plasmid		
pCR8/GW/TOPO	pUC19 derivative, spectinomycin-resistant	Invitrogen
pCR2.1 TOPO	Kanamycin-resistant	Invitrogen
ASG1	pCR8/GW/TOPO with ΔpilB deletion construct	This study
ASG2	pCR8/GW/TOPO with ΔpilA1 deletion construct	This study
ASG3	pCR8/GW/TOPO with ΔpilA2 deletion construct	This study
Primer[a]		
1pilB	CCATGCAGCGTTTCCATC	This study
2pilB	AGCTGGCAATTCCGGGAAAAGTTCTCTGGTTA	This study
3pilB	TAACCAGAGAACTTTTCCCGGAATTGCCAGCT	This study
4pilB	GGTGTTGTTGATGCTCAGAAGAACTCGTCA	This study
5pilB	TGACGAGTTCTTCTGAGCATCAACAACACC	This study
6pilB	ATCTTGCTGCAGCCATTG	This study
1pilA1	GCAATGTCCTTCGGAGTGAT	This study
2pilA1	AGCTGGCAATTCCGGGTGTATACCTTCAATAA	This study
3pilA1	TTATTGAAGGTATACACCCGGAATTGCCAGCT	This study
4pilA1	TGCTGTGTGTATTCATCAGAAGAACTCGTCAAGAA	This study
5pilA1	TTCTTGACGAGTTCTTCTGATGAATACACACAGCA	This study
6pilA1	GATTGCACACCGTAGCTCCT	This study
1pilA2	CCAGGATGATCAGGAGCT	This study
2pilA2	CCAGCTGGCAATTCCGGGATGAATCCTTAAATAG	This study
3pilA2	CTATTTAAGGATTCATCCCGGAATTGCCAGCTGG	This study
4pilA2	TGTTGTTGCTGGTGTTAATCAGAAGAACTCGTCAAGAA	This study
5pilA2	TTCTTGACGAGTTCTTCTGATTAACACCAGCAACAACA	This study
6pilA2	AACCTGCGGCTGTTCTTA	This study

[a] Primer sequences are presented as 5' to 3'.

Table 4.1. Strains, plasmids, and primer sequences used in this study.

Appendix

Xylella fastidiosa: A Re-emerging Plant Pathogen that Threatens Crops Globally

Castro C, DiSalvo B, Roper MC. Xylella fastidiosa: A reemerging plant pathogen that threatens crops globally. PLoS Pathog. 2021;17: e1009813.

Xylella fastidiosa is a fastidious, gram-negative bacterium in the family *Xanthomonadaceae* and is a major threat to agricultural crops and ecological and ornamental landscapes in the world. This bacterium is quite remarkable in regards to its very broad host range that includes over 600 plant species belonging to 63 diverse plant families. It is specifically limited to the xylem tissue of its plant hosts [1]. In some of these hosts it causes severe and devastating disease. However, in the vast majority of its hosts it is considered a benign commensal.

X. fastidiosa is endemic to the Americas. Historically, Europe was considered to be free of *X. fastidiosa*, but the bacterium was recently detected in Italy. In 2013, olive trees in the Apulia region of southern Italy began exhibiting leaf scorch symptoms that were later confirmed to be caused by *X. fastidiosa*. Since then, thousands of olive trees have died and *X. fastidiosa* has been detected in various plants species in France, Spain, and Portugal [1–3]. *X. fastidiosa* has been responsible for significant economic losses in regions like the US, Italy, and Brazil. For example, *X. fastidiosa* subsp. *fastidiosa*, the causal agent of Pierce's disease of grapevine, leads to crop losses of approximately $104 M and costs growers approximately $50 M in preventative strategies each year for the California viticulture industry [4,5]. In the Apulia region, *X. fastidiosa* subsp. *pauca* infection in olive orchards is projected to cost Italy up to €5.2 billion over the next 50 years if trees are not replaced [6]. Current management strategies to minimize *X. fastidiosa* spread in the field include removal of infected plants, severe pruning, and control of insect vectors with insecticides. The development of resistant plant lines is also

an active area of research and recently five new PD resistant grape varieties were commercially released to the grape industry [7].

The *X. fastidiosa* species is subdivided into multiple subspecies that include subsp. *fastidiosa*, *multiplex* and *pauca* [8]. The subspecies designations are loosely associated with host range, but some strains can infect multiple hosts. In general, disease symptoms associated with these *X. fastidiosa* strains are most commonly characterized by marginal leaf necrosis or leaf scorching like those observed in grapevines infected with *X. fastidiosa* subsp. *fastidiosa*. However, symptoms caused by *X. fastidiosa* subsp. *pauca* can be characterized by foliar wilt and interveinal chlorosis and symptoms caused by *X. fastidiosa* subsp. *multiplex* in some hosts can exhibit dense canopies and reduced fruit size [1]. *X. fastidiosa* has no free-living component of its lifestyle and has only been found associated with its plant and insect hosts.

Xylella fastidiosa has a unique association with its xylem sap-feeding insect vectors.

X. fastidiosa is obligately vectored by xylem-feeding hemipteran insects primarily belonging to the sharpshooter leafhopper (Cicadellidae) and spittlebug (Cercopidae) families (Figure 1) [9–11]. These insects are polyphagous (i.e., they feed on many plant species) and are present in warm regions across the globe [11]. *X. fastidiosa* is acquired when the insect feeds on the xylem sap of an infected plant. The bacteria colonize and multiply in the insect foregut (mouthparts) in a persistent, but non-circulative manner [10,12]. This type of pathogen-vector relationship is unique among insect-vectored plant pathogens because the bacterial cells propagate within the insect mouthparts but do not

circulate throughout the body of the insect, whereas most propagative pathogens circulate within the insect. When sharpshooters feed on the xylem of infected vines, *X. fastidiosa* attaches to and colonizes the insect foregut where it forms adhesive biofilms (Figure 1). *X. fastidiosa* experiences extreme shear stress during the xylem sap ingestion and egestion processes that occur during insect feeding. During transmission into a healthy vine, bacterial cells dislodge from the insect foregut, presumably as a result of the high shear stress created during feeding, and are deposited directly into the xylem of healthy vines [13]. There is no apparent specificity between a particular *X. fastidiosa* subspecies and insect vector species. In fact, individual glassy-winged sharpshooter (GWSS) (*Homalodisca vitripennis*) can acquire more than one *X. fastidiosa* subspecies in its foregut and can potentially transmit these strains to a variety of plants where the bacterium can behave as pathogen or a commensal endophyte [2,14].

In the context of Pierce's disease of grapevine caused by *X. fastidiosa* subsp. fastidiosa, the pathosystem with the broadest literature base, the two xylem-feeding insects transmit *X. fastidiosa* that have received the most research focus are the blue-green sharpshooter (BGSS) (*Graphocephala atropunctata*) and the GWSS. The BGSS is native to riparian areas in California and feeds on new plant growth that emerges in the spring [9,10]. The GWSS is invasive to California and was introduced into Southern California approximately in 1989 [29]. The introduction of this invasive pest drastically changed the epidemiology of PD in the southern part of California because GWSS can feed on both green and dormant woody tissues enabling transmission even in winter. In addition, GWSS can fly longer distances than native sharpshooter species, which could

explain how PD incidence was elevated to epidemic proportions in Southern California. Subsequently, there has been a concerted effort among growers and the California Department of Food and Agriculture to control vector populations and prevent the spread of GWSS. The predominant vector linked to Olive Quick Decline Syndrome in Italy is the meadow spittlebug, *Philaenus spumarius* [15].

Xylella fastidiosa **colonizes host compartments that are primarily non-living.**

As far as presently known, *X. fastidiosa* interacts primarily with non-living tissues in both its insect and plant hosts. These include the cuticular surface of the insect foregut and the plant xylem, which is non-living at maturity (Figure 1). The xylem consists of a network of vessels that are connected by pit membranes. These are thin, porous structures composed of primary plant cell wall, which allow for the passage of water but prevent the movement of pathogens and air embolisms. *X. fastidiosa* produces plant cell wall degrading enzymes, a polygalacturonase and several endoglucanases, that act in concert to degrade pit membranes allowing *X. fastidiosa* to breach this barrier and move from vessel to vessel to achieve systemic colonization [16–18]. *X. fastidiosa* is also a prolific producer of outer membrane vesicles that also modulate xylem colonization [30]. Interestingly, *X. fastidiosa* does not possess a Type III secretion system (T3SS) typical of other pathogenic bacteria that enables them to inject cognate Type III effectors into living host cells, likely because the bacterium interacts primarily with non-living cells. Instead of relying on T3SS effectors to bypass host immunity, *X. fastidiosa* delays early plant recognition in grapevines by camouflaging itself with a rhamnose-rich O-antigen, the

most external portion of its lipopolysaccharide layer as one mechanism that allows it to skirt initial triggering of the grape immune system to establish itself in the plant [19]. It is not known which living plant tissues are primarily responsible for initiating and propagating a response to *X. fastidiosa*, but it is likely the living xylem parenchyma cells adjacent to the xylem vessels.

One of the remarkable internal symptom phenotypes of infected grapevines is the prolific production of tyloses in response to *X. fastidiosa* colonization of the xylem (Figure 1). Tyloses are outgrowths of the living xylem parenchyma cells that protrude into the xylem and are part of the plant defense response. Their role, in part, is to slow or prevent pathogen movement within the xylem. However, overproduction of tyloses can cause a reduction in hydraulic conductivity within the xylem that is detrimental to the plant [20,21]. In PD-infected vines, tyloses become the dominant form of xylem occlusion during the early stages of disease and as a consequence, infected vines have a significant loss in hydraulic conductivity. Tyloses exacerbate PD symptoms and it is thought that this uncontrolled production of tyloses is what ultimately leads to the demise of the plant [24].

Another notable feature of *X. fastidiosa's* behavior in planta is the manner in which it regulates its own biofilm formation as it colonizes the xylem. In general, entering into and maintaining robust biofilms is linked to promoting virulence for many bacterial pathogens [23]. On the contrary, mutant strains of *X. fastidiosa* that are impaired in biofilm formation and effectively locked in a planktonic phase have a hypervirulent phenotype in grapevines [24–27]. Thus, it is speculated that *X. fastidiosa* enters the

surface adhesive biofilm state as a means to attenuate its own virulence by controlling its movement in planta by adhering to the xylem wall. This self-limiting behavior during parasitism in symptomatic/susceptible hosts may be a remnant from its lifestyle as a commensal in non-symptomatic hosts where tightly regulating and limiting rapid movement in the plant would promote a commensal interaction rather than a parasitic interaction.

X. fastidiosa acts as both a commensal and a pathogen depending on its host environment.

The bulk of the research on *X. fastidiosa* is biased towards isolates that are pathogenic in economically important hosts. The mechanism by which *X. fastidiosa* causes disease only in certain hosts, but not others has not been fully elucidated and its interactions with commensal hosts is largely understudied. However, it is speculated that compatibility between xylem pit membrane carbohydrate composition and *X. fastidiosa*-secreted cell wall-degrading enzymes mediate disease onset and progression [18,28]. In addition, the O-antigen is a critical component in evading initial immune recognition in the susceptible grapevine immune system and it is tempting to speculate that O-antigen composition dictates the type of symbiotic association with the plant-commensalism vs. parasitism [19]. Understanding the mechanisms that underlie how different *Xylella*-plant host interactions skew towards parasitism or commensalism is an area of research that is ripe for exploration.

Literature Cited

1. Rapicavoli J, Ingel B, Blanco-Ulate B, Cantu D, Roper C. Xylella fastidiosa: an examination of a re-emerging plant pathogen. Mol Plant Pathol. 2017. doi:10.1111/mpp.12585

2. Chatterjee S, Almeida RPP, Lindow S. Living in two Worlds: The Plant and Insect Lifestyles of Xylella fastidiosa. Annu Rev Phytopathol. 2008;46: 243–271.

3. Saponari M, Boscia D, Nigro F, Martelli GP, Others. Identification of DNA sequences related to Xylella fastidiosa in oleander, almond and olive trees exhibiting leaf scorch symptoms in Apulia (Southern Italy). J Plant Pathol. 2013;95. Available: https://www.cabdirect.org/cabdirect/abstract/20153279019

4. Tumber K, Alston J, Fuller K. Pierce's disease costs California $104 million per year. Calif Agric. 2014. Available: http://calag.ucanr.edu/Archive/?article=ca.v068n01p20

5. Alston JM, Fuller KB, Kaplan JD, Tumber KP. Assessing the returns to R&D on perennial crops: the costs and benefits of Pierce's disease research in the California winegrape industry. Aust J Agric Resour Econ. 2015;59: 95–115.

6. Schneider K, van der Werf W, Cendoya M, Mourits M, Navas-Cortés JA, Vicent A, et al. Impact of Xylella fastidiosa subspecies pauca in European olives. Proc Natl Acad Sci U S A. 2020. doi:10.1073/pnas.1912206117

7. Quinton A. UC Davis releases 5 grape varieties resistant to Pierce's disease. In: ANR Blogs [Internet]. 18 Dec 2019 [cited 3 May 2020]. Available: https://ucanr.edu/blogs/blogcore/postdetail.cfm?postnum=39023

8. Nunney L, Vickerman DB, Bromley RE, Russell SA, Hartman JR, Morano LD, et al. Recent evolutionary radiation and host plant specialization in the Xylella fastidiosa subspecies native to the United States. Appl Environ Microbiol. 2013;79: 2189–2200.

9. Hill BL, Purcell AH. Acquisition and retention of Xylella fastidiosa by an efficient vector, Graphocephala atropunctata. Phytopathology. 1995. Available: https://www.apsnet.org/publications/phytopathology/backissues/Documents/1995Articles/Phyto85n02_209.PDF

10. Almeida RPP, Blua MJ, Lopes JRS, Purcell AH. Vector Transmission of Xylella fastidiosa: Applying Fundamental Knowledge to Generate Disease Management Strategies. Ann Entomol Soc Am. 2005;98: 775–786.

11. Krugner R, Sisterson MS, Backus EA, Burbank LP, Redak RA. Sharpshooters: a review of what moves Xylella fastidiosa. Austral Entomology. 2019;58: 248–267.

12. Purcell AH, Finlay AH. Evidence for noncirculative transmission of Pierce's disease bacterium by sharpshooter leafhoppers. Phytopathology. 1979. Available: https://www.apsnet.org/publications/phytopathology/backissues/Documents/1979Articles/Phyto69n04_393.PDF

13. Backus EA, Shugart HJ, Rogers EE, Morgan JK, Shatters R. Direct Evidence of Egestion and Salivation of Xylella fastidiosa Suggests Sharpshooters Can Be "Flying Syringes." Phytopathology. 2015;105: 608–620.

14. Stenger DC, Burbank LP, Krugner R, Sisterson MS. Individual field-collected glassy-winged sharpshooter vectors harbor sequences from two Xylella fastidiosa subspecies. Eur J Plant Pathol. 2019;155: 329–338.

15. Bodino N, Cavalieri V, Dongiovanni C, Simonetto A, Saladini MA, Plazio E, et al. Dispersal of Philaenus spumarius (Hemiptera: Aphrophoridae), a Vector of Xylella fastidiosa, in Olive Grove and Meadow Agroecosystems. Environ Entomol. 2021;50: 267–279.

16. Roper MC, Greve LC, Warren JG, Labavitch JM, Kirkpatrick BC. Xylella fastidiosa requires polygalacturonase for colonization and pathogenicity in Vitis vinifera grapevines. Mol Plant Microbe Interact. 2007;20: 411–419.

17. Pérez-Donoso AG, Sun Q, Roper MC, Greve LC, Kirkpatrick B, Labavitch JM. Cell wall-degrading enzymes enlarge the pore size of intervessel pit membranes in healthy and Xylella fastidiosa-infected grapevines. Plant Physiol. 2010;152: 1748–1759.

18. Ingel B, Jeske DR, Sun Q, Grosskopf J, Roper MC. Xylella fastidiosa Endoglucanases Mediate the Rate of Pierce's Disease Development in Vitis vinifera in a Cultivar-Dependent Manner. Mol Plant Microbe Interact. 2019; MPMI04190096R.

19. Rapicavoli JN, Blanco-Ulate B, Muszyński A, Figueroa-Balderas R, Morales-Cruz A, Azadi P, et al. Lipopolysaccharide O-antigen delays plant innate immune recognition of Xylella fastidiosa. Nat Commun. 2018;9: 390.

20. McElrone AJ, Grant JA, Kluepfel DA. The role of tyloses in crown hydraulic failure of mature walnut trees afflicted by apoplexy disorder. Tree Physiol. 2010;30: 761–772.

21. Collins BR, Parke JL, Lachenbruch B, Hansen EM. The effects of Phytophthora ramorum infection on hydraulic conductivity and tylosis formation in tanoak sapwood. Can J For Res. 2009;39: 1766–1776.

22. Sun Q, Sun Y, Walker MA, Labavitch JM. Vascular occlusions in grapevines with Pierce's disease make disease symptom development worse. Plant Physiol. 2013;161: 1529–1541.

23. Koo H, Allan RN, Howlin RP, Stoodley P, Hall-Stoodley L. Targeting microbial biofilms: current and prospective therapeutic strategies. Nat Rev Microbiol. 2017;15: 740–755.

24. Gouran H, Gillespie H, Nascimento R, Chakraborty S, Zaini PA, Jacobson A, et al. The Secreted Protease PrtA Controls Cell Growth, Biofilm Formation and Pathogenicity in Xylella fastidiosa. Sci Rep. 2016;6: 31098.

25. Newman KL, Almeida RPP, Purcell AH, Lindow SE. Cell-cell signaling controls Xylella fastidiosa interactions with both insects and plants. Proc Natl Acad Sci U S A. 2004;101: 1737–1742.

26. Burbank LP, Stenger DC. The DinJ/RelE Toxin-Antitoxin System Suppresses Bacterial Proliferation and Virulence of Xylella fastidiosa in Grapevine. Phytopathology. 2017;107: 388–394.

27. Guilhabert MR, Hoffman LM, Mills DA, Kirkpatrick BC. Transposon mutagenesis of Xylella fastidiosa by electroporation of Tn5 synaptic complexes. Mol Plant Microbe Interact. 2001;14: 701–706.

28. Sun Q, Greve LC, Labavitch JM. Polysaccharide compositions of intervessel pit membranes contribute to Pierce's disease resistance of grapevines. Plant Physiol. 2011;155: 1976–1987.

29. Varela, L.G., Smith, R.J., and Phillips, P.A. 2001. Pierce's Disease. University of California Davis, UC ANR Publication 21600

30. Ionescu M, Zaini PA, Baccari C, Tran S, da Silva AM, Lindow SE: Xylella fastidiosa outer membrane vesicles modulate plant colonization by blocking attachment to surfaces. Proc Natl Acad Sci U S A 2014, 111:E3910–8.

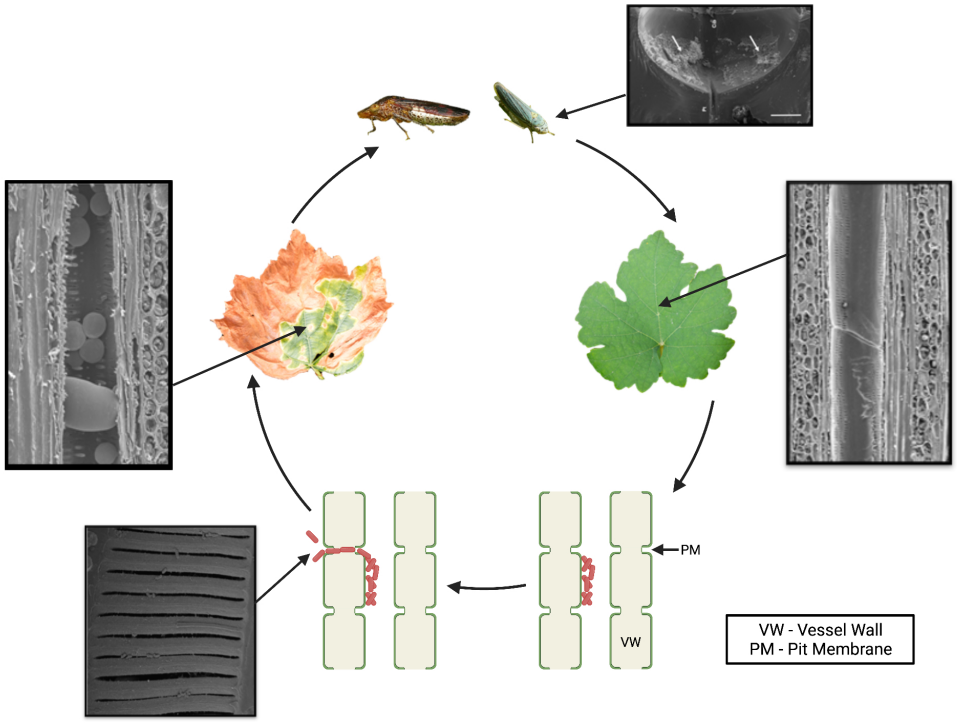

Figure 1. Pierce's disease of grapevine cycle. *Xylella fastidiosa* is acquired by its xylem-feeding insect vectors, such as the glassy-winged sharpshooter and the blue green sharpshooter, during the feeding process. Once acquired it colonizes the insect's foregut and forms robust biofilms (indicated by white arrows). *X. fastidiosa* is transmitted to a new host plant when the insect vector feeds on a new plant and deposits *X. fastidiosa* cells directly into the plant xylem. *X. fastidiosa* achieves systemic colonization of the xylem by enzymatic degradation of the xylem pit membranes that connect adjacent xylem vessels. *X. fastidiosa* colonization induces prolific production of balloon-shaped defense-related protrusions called tyloses in the xylem. Systemic colonization and vessel occlusion by bacterial biofilms and excess tylose production lead to PD symptom development. Photo credit for the blue green sharpshooter: Rodrigo Krugner. Photo credit for the xylem longitudinal sections: Qiang Sun. Pit membrane photo reprinted from Ingel et al., 2019, Molecular Plant-Microbe Interactions Vol. 32, No. 10: 1402-1414. Insect foregut image reprinted from Rapicavoli et al., 2015, Applied and Environmental Microbiology Vol 81, No. 23: 8145-8154. Created with BioRender.com.